THE UNIVERSITY *of* EDINBURGH

MONITORING THE STABILITY OF DENTAL IMPLANTS USING ACOUSTIC EMISSION METHOD

Zannar Ossi

A dissertation submitted for the degree of Doctor of Philosophy

University of Edinburgh

November 2012

DECLARATION

I hereby declare that this thesis describes my own work, of my own composition and has not been submitted as part of any other higher degree.

Zannar Ossi
November 2012

ACKNOWLEDGEMENTS

I have been very fortunate to receive a great deal of supports throughout the course of my research. I would like to express my gratitude to my supervisors, Professor Richard J. Ibbetson and Professor R. (Bob) L. Reuben, who were abundantly helpful and offered invaluable assistance, support and guidance.

Many thanks are due to my friends and colleagues at the Edinburgh Dental Institute and Heriot-Watt University. Special thanks to my friend Wael Abdou and Stuart Morman for their help. I would like to express my love and gratitude to my beloved family.

ABSTRACT

This thesis relates to the feasibility of monitoring dental implants using the transmission of Acoustic Emission (AE) from an intra-oral source to a sensor mounted on the patient's face. A number of *in vitro* and *in vivo* experiments have been carried using different AE sources on teeth and dental implants with the ultimate aim of defining the characteristics of the AE signatures in the time- and frequency-domains that are affected by the implant-bone interface.

An initial feasibility study was carried out to assess the transmission of simulated AE signals through human teeth and hard and soft tissues by biting on different types of hard food. The tests demonstrated that the transmission of AE signals through human tissues was feasible. However, the source was not reproducible. Further preliminary experiments were carried out to assess the transmission of AE in various dental materials as well as in bone and bone-implant combinations in various states of hydration.

The main systematic body of work centred around establishing whether AE signals could discriminate between implants with different amounts of contact with bone. AE signals were generated by applying a standard impulse source through a specially-designed abutment onto dental implants of various sizes (large and small) inserted in bovine ribs under tight and loose fitting conditions. The findings suggested that this simple transmission test was able to assess the quality of the contact between the implant and the bone in the *in vitro* situation and that it might be possible to extend this to the clinical environment. The (standard) pencil lead break method was not suitable for use intra-orally, so a more suitable source for *in vivo* testing needed to be developed. After considering various options a continuous source (based on an air jet) was developed and this was applied to dental implants in the same set of systematic tests as for the pencil lead source. The analysis revealed that the air jet source was a little better at discriminating between the various implant contact conditions.

Finally, an *in vivo* study was conducted to assess the characteristics of the transmitted AE form air jet source applied to the dental implants of a number of volunteers. The findings demonstrated that the AE transmission through the implants, soft and hard tissues using an air jet source was feasible, with the degree of transmission depending on a number of variables, some related to the patients themselves and some related to other, tractable engineering factors.

The overall conclusion of the work is that the technique is very likely to be successful for monitoring implant stability, and is feasible to apply with minimum invasion to patients whose implants have been newly installed. An *in vivo* study in which the test is applied to patients during the stages of stabilisation of their implants is required in order to validate the technique.

TABLE OF CONTENTS

LIST OF FIGURES

LIST OF TABLES

Chapter 1

INTRODUCTION

1.1 Research context

Titanium implants have been used increasingly since the 1970s. The first placement of a craniofacial implant for a bone-anchored hearing aid was performed in 1965 (Branemark *et al.* 1969). Today millions of edentulous and partially dentate patients from all over the world have been treated with dental implants to provide support for prostheses replacing missing teeth.

The two most important factors for survival of the dental implant are its primary stability and the integrity of the osseo-integration process post-implantation (Uribe *et al.* 2005). Assessment of these two factors has remained a challenge for dentists due to the lack of an effective and non-invasive device for accurate measurement of stability at the bone-implant interface.

Various techniques and instruments have been proposed to test implant stability and osseo-integration including Periodontal Probing, Percussion, Radiographic Assessment, Damping Capacity Assessment (Periotest, Siemens, AG, Bensheim, Germany), Resonance Frequency Analysis (Osstell Integration Diagnostics AB, Savedalen, Sweden) and Reverse Torque. However, these techniques have limitations in obtaining results which are reproducible to the degree of accuracy required.

Acoustic Emission (AE) is a widely used monitoring technique in engineering. Application in medicine is generally limited to orthopaedics whilst in dentistry it has been used for laboratory studies of dental materials; it is more sensitive in many applications than other non-destructive testing (NDT). The principle of AE is the generation of ultrasonic waves within, or on the surface of a solid as a result of some impulsive release of energy. An AE sensor is utilised to capture the waves to facilitate

analysis of the signals in order to characterise and understand the behaviour of the material.

1.2 Objective and scope of present research work

The primary aim of this study was to assess the feasibility of using Acoustic Emission as a method for monitoring the stability of dental implants. The method had potential as it was non-invasive and potentially applicable to *in vivo* use within the oral cavity.

The objectives were:

a. To test the basic transmission of AE signals within the human oral cavity.
b. To understand and characterise the AE signals detected through large and small implants fitted in bovine ribs under tight and loose fitting conditions respectively.
c. To test the feasibility of the new AE source *in vivo.*

1.3 Programme of work

No studies had previously assessed the stability of dental implants using an AE technique. The methodology was therefore centred on a series of investigations firstly *in vitro* and subsequently *in vivo*. Initially a basic transmission test was performed *in vivo* by a subject biting on various types of hard and brittle food to assess the potential of AE transmission from the oral cavity, and some basic transmission tests were carried out on bone and dental materials. The main *in vitro* experiments were set up by inserting large and small size implants in bovine ribs under tight and loose fitting conditions. The second series of experiments used a well-known standardised technique in Acoustic Emission studies which was the pencil lead break test (Hsu-Neilson). This was selected as a reference source to determine whether differences in implant sizes and degree of contact with bone could be detected. In a third series of experiments, a new energy source suitable both for Acoustic Emission and use inside the oral cavity was developed and characterised by comparing it with the Hsu-Neilson test. The final part of the programme of work was

to derive a method appropriate for use with implants within the mouth and to assess the results which were obtained from participants in the study.

1.4 Thesis outline

Chapter 1: Introduction. This chapter describes how the basis for the present work was inspired and addresses its contribution to the development of an AE method in monitoring dental implants.

Chapter 2: Literature Review. The first section reviews the biological aspects of osseo-integration of dental implants. The second section summarises the criteria and factors that affect the success and failure of dental implants. The third section describes the current methods of assessing implant stability. This is followed by a section which introduces and reviews AE as potentially a more sensitive and non-invasive method. Finally a Statement of the Problem and the Aims and Objectives of the study are described.

Chapter 3: Experimental Procedures. This chapter describes the experimental apparatus, materials and methods used for the research including the analysis techniques. Five series of experiments were carried out using various AE sources to study the transmission of AE signals.

Chapter 4: Results, Analysis and Discussion. This chapter presents the experimental results from all five experiments and an overall interpretation of these results, covering the important aspects related to the transmission of AE signals.

Chapter 5: The main conclusions and recommendations for future work are presented.

1.5 Contribution to knowledge

AE had never been used in monitoring dental implant stability, nor had an air jet been used previously as an AE source, nor has an AE transmission test been carried

out on a living subject. Hence developing a unique air jet device in the dental environment which was suitable for intra-oral use, and its application with an AE technique in monitoring dental implants are, to the author's knowledge, significant contributions. This provides a potential alternative, non-invasive and sufficiently sensitive technique for examining and understanding the bone/implant interface.

Chapter 2

LITERATURE REVIEW

This chapter is divided into four main sections. The first section reviews some aspects of the biology of osseo-integration, including the phases of healing of the bone around the dental implants after the insertion. The second section summarises the factors that affect implant success and failure. The third section briefly describes the current methods used to monitor the stability of dental implants. The fourth section summarises the state of knowledge on Acoustic Emission techniques applied in the medical field.

2.1 Biology of osseo-integration

The American Dental Association defines a dental implant as "material inserted or grafted into tissue; dental implant-device specially designed to be placed surgically within or on the mandibular or maxillary bone as a means of providing for dental replacement; endosteal (endosseous); eposteal (subperiosteal); transosteal (transosseous)" (ADA 1995-2000).

The concept of osseo-integration has been defined at multiple levels such as clinically (Adell *et al.* 1981), anatomically (Branemark 1983), histologically and ultra-structurally (Linder *et al.* 1983).

Branemark *et al.* (1969) define osseo-integration as a direct and load-bearing union between a titanium implant and vital bone without in-growth of fibrous tissue at the interface. Defined osseo-integration is a histological event that occurrs gradually over a period of time; it is essential for implant stability before and during loading and must be correctly established for successful long-term function.

Figure 2.1 shows a schematic summary of the healing around a dental implant (Rigo *et al.* 2004).

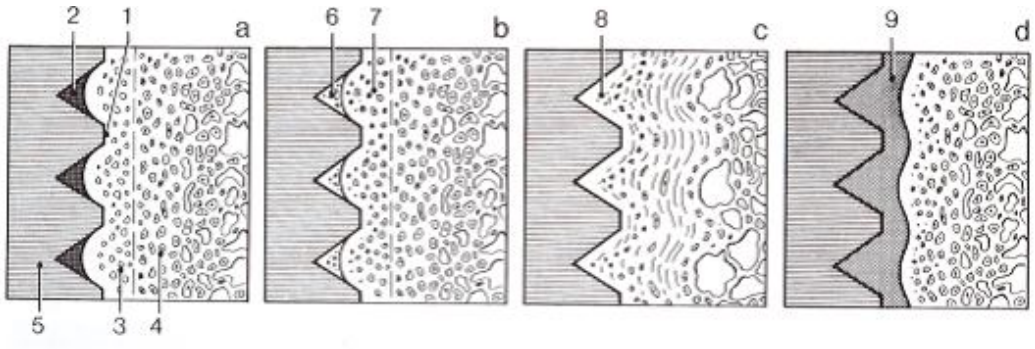

Figure 2.1: Schematic summary of the biology of osseo-integration

a) The screw-thread immediately after implant placement. It is vital to create immediate stability after insertion and during the initial healing phase. (*1*) Immobilization: contact between the fixture and bone. (*2*) Hematoma in a confined cavity, which is bordered by the fixture and bone. (*3*) Bone, despite careful preparation is thermally and mechanically damaged. (*4*) Unmolested bone tissue. (*5*) Fixture.
b) The haematoma transforms into new bone during the initial healing period. (*6*) Damaged bone tissue heals through revascularisation, demineralisation and remineralisation. (*7*).
c) Direct contact between bone and screw-thread is formed without intermediate tissues after the initial healing period. (*8*) Implant/bone interface area is remodelled in response to functional loading.
d) Failure of osseo-integration leads to formation of non-mineralised connective tissue at the implant-bone interface. (*9*) A form of pseudoarthrosis, which could be due to trauma during bone preparation, infection, early functional loading during initial healing period prior to adequate mineralisation and the organization of hard tissue, as well as later in the process, through supra-laminal loading, sometimes occurring several years after initial osseo-integration had been achieved.

Davies (1998) describes the process of osseo-integration at a cellular level, in the initial stage, the blood cells from the capillary venues migrate into the tissue surrounding the dental implants. The adhesion and aggregation of platelets on the surface of the

implants is completed as a result of biochemical change. A collagen network is then formed by fibroblasts and red bone marrow which act as a scaffold (osteoconduction) for the migration of osteogenic cells (osteoinduction). Osteoid tissues and new trabecular bone remodel into lamellar bone in direct contact with the implant surface (osseo-integration) (Branemark 1990; Meyer *et al.* 2004).

The trabecula bone is formed by osteoblasts over 3 to 4 months: it is followed by gradual conversion to compact bone around the periphery of the dental implant (Tortora and Grabowski 2000).

Misch, *et al.* (2001) classify three types of bone developed around osseo-integrated dental implants: lamellar bone, woven bone and composite bone. Lamellar bone is the most organized, highly mineralised, and strongest of the bone types and is the most desirable next to an implant. Woven bone is also called immature bone since it is unorganised, less mineralised, and has less strength than the other types. Composite bone is a combination of lamellar and woven bone.

2.2 Factors influencing the success and failure of dental implants

The main classes of factor which affect the success of an implant are the bone quality, criteria of success and factors influencing the failure. These are discussed in turn below.

2.2.1 Bone quality and morphology

Throughout the literature, bone morphology and density have been important predictors of implant success, which led to the importance of classifying the alveolar resorption during the planning of implant therapy.

Lekholm & Zarb (1985) listed four bone qualities found in the anterior regions of the jawbone:

Type I. Homogeneous compact cortical bone;

Type II Thick layer of cortical bone surrounding a dense trabecular bone;

Type III Thin cortical layer and dense trabecular bone;

Type IV Thin cortical layer of compact bone surrounding a low-density trabecular bone
Atwood (1971) and (1979) stated the common characteristics of the edentulous mandible as a result of resorption during certain stages of mandibular atrophy.

Nishimura *et al.* (1992) stated that two weeks post extraction, bone resorption and formation at the edge and the base of the socket respectively could be observed. Tallgren (1972) found the rate of resorption in the first 5 years post-extraction of the tooth was highest and it reduced afterwards. It was also found that the resorption was constant throughout life and the rate of resorption differed according to the location in the jaws; the reduction of the resorption rate was four times faster for anterior residual ridge height in the mandible than in the maxilla.

Cawood & Howell (1988) found horizontal and vertical resorptions taking place in the maxilla, anterior and premolar areas of the mandible; however only vertical resorption was found in the molar area of the mandible. Douglass *et al*. (1993) found that resorption in bone height was more common in the mandibular posterior region than anterior area.

Lekholm & Zarb (1985) classified atrophy for the maxilla and mandible from A to E:
A Most of the alveolar ridge was present;
B Moderate residual ridge resorption had occurred;
C Advanced residual ridge resorption had occurred and only basal bone remained;
D Some resorption of basal bone had started;
E Extreme resorption of the basal bone had taken place.

The quality of the alveolar bone has been found in several studies to be the most important factor for achieving the primary stability of a dental implant (Jaffin and Berman 1991; Johns *et al.* 1992). Other studies further support this finding and that the failure rate of dental implants is higher in poor-quality bone (Jemt and Lekholm 1995).

Albrektsson *et al.* (1988) carried out a retrospective study for five to eight years on 8,139 dental implants. The implant success rate was found to be 99.1% in the mandible

and 84.9% in the maxilla. The implant failure rate in bone of poor quality and quantity was higher than where quality and quantity were good.

Hutton *et al.* (1995) in a 3-year follow up prospective study reported on the status of 120 overdentures and 444 dental implants. Maxillary overdenture failure rates (27.6%) were nearly nine times greater than those for mandibular overdentures (3.3%). Adell *et al.* (1981) and (1990) reported on two classical long-term 15-year follow-up studies; they found success rates of 95% in the maxilla and 99% in the mandible.

Jaffin & Berman (1991) in 5-year study of 1,054 maxillary implants placed in softer bone reported that, the failure rates for type I, II and III bone were 3% compared with 35% in type IV bone. They attributed the high failure rate partly to the difficulty in achieving initial stability after implant placement in the softer bone of the posterior maxilla.

Bone volume plays a great role in implant success rate. Misch (1993) stated that longer and wider implants had greater surface areas, which resulted in less concentrated stress being transmitted to the bone. For root form implants, each 0.25mm increase in diameter corresponded to an increase in surface area of approximately 5-8%. An implant which was 3mm longer provided more than a 10% increase in surface area.

The crestal bone region is most commonly affected in early bone loss. Saadoun & LeGall (1992) stated that the width of the implant had more impact on the bone loss than the length. Misch (1993) also confirmed that the crestal region received most stress after loading the implant. Therefore the length of the implant is not completely effective in decreasing the load around the implant.

Block *et al*. (1990) in an animal study showed stronger correlation between the pull out force for extraction and the implant length than for its diameter. A minimum implant length of 10mm and 6mm was required in maxilla and mandible respectively for a dental implant to be successful.

2.2.2 Criteria for success of dental implants

Several criteria for success of the dental implants have been proposed. The most common are listed below: these were proposed by Albrektsson *et al.* (1986) and Albrektsson and Isidor (1994).

1. An individual, unattached implant was immobile when tested clinically.
2. Radiographic examination did not reveal any peri-implant radiolucency.
3. After the first year in function, radiographic vertical bone loss was less than 0.2 mm per annum.
4. The individual implant performance was characterised by an absence of signs and symptoms such as pain, infection, neuropathies, paraesthesia, or violation of the inferior dental canal.
5. As a minimum, the implant should fulfil the above criteria with a success rate of 85% at the end of a 5 year observation period and 80% at the end of a 10 year period.

Those criteria were reviewed by (Albrektsson and Isidor 1994) and further suggestions were added. These were average bone loss <1.5 mm in the first year in service, and thereafter <0.2 mm annually. Many other suggested success criteria were similar as shown in Table 2.1.

Author	**Bone Loss**	**Radiographic Evaluation**
(Schnitman and Shulman 1979)	Bone loss no greater than a third of the vertical height of the implant	No suggested criteria
(Smith and Zarb 1989)	Mean vertical bone loss <0.2 mm annually after the first year in service	No evidence of peri- implant radiolucency as assessed on an undistorted radiograph
(Wennström and Palmer 1999)	Maximum bone loss of 2mm between prosthesis installation and the 5th year, with the majority of the loss occurring during the first year	No suggested criteria
(Ostman *et al.* 2008)	Success grade 1 <2 mm bone loss during the first year in service Success grade 2 <3 mm bone loss the fi year in service	No radiographic signs of pathology No radiographic signs of pathology

Table 2.1: Criteria for success of dental implants

Several studies suggested different parameters for success:

1. Biocompatibility of the implant material (Albrektsson *et al.* 1981)
2. Macroscopic and microscopic nature of the implant surface (Skalak 1983)
3. The surgical technique (Ericsson *et al.* 1994)
4. An undisturbed healing phase (Schatzker *et al.* 1975)
5. The subsequent prosthetic design and long-term loading phase. This reconciled considerations of design, materials used, location of implants and anticipated loading together with hygienic and cosmetic considerations (Albrektsson *et al.* 1981)

2.2.3 Factors influencing implant failure

Dental implant failure generally refers to the situation when an implant did not fulfil its purpose for any reason; this might be caused by different factors. The clinical performance of osseo-integrated dental implants was first evaluated by the Swedish National Board of Health and Welfare in 1975 (Bergman 1983). Three main criteria were used, these were periodontal (gingival index, plaque index and pocket depth), prosthetic (type of occlusion) and radiographic parameters (absence of peri-implant radiolucency).

2.2.3.1 Operator and material related factors

Several studies have shown that operator skills and experience play a great role in outcome of dental implant therapy (Weyant 1994). The failure rate of dental implant for surgeons who had placed less than 50 implants was almost twice as high as for those who had placed over 50 implants (Weyant 1994; 1996).

Surgical preparation and technique at the implant site are also important. Bacterial contamination may cause a zone of necrosis surrounding the inserted implant. Iyer *et al.* (1997) reported the degree of trauma influenced the extent of the zone of necrosis.

Lundskog (1972) and Eriksson and Albrektsson (1983) reported several *In vivo* experimental investigations which showed that the damage to the bone could be caused by heat generated during the drilling of the implant site without adequate cooling.

2.2.3.2 Biomaterial related factors

Pure and alloyed titanium has been used in many medical treatments as a material of choice due to its high corrosion resistance and good mechanical performance (Niinomi 1998). The high biocompatibility of pure titanium is due to the absence of toxic effects on fibroblasts and macrophages and a lack of inflammatory response in peri-implant tissues (Mostardi *et al.* 1999). The biocompatibility of titanium alloys is due to a passively formed oxide film on their surface which makes it the most commonly used material in implant therapy in dentistry (Long and Rack 1998). Although the initial success rate of dental implants was found to be almost 100%, a number of studies have shown that the final result of the treatment could be compromised by many complications (Sones 1989; Taylor 1998).

Esposito *et al.* (1998) classified implant failures into biological, mechanical failures of the components and functional failures.

2.2.3.3 Biological failure

Biological failure of dental implants is defined as inadequate establishment (e.g. interference with healing process) or maintenance of the osseo-integration by the host tissue (Esposito *et al.* 1998).

Systemic conditions such as diabetes mellitus and osteoporosis can contribute to dental implant failure. Fiorellini and Nevins (2000) reported that diabetes delayed wound healing, which logically affects the osseo-integration process. An 85% success rate was reported in diabetic patients, most failures occurred in the first year after implant loading. Olson *et al.* (2000) also reported that patients who had diabetes for longer periods had a higher occurrence of dental implant failure.

Several reports have been written on the success of dental implants in patients with osteoporosis, Roberts *et al.* (1992) and Dao *et al.* (1993) reported that a diagnosis of osteoporosis at one particular part of the skeleton, was not necessarily seen at another distant site, local rather than systemic bone density seemed to be the predominant factor.

2.2.3.4 Mechanical complications

A restored dental implant consists of a set screw, abutment and the implant. Zarb and Schmitt (1990), Jemt *et al.*(1992) and Becker and Becker (1995) in retrospective studies observed the fixed prostheses supported by dental implants, found that each of these components could be fractured by fatigue forces and the screw problem was the most commonly reported mechanical failure which mainly occurred in the first year of function.

The reported frequency of the fracture of implant components varies widely. Adell *et al.* (1981) studied 2768 fixtures installed in 410 edentulous jaws of 371 consecutive patients in retrospective study over period of 15 years. They found that an implant fracture frequency of 3.5% in Brånemark implants. Most of those fractures occurred after 5 years of fixture installation. Naert *et al.* (1992) observed 589 consecutive implants supporting complete fixed prostheses They recorded the component complications as follows: fixture fracture (3/564), abutment screw fracture (5/564), gold screw fracture (7/564). It was also reported that most fractures occurred in maxillary prostheses, but only 2% of the tooth veneer fractured in type II prostheses in the mandible.

Lekholm *et al.* (2006) in retrospective review of 17 partially edentulous patients over 20 years follow up, found that fractures of the ceramic, loosening of the locking screw and fractures of the abutment were the most common mechanical complications. Jemt and Johansson (2006) reported that minimal mechanical complications occurred in a 15-year follow-up period on 76 patients with fixed prostheses in the maxilla: they found that the

prosthetic design, unfavourable loading, and fatigue were possible causes for mechanical failure.

2.2.3.5 Geometry of dental implants

Various geometries of dental implants have been used, the root-shaped dental implants are currently the most common (Sennerby *et al.* 2005).

Implant design:
Numerous investigations demonstrated that high primary stability could be achieved by using screw-shaped implants in contrast to cylindrical ones (Branemark *et al.* 1969; Lundskog 1972; Carlsson *et al.* 1986). Albrektsson (1993) observed continuous bone loss around cylindrical implants. Lekholm *et al.* (1994) found high survival rates and minimal marginal bone resorption with screw-shaped implants. The advantages of the screw-shaped implants might have been that: (i) they engaged the bone better at the implant site during insertion and consequently their stability was less dependent on press-fit and rapid bone integration, (ii) firm stability between the thread flanks and the head of an implant could be achieved by an axial compression of the bone, (iii) during functional loading of the implant, the threads ensured an even distribution of loading stresses over the interface.

Implant length:
Friberg *et al.* (1991) in retrospective study followed up 4,641 Brånemark dental implants, they reported that generally the shorter implants were less successful than longer ones in situations of advanced jaw resorption and poor bone quality. However, Deporter *et al.* (2002) in a 10 year prospective clinical trial showed a 92.7% survival rate of short sintered porous-surfaced dental implants used with mandibular complete overdentures.

Hagi *et al.* (2004) reviewed 12 published studies examining the relationship between short dental implant failure rates and their surface geometry such as length and location (maxilla versus mandible). It was found that (i) greater failure rates were observed in

machined-surface implants comparing to those with textured surfaces; (ii) shorter implants had higher failure rates than longer ones except for the sintered porous-surfaced implants.

Das Neves *et al.* (2006) found that longer and wider implants had a higher success rate than short ones; in several follow up studies 16,344 implant placements produced 786 failures (4.8%). They found that 3.75 x 7 mm implants had a failure rate of 9.7% compared to 6.3% for 3.75 x 10 mm implants.

Both Ostman *et al.* (2005) and Miyamoto *et al.* (2005) found that increasing implant length resulted in decreasing primary stability as measured using Resonance Frequency Analysis (RFA). This might have been because long Brånemark implants had a reduced diameter in the coronal direction to reduce frictional heat. Ivanoff *et al.* (1996) in a rabbit model demonstrated higher removal torque for long compared with short implants.

Implant diameter:

The choice of the implant diameter is based on both surgical and prosthetic requirements. Ivanoff *et al.* (1997) in an animal study found a significant increase in the removal torque following an increase in implant diameter in integrated implants in rabbit tibia. The authors suggested that the shear resistance was due to the presence of supportive cortical bone.

Ivanoff *et al.* (1999) studied the relationship between the diameter of implants and survival rates and marginal bone remodelling. The 3- to 5-year retrospective report found a significant difference between implant failures associated with implant diameter P-value < 0.05, with a higher failure rate for the 5.0-mm-diameter compared with those of 3.75 and 4-mm. diameter. However, Langer *et al.* (1993) suggested that high primary stability could be gained with wide diameter screw-shaped self-tapping dental implants, which might be useful where bone quality was poor and in posterior regions of the mouth when bone height was reduced. The advantages of wider implants also include

increased implant surface topography and the possibility of higher marginal and lateral cortical bone engagement.

Implant surface:
The initial implant surface design was machined; osseo-integration required several months for those implants according to the classical protocols (Albrektsson and Sennerby 1991). Currently, a huge number of experimental investigations have demonstrated that the implant surface topography influenced the bone response and osseo-integration. Buser *et al.* (2004) reported that the roughness of the surface of dental implants increased bone apposition whilst hydrophilic surfaces favoured the interactions with biological fluids and cells when compared with the hydrophobic ones.

Buser *et al.* (1991) and Davies (1998) emphasised the important role of the roughness of the implant surface with regard to bone healing; the rough surface of titanium dental implants provided a higher degree of bone to implant contact (BIC).

Various surfaces for titanium implants have been proposed to enhance osseo-integration. Hydroxyapatite coatings, titanium plasma spraying and blasting procedures have been compared in several clinical and histomorphometric studies. The sandblasted and thermo-acid-etched implant surface was found to be superior to the other surfaces in regard to BIC (Sullivan *et al.* 1997; Davies 1998; Lazzara *et al.* 1998; Lazzara *et al.* 1999).

2.2.3.6 Loading of dental implants

Chapman (1989) stated that occlusal loading could be critical for implant success and longevity. The potential load created by tooth contacts could have a dramatic impact on the attachment between the bone and the surface of the titanium implant. Periodontal ligaments in natural dentitions have the capacity to absorb the occlusal forces, while the bone-implant interface seemingly had no capacity to allow movement of the implant

Geng *et al.* (2001) stated that the load on dental implants was the key factor influencing success and failure. The generated load depended on the type of loading, the material properties of the implant and prosthesis, the quality and quantity of the surrounding bone, the implant surface structure, the implant geometry, its length, diameter, and shape.

Gibbs *et al.* (1981), Chapman (1989) and Weinberg and Kruger (1995) reported that the failure of a dental implant occurred when the occlusual forces exceeded the capacity of the interface to absorb stress. There were several biomechanical factors described that contributed to overload of dental implants, such as occlusal interferences, bone type and parafunctional habits (bruxism).

Isidor (1997) reported the relationship between excessive loading, marginal bone loss and implant mobility. Quirynen *et al.* (1992) reported the effects of overload on marginal bone loss in a clinical study of 98 patients with fixed prostheses.

Aparicio *et al.* (2003) reviewed three loading schemes.
1. Immediate/Direct loading: The prosthesis is attached to the implants immediately after implant placement.
2. Early loading: The implant is restored earlier than the conventional healing period of 3 to 6 months.
3. Delayed loading: The implant is restored after the conventional healing period of 3 to 6 months.

2.2.3.7 Insertion torque

Ottoni *et al.* (2005) described the insertion torque as a compressive stress on the adjacent bone during implant placement; the implant bed being slightly narrower than the diameter of the implant increased the primary stability.

Insertion torque analysis quantified the amount of force during the placement and this correlated with bone density (Turkyilmaz *et al.* 2007). Song *et al.* (2007) stated

that the increase in insertion torque showed an increase of the thickness of the cortical bone which allowed assumptions to be made about the quality of the bone support available for the implant.

Lim *et al.* (2008) reported a significant increase in insertion torque with increasing diameter and length of implant. Chaddad *et al.* (2008) reported that insertion torques with values of less than 15 Ncm correlated with failure of implants having both machined and treated surfaces.

2.3. Current methods of monitoring the stability of dental implants

Several methods and techniques have been used for monitoring the stability of dental implants.

2.3.1 Periodontal probe

An examination with a periodontal probe is considered to be the main tool for assessing periodontal health in everyday practice. The diagnostic value and possible trauma of probing around dental implants has been studied thoroughly. Schou *et al.* (2002) discussed the difference between the probing measurements around teeth and dental implants including the factors that influenced the probe penetration around dental implants such as their surface roughness and their threads. Spray *et al.* (1978) reported that the lack of accuracy of this method was due to variability in the diameter of the probe and the applied probing force. Therefore, it was not possible to identify the histologic level of the connective tissue attachment. On the other hand Lang *et al.* (1994) suggested that the condition of the periodontal tissues could be assessed using a probe with light forces (0.2-0.25 N) to avoid tissue trauma and under healthy conditions the pocket depth around dental implants ranged between 2-4 mm.

2.3.2 Percussion test

The percussion test is a simple method that can be used to estimate the level of integration (Meredith 1998). It measures the stability of an integrated dental implant

by simply tapping on the healing abutment with the handle of a dental instrument such as dental mirror. An integrated implant produces a high pitched sound (as if tapping on a marble) while a non-integrated implant produces a low and dull sound. The tone changes during the healing process as a result of increasing implant-bone interface contact.

The disadvantage of this method is that good listening skills are required by the operator and hence it can be subjective, therefore it is not an accurate method.

2.3.3 Radiographic assessment

The radiograph is the most commonly used diagnostic/monitoring method to evaluate the amount of available bone for implant placement and around a previously placed implants, Hermann *et al.* (2001) stated that radiographs could be used to measure the crestal bone level which was an indicator of the success of a dental implant.

Radiographs provide only a two-dimensional image of a three-dimensional structure, therefore visualising osseous defects such as buccal dehiscences might be difficult. Spray *et al.* (2000) reported that intra-oral radiographs illustrated clearly the mesial and distal marginal bone levels. However, early bone loss often occurs on the facial aspect of the implant. Sophisticated technology, such as computer scanning tomograms might offer a better diagnostic image. However their routine use generally has a risk radiation overdose as well being expensive.

2.3.4 Periotest

The Periotest (Seimens, AG, Bensheim, Germany) instrument initially was developed to measure the stiffness of the natural dentition and hence the condition of the periodontium; at a later stage it was used in oral implantology to measure the bone/implant interface. It involved a damping capacity assessment, measuring the deflection/deceleration of a tooth or implant that had been struck by a small pistil fired from within the instrument's hand piece. The handpiece had an electronically controlled translational hammer bearing an 8-gram rod with a sensor at its tip. When activated, the

rod tapped the implant abutment up to 16 times in four seconds with an action similar to that of a retractable ballpoint pen. The contact time of the accelerated pistil against the implant, which moved according to the strike, was calculated to produce a value called the Periotest t value (PTV), which ranged with decreasing stability of the tooth or implant, from 8 to 50 PTV units.

Manz *et al.* (1992) reported in two *in vitro* studies, the high degree of repeatability and inter-examiner and intra-examiner reliability of this method. However a number of studies demonstrated that several variables influenced the Periotest value. For example angulation, striking point and abutment length (Derhami *et al.* 1995; Truhlar *et al.* 1997).

2.3.5 Reverse torque

This method was first proposed by Roberts *et al.* (1984) and developed further by Johansson and Albrektsson (Johansson and Albrektsson 1987; Johansson and Albrektsson 1991). It measured the torque level at the breaking point of the bone-implant contact.

Sullivan *et al.* (1996) reported that a removal torque value (RTV) from 45 to 48 Ncm as an indirect measurements of BIC and a RTV of 20 Ncm might be an acceptable indication of successful implant integration.

Removal torque has been criticized as being destructive by Adell (1985); there was a risk of irreversible plastic deformation of the peri-implant bone and of causing implant failure when an unnecessary load was applied to an implant that was still undergoing osseo-integration.

2.3.6 Pulsed oscillation waveform

Kaneko (1991) was the first to describe this method of analysing the mechanical vibration characteristics of the implant-bone interface using a forced excitation steady-state wave.

This device consisted of an electric driver and receiver, pulse generator and oscilloscope.

The frequency and amplitude of an excited implant were displayed on the oscilloscope screen. Kaneko *et al.* (1986) in an *in vitro* study demonstrated that the sensitivity of this device depended on the direction and position of the load; also the sensitivity was low for assessment of rigidity of a dental implant.

2.3.7 Resonance frequency analysis

Meredith *et al.* (1996) reported the use of sonic resonance frequency measurements to assess the values of the implant-bone interface. Currently, two machines are in clinical use: Osstell (Integration Diagnostics, Goteborgsvangen, Sweden) and Implomates (Bio Tech-One, Taipei Hsien, Taiwan). The principle of this natural frequency detecting device is to measure the stiffness of the bone/implant interface by calculating the resonance frequency resulting from the reaction to oscillations applied to the implant-bone system (Meredith *et al.* 1996).

Barewal *et al.*(2003), Franke *et al.*(2003) and Huang *et al.* (2003) and a number of other studies tried to verify the parameters that affected RFA values in various settings. Unfortunately none of the data in those studies could demonstrate the validity of RFA in the assessment of implant-bone contact.

Ito *et al.* (2008) used the Osstell transducer to measure RF of implants placed in the tibia of mini-pigs and found that there was no correlation between RF and histological implant-bone contact. Schliephake *et al.* (2006) reported that there was neither correlation between bone-implant contact nor peri-implant bone density and RFA values. Nkenke *et al.* (2003) in cadaver studies demonstrated that RFA values did not correlate with bone density or with bone-implant contact at the time of implant placement.

2.4 Acoustic Emission

The term Acoustic Emission (AE) is used to describe both a technique and the phenomenon upon which the technique is based. AE is defined as 'the class of phenomena whereby transient elastic waves are generated by a rapid release of energy from a localised source or sources within a material, or the transient elastic wave(s) so generated' according to ANSI/ASTM standards (ASTM STP 505 American Society for Testing and Materials, Philadelphia, D1907, 1972). It is reported that AE was used as early as 6,500 BC; potters were known to listen for audible sounds during the cooling of their ceramics, signifying structural failure. Elastic deformation in solid materials occurs when load is applied, some permanent microscopic deformation may occur, which leads to the release of elastic wave AE.

The elastic wave which carries strain energy can be recorded by an AE sensor mounted on the structure's surface and detects any emissions that are above a certain threshold level, and then converts them to voltage signals. AE signals are normally small and may contain background noises such as those which are environmental and mechanical. Therefore a threshold level, amplification and filtering are required for signal processing.

The first major work on AE was published in a PhD thesis written by Kaiser (1950), entitled "Results and Conclusions from Measurements of Sound in Metallic Materials under Tensile Stress." Soon after becoming aware of Kaiser's work, Schofield (1961) initiated the first research program in the United States to look at the materials engineering applications of Kaiser's research. This was generally recognized as the beginning of modern day Acoustic Emission testing.

Coupling agent:

Use of a suitable acoustic couplant (e.g. grease or water-based gel) is necessary to improve the reliability of AE detection. Colombo *et al.* (2005) stated that correct and intimate coupling of an Acoustic Emission sensor to the surface of a specimen was very important for obtaining good measurements. The couplant material is used to remove any air from the interface as the acoustic impedance of air is much lower

than that of the sensor face or material surface and can cause considerable loss in transmission (Cros *et al.* 2000).

A number of studies (Hill and El-Dardiry 1981; Li and Nordlund 1993) showed the influence of coupling on the transmission of AE energy from the specimen to the sensor.

Application of the AE technique:
The AE technique offers the advantages of being a non-stop method which can monitor the condition of the material under investigation throughout the test. It is non-localized and has the ability to examine large volume objects (Williams 1980).

Billi *et al.* (2000) applied the AE method in testing the damage to the hydroxyapatite coating on dental implants during the whole cycle of fatigue. The method allowed following the progression of the damage and established the exact fatigue life of each coating with a good degree of approximation.

Furthermore, it was found that AE was highly sensitive in assessing composite materials, it was able to detect microcracks, material deformation, solidification, friction, impact, flow, phase transformations, and the stress released when matrix crazing, fibre breakage, debonding, or any other microstructural failure occurred. Hamstad (1985), Hamstad and Moore (1986), Alander *et al.* (2004) and Fennis *et al.* (2005) stated the advantages of using the AE method to test and analyse fibre reinforced composites included the ability to obtain real time data and the high sensitivity of the method.

AE has been confirmed to be a powerful technique able to provide complementary information on the behaviour of materials; hence it has been widely used in materials testing and has been applied in the analysis of fracture behaviour of different types of biomaterials such as ceramics.

For example, Asaoka *et al.* (1992) used an AE technique to study the viscoelastic behaviour of dental porcelain during heat treatments. Qi (1997) investigated failure

mechanisms of composite materials using an AE method. Schrooten *et al.* (1999) used AE analysis for evaluation of the adhesive strength of a plasma sprayed bioactive glass (BAG) coating on dental implants *in vitro*. Lin *et al.* (2000) used an AE method to study the fracture behaviour of a repaired acrylic resin denture subjected to flexural loading.

Vallittu (2002) suggested that the AE technique could be used in evaluating the initial phases of fracture propagation in porcelain fused to metal crowns.

Wang and Darvell (2008) proposed that AE was effective in detecting crack formation when load was applied to amalgam and glass ionomer cement (GIC).

AE techniques have also been widely used to monitor and measure removal of bone cement from the femoral canal in hip prosthesis loosening and also in monitoring the integrity of the cement–metal interface of total joint components *in vitro* (Schmidt and Nordmann 1994; Davies *et al*. 1996).

AE techniques suffer from several disadvantages:

1. The parameters of the acquired AE signals depend on the test equipment used, e.g. the precise frequency of operation, sensitivity of the transducer and amplifier gains. All experiments must be carried out using identical equipment if repeat measurements on the same structure were required.
2. The effect of geometry and materials' properties of the structure on transmission of the AE signal is not fully understood. Therefore, it is not possible to compare the AE signals recorded from structures of different geometries with any degree of certainty.
3. The experimental set up can affect the parameters of the measured signals such as the maximum amplitude, if the relative location of the source were different in each case.

The current method can only give a quantitative indication of the change in state of the component rather than a quantitative indication of an absolute level of change.

Summary of literature review:

Evidence from the presented literature review indicates that there is lack of a reliable prognostic indicator for implant stability. The AE method has proven in many

industries to be reliable and accurate monitoring method and may have potential for application in assessing the stability of dental implants.

Chapter 3

APPARATUS AND DESCRIPTION OF THE EXPERIMENTS

3.1 Introduction

This chapter describes the material specifications, experimental apparatus and procedures used for this work. Firstly the features and specification of the apparatus common to all experiments are described and then the details of each of five series of experiments are presented, including the design and calibration of an air jet device. This was specifically developed for this study, in the search for a non-invasive source of AE energy to assess the feasibility of the AE technique in monitoring the stability of the dental implants,

At an early stage in this study, it was essential to determine if it were possible for an AE source on a tooth to be transmitted with reasonable fidelity to a sensor mounted on the face, essentially a basic transmission test of AE signals through soft and hard human tissues. In order to generate AE in the oral cavity an impulsive source was required, and it was recognised that biting on certain types of food might release AE energy. Because it was not known what characteristics such a source would have, the first experiment assessed AE transmission through the jaws and soft tissues using different types of food to generate burst-like signals. Fundamentally, this provided a demonstration that AE could be generated in the mouth without harm and that the waves could be transmitted through bone and soft tissues to an external sensor. Secondarily, the tests allowed an assessment of whether different sources could be distinguished despite the damping effects of the soft tissues such as fat, muscles and skin.

Next, it was essential to determine whether it was possible to discriminate between implants that had good bone contact and those that did not, and so the second series of experiments were designed to assess this. In order to minimise the variables, the experiments were done *in vitro* using a standard Hsu-Nielsen source (pencil lead break) which was a well-established technique in the calibration of AE systems, and it was used in this study to generate AE signals on large and small dental implants

inserted in bovine ribs in tight and loose fitting conditions, and with the ribs in wet and dry conditions.

To apply the AE technique in assessing the implant/bone interface, it was necessary to demonstrate the application of a standard source clinically. Since the pencil lead break was not suitable for intra-oral use, a different AE source was required. There were several other existing sources used to calibrate AE systems, such as the breakage of a glass capillary tube and a high voltage discharge, which were not suitable. However, the Helium Gas Jet source was one established source which worked by directing a jet of helium gas onto a surface. To avoid the use of helium gas, it was necessary to adapt this standard source to use a compressed air jet, which was readily available in dental clinics. Because the jet was a continuous source (whereas the pencil lead was a discrete source), it was necessary to establish that the implant/bone interface could be assessed using the air jet as had been done using the Hsu-Nielson source.

Having determined that discrimination between implants of different dimensions and with differing amounts of bone contact was possible using an air jet as the energy source. The final stage of the investigation was to assess the usefulness of the technique when used *in vivo* with participants who had been provided with dental implants. *In vivo* experiments were performed on participants having two mandibular implants in the anterior portion of the mandible. These implants had been provided to assist in retaining a mandibular complete removable prosthesis. The implants were assessed using the same procedures as for the *in vitro* bone tests and the results correlated with the dimensions of the implants, whilst recognising the possible variability in transmission between participants.

3.2 Signal processing

In general, there are three types of AE signals, burst, continuous and mixed. Burst signals are transmitted from individual events occurring on materials and take the form

of discrete transients (Figure 3.1a). Continuous signals resulted from time and/or successive emission events from one or more sources (Figure 3.1b).

Figure 3.1c shows mixed signals which are a combination of burst and continuous signals.

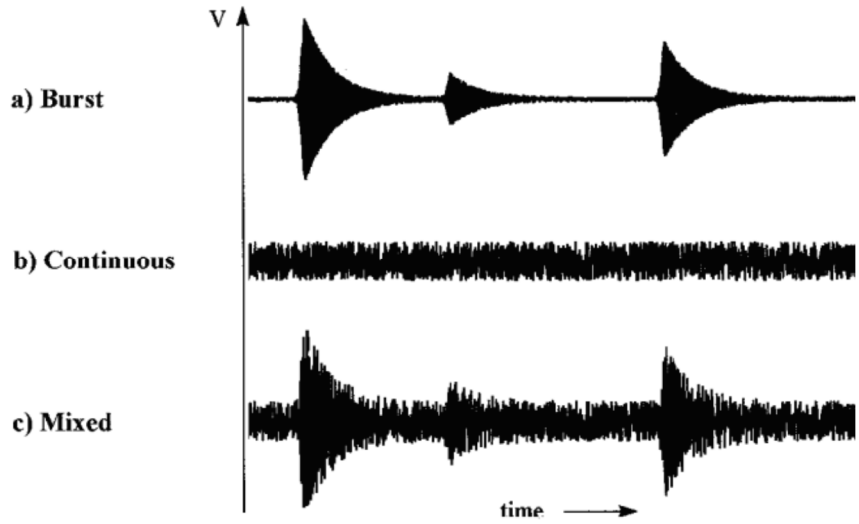

Figure 3.1: AE signals

Various parameters are commonly used in AE to identify the nature of the sources (Figure 3.2).

Amplitude, A, is the greatest measured voltage in a waveform and is measured in decibels (dB). This is an important parameter in Acoustic Emission inspection because it determines the detectability of the signal. Signals with amplitudes below the operator-defined, minimum threshold would not have been recorded.

Rise time, R, is the time interval between the first threshold crossing and the signal peak. This parameter is related to the propagation of the wave between the source of the Acoustic Emission event and the sensor. Therefore, rise time is used for qualification of signals and as a criterion for noise filter.

Duration, D, is the time difference between the first and last threshold crossings. Duration can be used to identify different types of sources and to filter out noise.

Like counts (N), this parameter relies upon the magnitude of the signal and the acoustics of the material.

MARSE, E, sometimes referred to as energy counts, is the measure of the area under the envelope of the rectified linear voltage time signal from the transducer. This can be thought of as the relative signal amplitude and is useful because the energy of the emission can be determined. MARSE is also sensitive to the duration and amplitude of the signal, but does not use counts or user defined thresholds and operating frequencies. MARSE is regularly used in the measurements of Acoustic Emissions.

Counts, N, refer to the number of pulses emitted by the measurement circuitry if the signal amplitude is greater than the threshold. Depending on the magnitude of the AE event and the characteristics of the material, one hit may have produced one or many counts. While this is a relatively simple parameter to collect, it usually needs to be combined with amplitude and/or duration measurements to provide quality information about the shape of a signal.

Threshold: the threshold voltage level is set to distinguish signal from noise. The AE events are counted only if the signals cross the threshold.

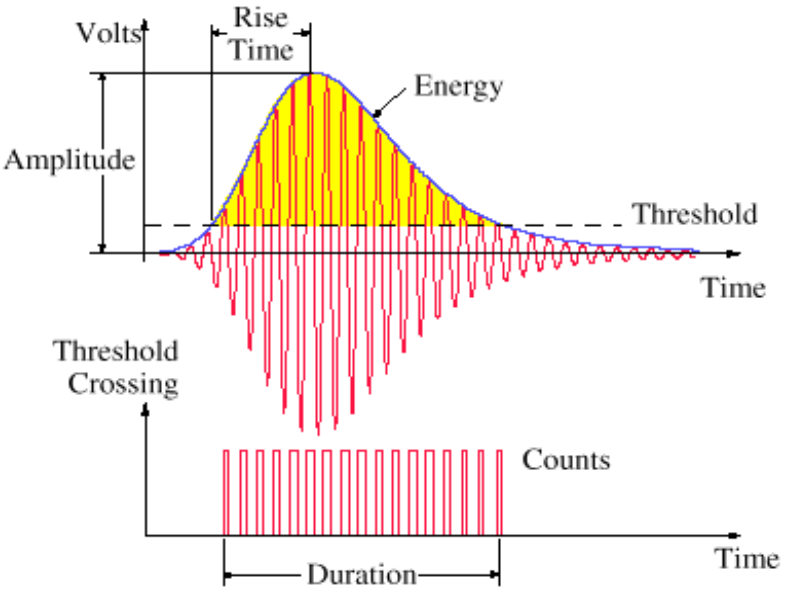

Figure 3.2: AE parameters

Two sources of AE were used in this study, Hsu Nielsen and air jet. Hsu Nielsen is the standard pencil lead fracture technique which produces a rapid release of AE energy within the test materials in the form of a burst AE signal. Figure 3.3 shows the AE signal produced by a pencil lead fracture.

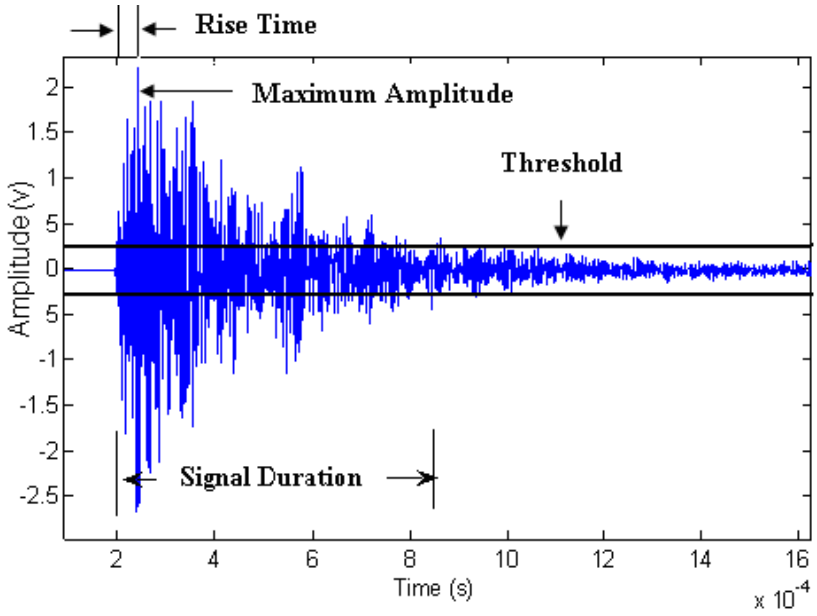

Figure 3.3: Typical AE signal caused by pencil lead break source

The air jet source produced continuous AE signals; a typical example of which is shown in Figure 3.4.

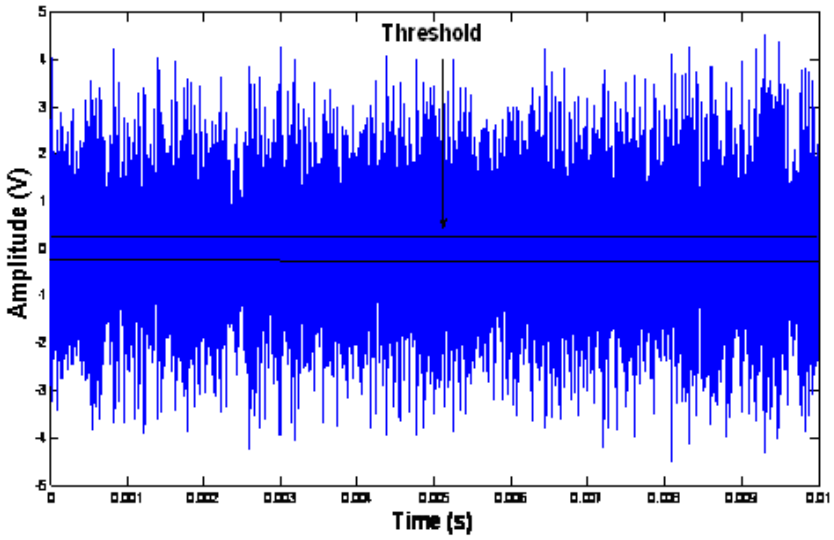

Figure 3.4: Typical AE signal caused by an air jet device source

A number of statistical methods were utilised in AE signal analysis in this work these are described in term below.

3.2.1 Trending

Trending was used to show how signals changed over time, typically a few tens of seconds (see below) in longer or excessive records. It was usually measured by the change in a particular feature.

3.2.2 AE energy

The energy analysis procedure involved squaring and integrating the time signal, the signal energy being proportional to the area under the curve. Each record typically contained 2.5 units in points and the integration consisted of adding together the absolute value of each of the points giving a value in V.s. In cases where the record length was longer, it was necessary to take this into account in the energy.

3.2.3 Frequency domain

The disadvantage of energy analysis is that it is calibration dependent; hence frequency analysis was used to determine if the energy distribution in the frequency domain, i.e. the ratio of proportions of the total energy, could be used instead. Accordingly, the time domain signal was converted to the frequency domain (spectrum) using a standard signal processing technique called the Fast Fourier transform (FFT).

High frequency: frequency ratio analysis

The AE energy is represented by the area of the spectrum in a given band (power spectral density x frequency). The spectra were normalised and divided into two equal bands, low frequency band ($0.5 \times 10^5 – 2 \times 10^5$ Hz) and high frequency band ($2 \times 10^5 – 4 \times 10^5$ Hz), as shown in Figure 3.5. The ratio of the energy in the high band to the low band is termed hereinafter “frequency ratio”.

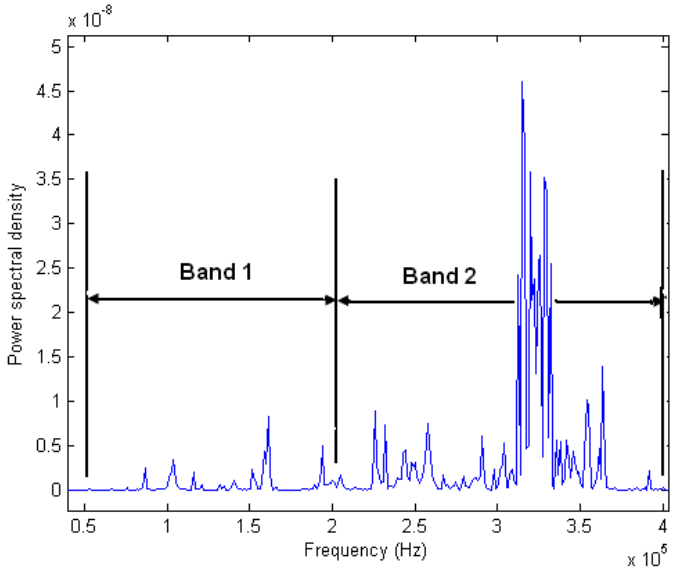

Figure 3.5: Frequency band division

Low frequency: sum of peaks analysis

In order to reveal lower frequencies in the signal a process of demodulated resonance analysis was used. This consisted of analysing the signal in the time domain.

3.3 Apparatus

This section describes the apparatus used in all experiments of this study.

3.3.1 AE system

An Acoustic Emission (AE) system normally consists of sensors, preamplifiers, filters and amplifiers. A schematic AE testing set up is shown in Figure 3.6. Figure 3.7 shows the AE apparatus used in this study.

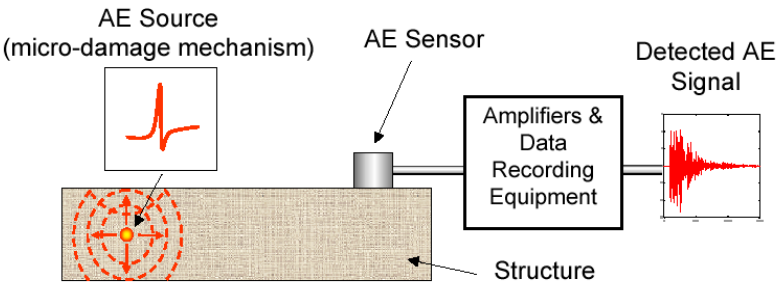

Figure 3.6: A typical AE system setup

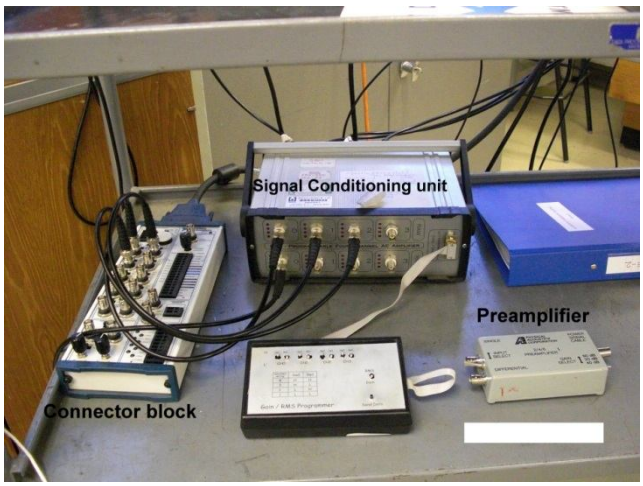

Figure 3.7: Connector block, preamplifier and signal conditioning units

AE sensor and coupling:

Throughout the study, one Physical Acoustics Corporation (PAC, New Jersey, USA) Micro-80D AE sensor was used which was based on Lead Zirconate Titanate (PZT), it had an operating frequency range of 0.1-1MHz and resonances at 325 KHz and 650 KHz. A schematic view of the sensor is shown in Figure 3.8.

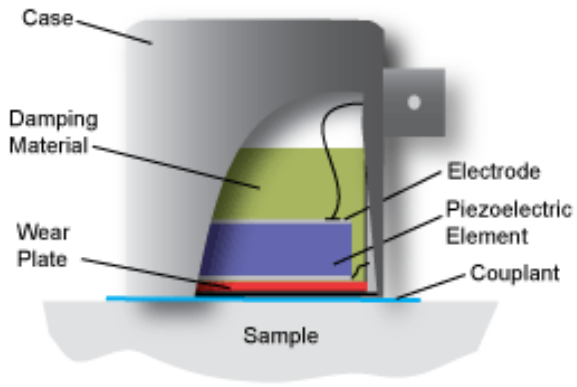

Figure 3.8: Schematic view of AE sensor

The AE sensor converts detected energy waves propagating through the material under examination into a time varying voltage signal. The sensors were 10 mm in diameter and 12 mm high. In order to obtain good coupling between the AE sensor and the specimen, in the *in vitro* experiments the surface of specimen was kept smooth and clean. Silicone grease was used as couplant to fill any gaps caused by

surface roughness and eliminate air which might otherwise have impaired AE transmission. In the *in vivo* experiments GEL-KAM fluoride oral gel (Colgate-Palmolive, UK) was used as the couplant between the AE sensor and the participant's facial skin.

Sensor calibration:

In order to check the consistency and accuracy of the sensors, calibration was performed for four Micro-80D sensors with numbers 93, 115, 127, and 99 at the same time by positioning them on a circular steel block with 38 cm diameter and 20 cm thickness, as shown in Figure 3.9 below. Ten pencil lead breaks were carried out in the centre of the steel block. The sensors were then taken off and remounted four times at the same position with vacuum grease applied, to analyse the effect of remounting the sensors on AE energy. The same procedures were performed with the sensors repositioned in different places around the steel block surface as shown.

AE signals were acquired at 5MHz sampling rate for 125000 points with the preamplifier gain at 40 dB and SCU gain at -12, the energy was calculated by squaring the raw signal and integrating the area after eliminating the noise threshold which was set at 1.5 maximum noise in the first 900 points.

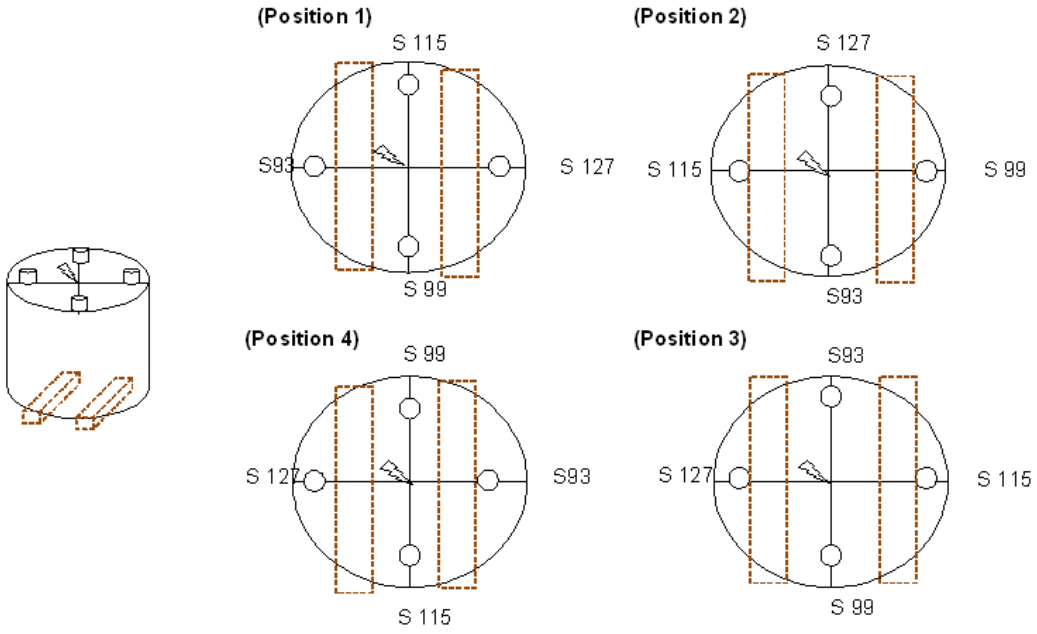

Figure 3.9: AE sensor calibrations

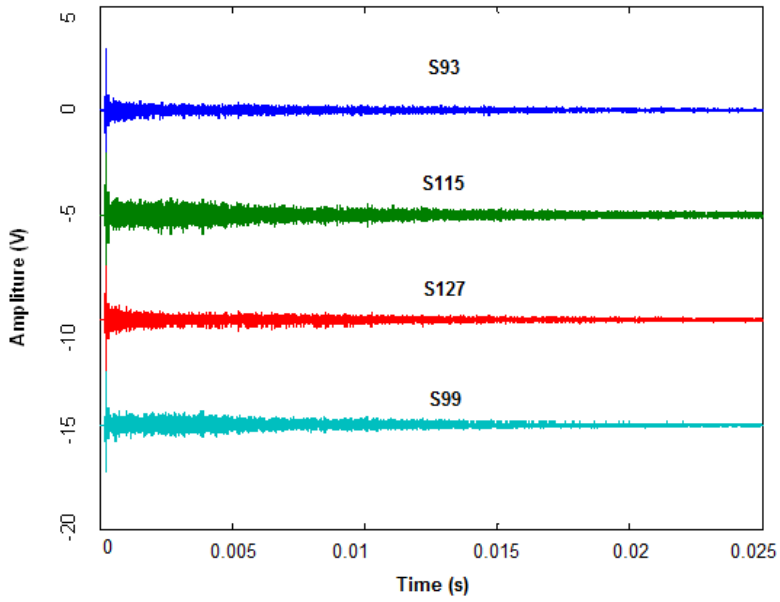

Figure 3.10: Typical raw AE signals within 0.025second for four sensors

Since only sensor number 93 was used throughout this study, the rest of this section shows only calibration results for this sensor. Figures 3.11-3.12 show AE energy distribution over all positions used in this study. The pencil lead was broken fifty times at each position. The calibration certificate for the sensor 93 is shown in Appendix A.

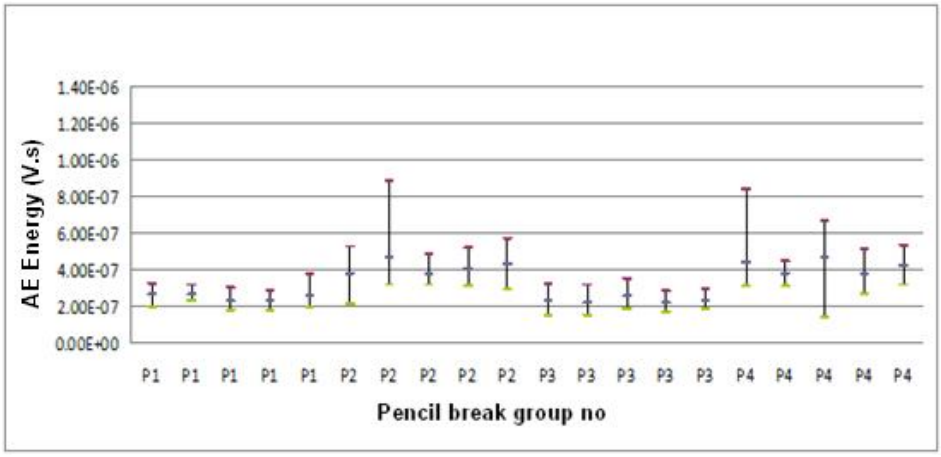

Figure 3.11: AE energy of sensor 93 calibration: AE energy per mounting per position

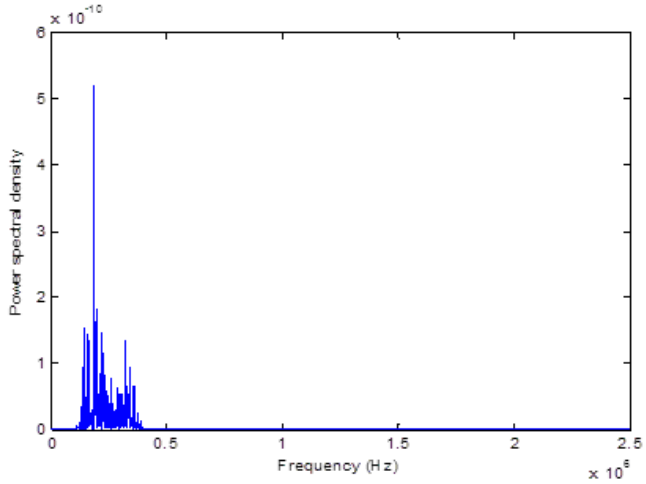
x 10^-10
Power spectral density
Frequency (Hz)
x 10^6

(a)

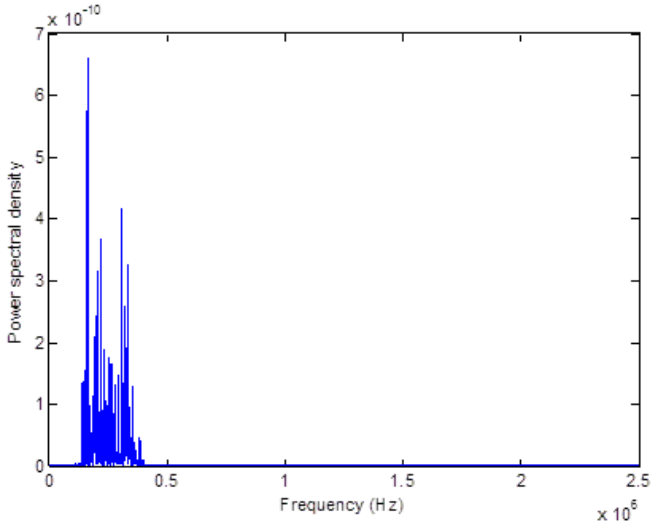
x 10^-10
Power spectral density
Frequency (Hz)
x 10^6

(b)

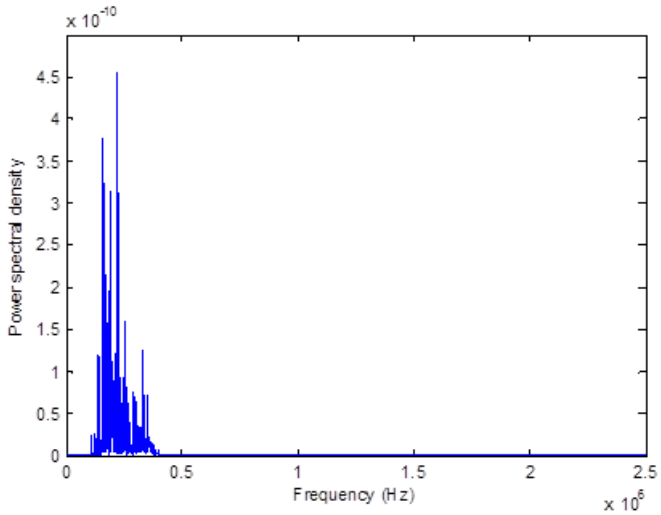
x 10^-10
Power spectral density
Frequency (Hz)
x 10^6

(c)

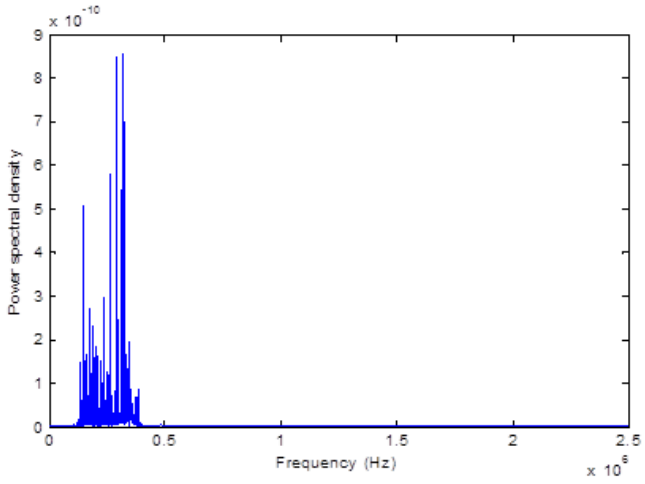

(d)

Figure 3.12: Frequency domains of four positions: (a) Frequency domain at position 1, (b) Frequency domain at position 2, (c) Frequency domain at position 3, (d) Frequency domain at position 4

A systematic investigation was carried out to measure the frequency quantitatively. First, both high and low pass filters were applied to each time domain signal. Then FFT was applied to both filtered signals to determine the frequency spectrum. Secondly, the integral of the high pass filter signal was obtained and divided by the integral of the low pass filter signal. This ratio is plotted for all positions.

Preamplifier:

A preamplifier of type PAC 1220A as shown in Figure 3.13 was used to amplify the AE signals to a level that could be comfortably transmitted by a short length of coaxial cable and converted by an Analogue to Digital Converter (ADC). This had a switchable 40/60 dB gain and internal band-pass filters from 0.1-1 MHz. The preamplifier was powered by a 28 V power supply and used a single connection for both power and signal. All data acquired in this work were in a raw format with the preamplifier gain set at 40dB or 60dB and the units of AE voltage were corrected to 40dB gain.

Figure 3.13: Preamplifier

Data acquisition (DAQ) system:

The experiments in this research centred on acquiring raw AE signals and the DAQ was based on an in-house built desktop PC with a 12 bit, National Instruments (NI), PCI-6115 board as shown in Figure 3.14. This board was used to acquire simultaneously the raw AE signals at 10m samples/second for one channel and employed a full length PCI slot. It was a multifunction analogue, digital and timing device without on-board switches or jumpers so that it could be configured and calibrated by software.

Figure 3.14: AE data acquisition card

The software-programmable gain can be set to 0.2, 0.5, 1, 2, 5, 10 or 50 and covers an input range from ± 200 mV to ± 42 V. The data can be sampled from 20k samples/second up to 10m samples/second at each channel with a total on board memory of 32 MB. The board supports only differential input configurations and has

an over-voltage protection at ± 42 V. For source location applications, it can be used to record raw AE signals (sampled at 5m samples/s) over up to four channels.

Computer software:

A 12 bit, National Instruments (NI), PCI-6115 DAQ board allowed raw AE to be sampled and stored simultaneously over four channels at up to 10M samples/s per channel with a total on board memory of 32MB. LabView126 software from NI was used to prepare programmes to control sampling frequency, input range, pre-trigger data, trigger channel and trigger level (Figure 3.15). MATLAB software was used to process the stored raw data and its Curve Fitting Toolbox was used to apply the moving source model.

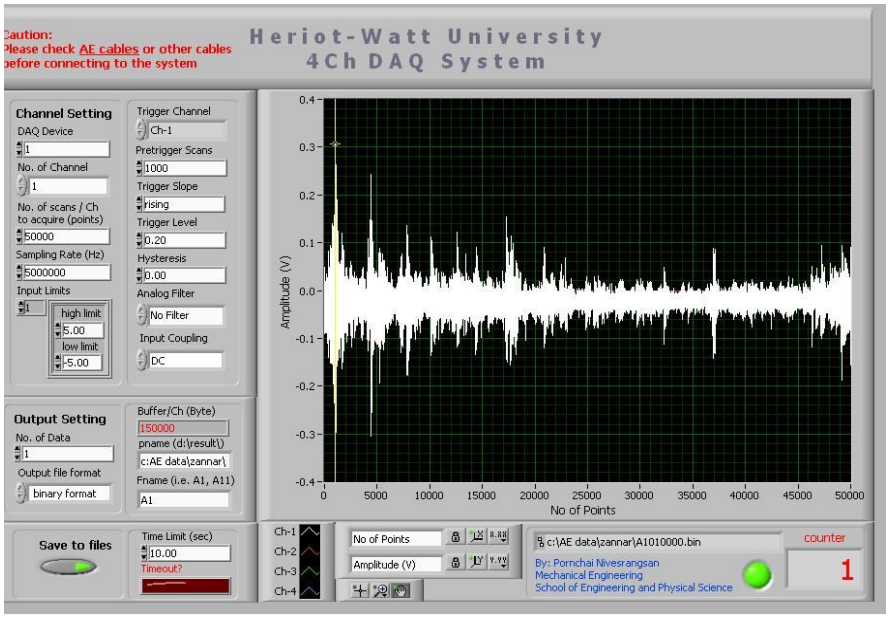

Figure 3.15: LabView front panel for 1-channel DAQ system

3.3.2 Sample collection, preparation and storage

Fresh bovine ribs from different animals (approximately 30 months old) with similar anatomical characteristics were obtained from a butcher's shop. These ribs served as a model of the human edentulous jawbone due to their macroscopic composition of cortical and medullary bone. On receipt, the samples were processed according to a protocol developed by Tricio *et al.* (1995), cleaned of soft tissue residues and

immediately immersed in 50% ethanol/saline solution. The experiments were performed at room temperature (23 ±2˚C) within the first three days of obtaining the ribs. To keep the samples hydrated during the experiments, they were wrapped in saline soaked gauze.

3.3.3 Fabrication of gold abutment

It was necessary to fabricate a customised gold abutment in order to facilitate the application of the Hsu-Neilson source. A cast-to U-Impl (U-Impl Implant System, Aarbergstrasse, Switzerland) was used to fabricate the gold abutment. The wax pattern (Plastodent®-Set, DeguDent GmbH, Germany) was carved to provide a 5mm height and 15mm diameter flat circular surface. The wax was allowed to cool and then smoothed and removed from the implant analogue. The pattern was sprued, mounted on a crucible-former, coated with surface wetting agent (Debubblizer®KERR, USA) and invested in graphite-free, phosphate-bonded investment material (MOLDAVEST®futura, Heraeus Kulzer Laboratory Products Division, Germany) in an X1 casting ring lined with cellulose. The mixing of the investment was under vacuum (Refer, Twister Pro, Germany) and followed the manufacturer's recommendations; for the wax pattern 60g of powder and 13ml special liquid were mixed. The mix was first stirred by hand until the powder was thoroughly wetted, then held under vacuum for 15 seconds before being spatulated under vacuum for further 60 seconds.

The ring was filled with the investment under vibration; 20 minutes after setting, the top of investment was scraped and the casting ring was transferred to a furnace (KaVo burnout furnace, type 5636, Germany) at 700˚C for 30 minutes prior to casting in an induction casting machine (Heraeus Kulzer, Heracast IQ, Germany). The casting was made in type IV yellow gold alloy (Bodent 60, Charles Booth, 49-63 Spencer Street, Birmingham, B18 6DE).

The casting (Figure 3.16) was quenched in cold water before divesting. Final removal of investment was accomplished by air-abrasion with 50µ aluminium oxide powder at a pressure of 5 bar. The sprue was removed using a separating disk and the

gold abutment was finished using brown and pink stones and then polished using a green rubber wheel. The adaptation and accuracy of the fit of the gold abutment were verified on a dental implant.

Figure 3.16: Cast gold abutment

3.3.4 Fabrication of metal clamps for mounting AE sensor

In order to achieve a stable mounting of the AE sensor on the bovine rib, a metal clamp was made from a stainless steel plate of 40mm width, 135mm length and 1mm in thickness. Two windows were cut on each side to enable direct mounting of the AE sensor on the rib and the gold abutment on the dental implants. Two screws and nuts were used to tighten the clamp into position on the bone.

3.3.5 Installation of dental implants in bovine ribs

A total of four holes 15mm apart were prepared in the middle of the bovine ribs using U-Impl surgical kit, as shown in Figure 3.18. The implant site preparation was carried out according to the manufacturer's guidelines as per Figures 3.19 and 3.20. Two sizes of dental implants were used, 8.5mm length × 3.5mm diameter and 13mm

length × 4.5mm diameter. One of each size was screwed into a hole of recommended diameter at the recommended torque of 25 Ncm, Group A (tight-fit); and one of each size being screwed into a pre-tapped hole to a lower torque of 5 Ncm, Group B (loose-fit).

Figure 3.18: U-Impl surgical kit and implant

Implant with 3.5Ø8.5mm length tight-fit condition

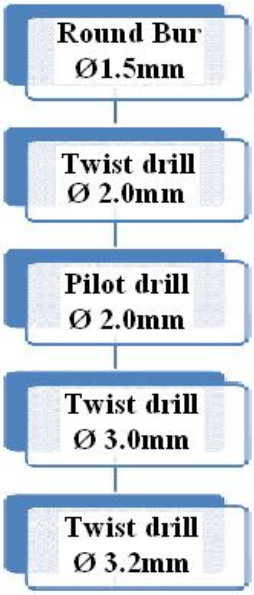

Implant with 3.5Ø8 8.5mm length loose-fit condition

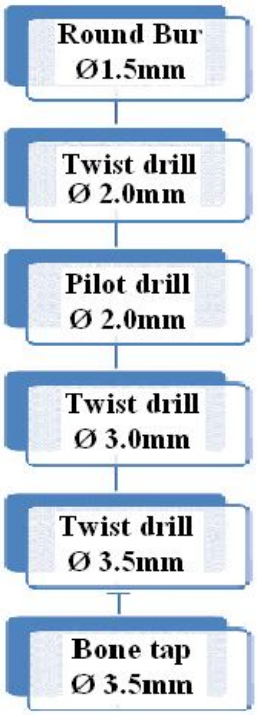

Figure 3.19: Drilling protocol for 3.5 diameter and 8.5mm length implant placement

Implant with 4.5Ø 13mm length tight-fit condition

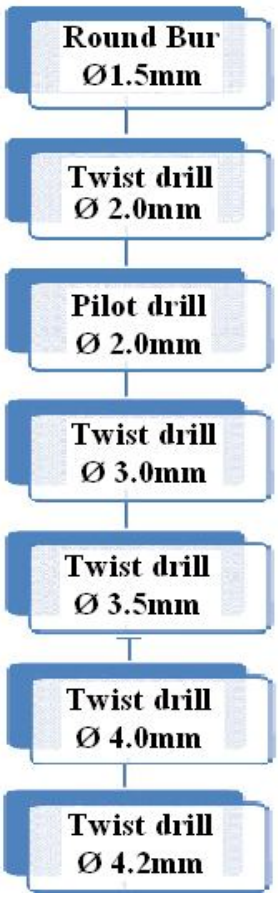

Implant with 4.5Ø 13mm length loose-fit condition

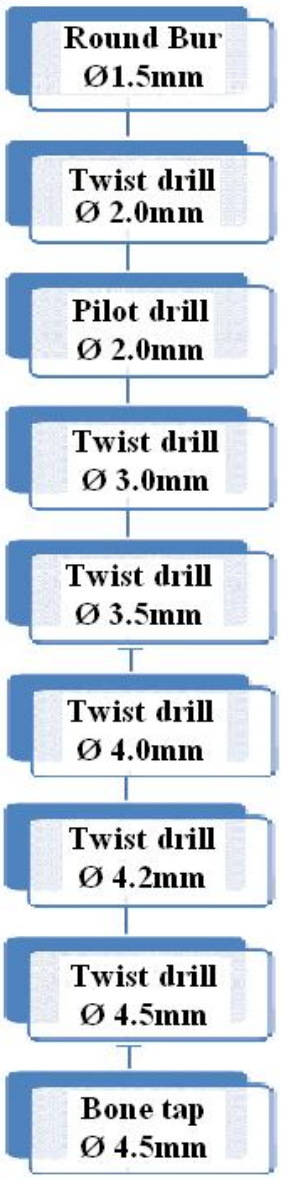

Figure 3.20: Drilling protocol for 4.5 dimension and 13mm length implant placement

Figure 3.21 shows schematically the arrangement of implants in a given bone and Table 3.1 shows a summary of the test conditions.

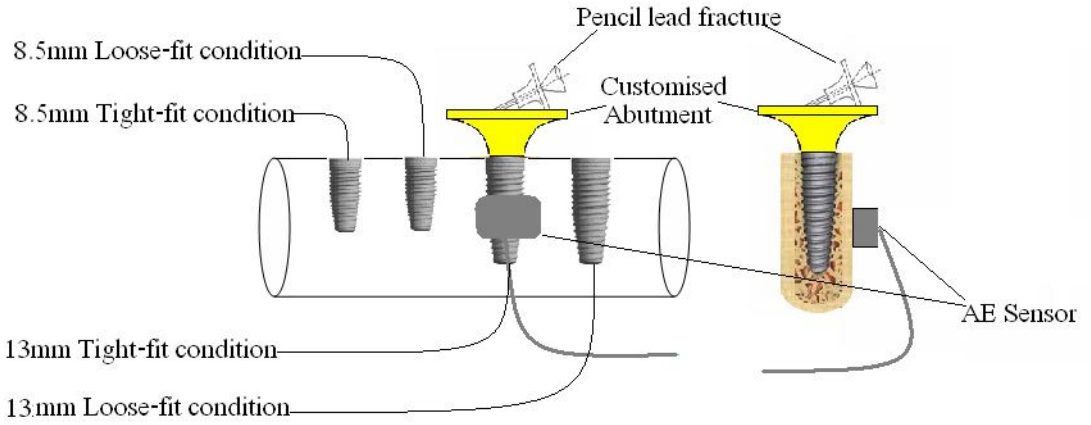

Figure 3.21: Schematic arrangements of implants in bovine bone

Groups	Implant Length mm	Implant Diameter mm	Hole Diameter mm	Number Implants	Insertion Torque N.cm
A	8.5	3.5	3.2	10	20-25
	13	4.5	4.2	10	20-25
B	8.5	3.5	Pre-tapped 3.5	10	2-5
	13	4.5	Pre-tapped 4.5	10	2-5

Table 3.1: Summary of implant conditions

3.3.6 Placement of AE sensors

In the *in vitro* experiments the sensor was held against the specimen test surface using in-house designed magnetic clamps and a customised metal plate as shown in Figure 3.22.

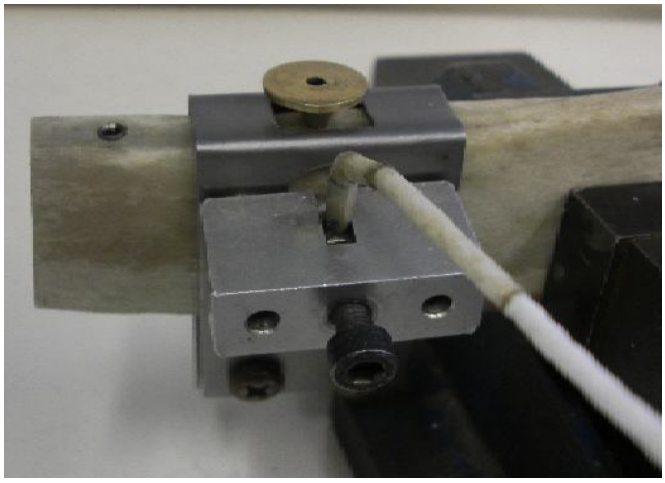

(a)

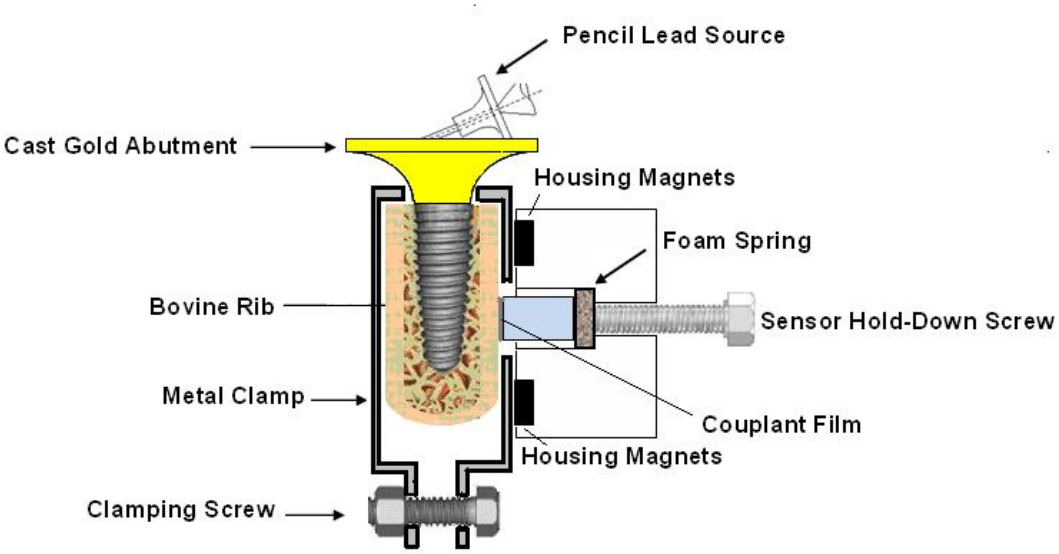

(b)

Figure 3.22: *in vitro* AE sensor placement: (a) AE sensor placement on the specimen tested, (b) Schematic view of AE sensor placement

In the *in vivo* experiment, the AE sensor was placed on subjects' faces in the area of mental foramen between lower 1st and 2nd premolars using a custom designed acrylic housing connected to a pair of patient safety glasses. Sticking plaster was placed over the sensor to secure it in position. The schematic view and clinical picture are shown in Figures 3.23 and 3.24.

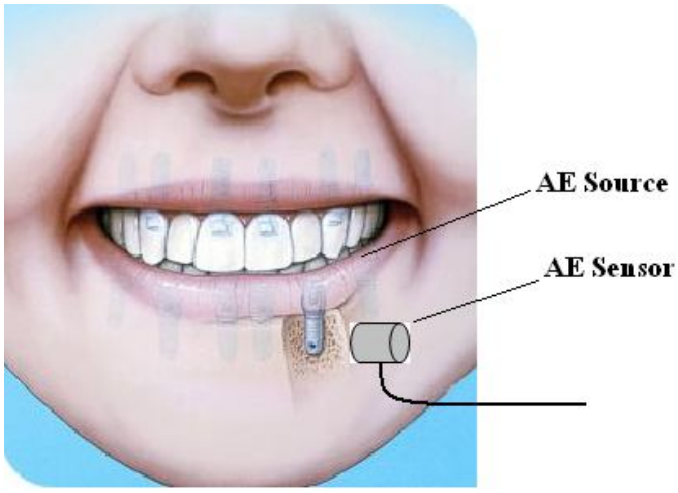

Figure 3.23: Schematic view of extra oral placement of AE sensor

Figure 3.24: Fixation of AE sensor on subject's face

3.3.7 Data collection and storage

Data in the form of AE signals from all experiments were collected and stored in a securely kept laptop computer (kept within Chief Researcher's locked office cupboard). In experiment 3 (*in vivo* study) the reference number connecting this data to an individual research subject recorded on a paper copy was kept locked and the key was in the Chief Researcher's safe within the Edinburgh Dental Institute.

3.3.8 Hsu-Nielson technique

The Hsu-Nielsen Device (HSU *et al.* 1977) is an aid to simulate an Acoustic Emission event using the fracture of a brittle graphite lead in a suitable fitting.

The Hsu-Nielsen source used in this experiment was an artificial source of AE. A mechanical pencil and an in-house machined guide ring (Nivesrangsan 2004) made of Teflon were used to generate simulated AE sources by breaking the 2H pencil lead, the so-called Hsu-Nielsen source. The standard guide ring helped to break the pencil consistently and ASTM standard (E976–99) (ASTM 1999) recommended that the pencil lead should be consistent (0.3 or 0.5 mm diameter, HB or 2H pencil lead) with a length of 2-3 mm. Accordingly, this research used a 2H, 0.5 mm diameter lead with a 3mm length to generate simulated AE sources. A schematic view and the dimensions in mm. of the Hsu-Nielsen source and guide ring were shown in Figures 3.25 and 3.26. As far as could be judged visually, the lead was broken under the

same conditions, in the same position, using the same length and the same orientation of the pencil for all experiments.

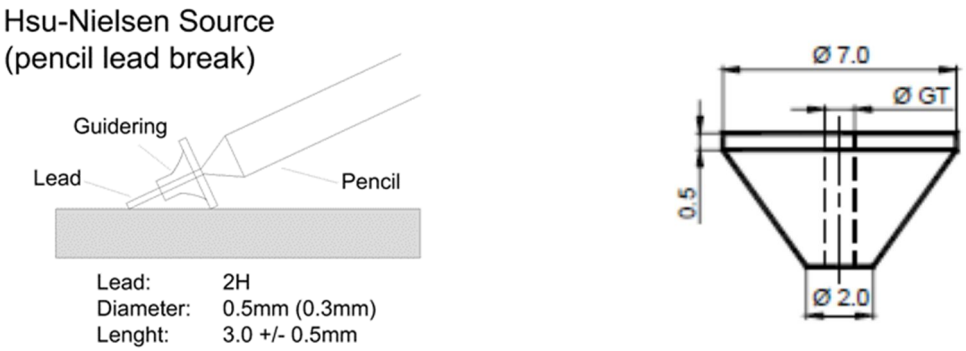

Figure 3.25: Schematic view and dimensions in mm. of Hsu-Nielsen source and guide ring

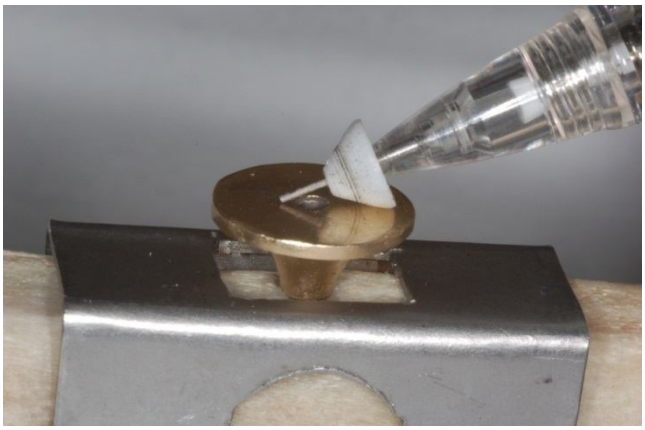

Figure 3.26: Hsu Nielsen simulations on customised gold abutment

The tip of the graphite pencil lead was pressed against the surface of the customised gold abutment until it fractured. This generated an intense acoustic signal, quite similar to a natural AE source that the sensor detected as a strong burst.

3.3.9 Application of water to the bovine ribs

Living bones are supplied with blood under constant pressure and other media such as collagens. Although the laboratory experiments were carried out on bovine ribs covered by a wet towel to maintain the moisture, there was lack of any sort of liquid supplied to the bones, which might have had an impact on the AE signals. Hence this

experiment was designed to maximise the presence of liquid inside the bovine rib by using two customised silicone adaptors constructed of silicone putty (Aquasil, DENTSPLY Caulk, 38 West Clarke Avenue, Milford, DE 19963) which were adapted to each end of the rib. A PVC tube of two metres length and 9mm diameter was secured to one end of the silicone adaptor with metal clamps, whilst the other end of the adaptor was secured to the bone with metal clamps. The PVC tube was attached to a 500ml water bottle filled with water as shown in Figure 3.27. The total depth of water was approximately two metres, which simulated the blood pressure of an average person.

$$\mathbf{P = a + I \times g \times h}$$

P = water pressure

a = atmospheric pressure (ignored in this study)

I = water density at room temperature (1000 kg/m^3)

g = gravitational constant (9.81 m/s^2)

h = water depth (2 m)

P is therefore approximate 19.62 KPa and is equivalent to 2.85 PSI

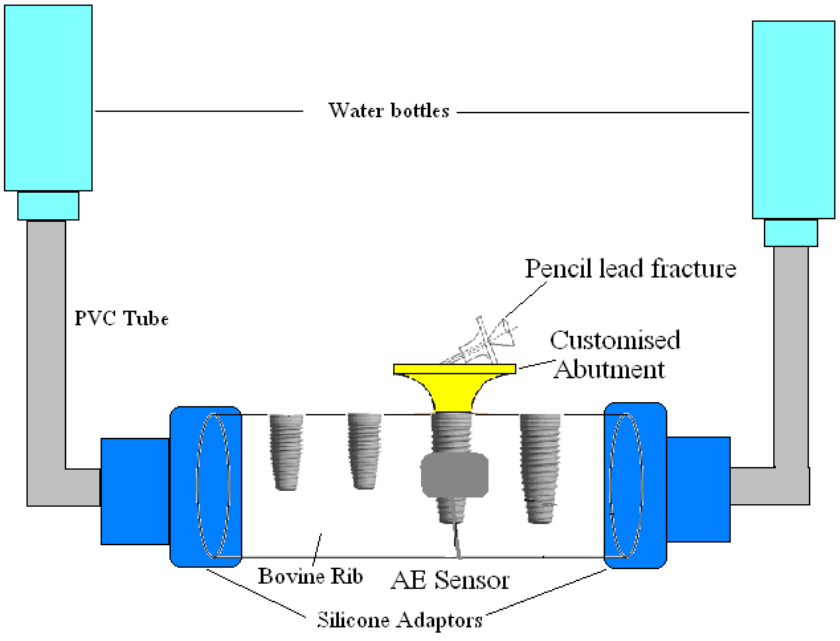

Figure 3.27: Wet bone experimental set up

3.3.10 Development and calibration of air jet technique

Compressed air was investigated as a potential alternative option to the Hsu-Nielson and helium gas jet techniques (Appendix B). It is readily available in all dental surgeries, since dental chairs operate on compressed air at a reasonably constant pressure of approximately 55 PSI. Development and construction of appropriate apparatus are required to allow the assessment of dental implants *in vivo*. In this section, a series of experiments carried out to develop the air jet device.

3.3.10.1 Initial feasibility test with 3-in-1 dental syringe

A basic exploration of the air jet method was performed as per Figure 3.28 showing the schematic set-up using compressed air from the 3-in-1 air-water syringe of a dental chair. The syringe was aimed at a metal plate with dimensions of 60x60x5mm at a distance of approximately 5mm. Ten puffs of air were blown onto the same location of the metal plate, AE data were collected by the AE sensor mounted on the back of the plate. The data were stored and processed as described in Section 3.3.2.

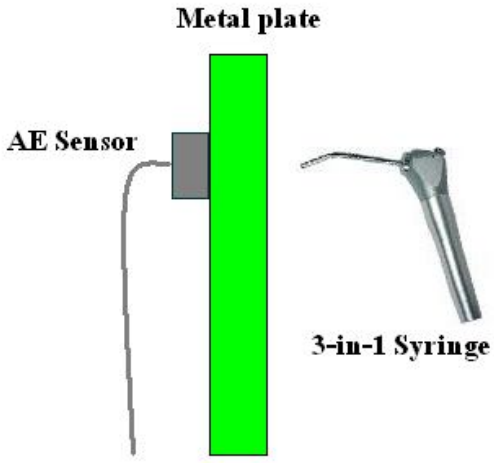

Figure 3.28: Schematic view of 3-in-1 dental syringe with metal plate

Figure 3.29 shows typical continuous AE signals produced by the compressed air released from the 3-in-1 syringe in 0.01 second.

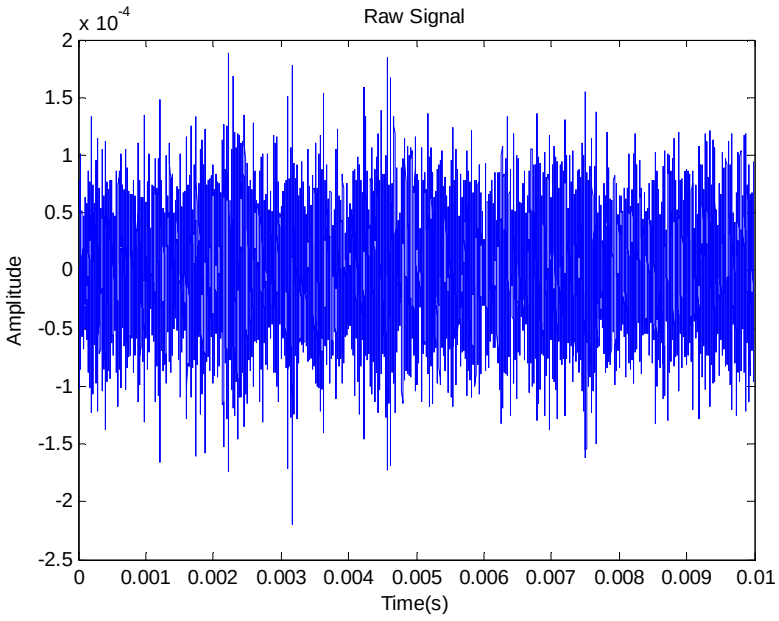

(a)

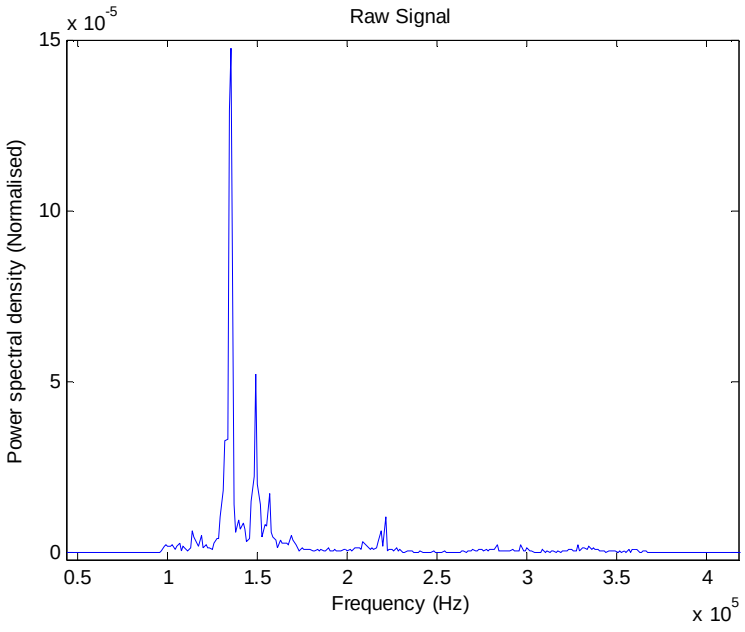

(b)

Figure 3.29: Typical AE signals produced by 3-in-1 dental syringe: (a) time domain, (b) frequency domain

Although AE signals were generated by the 3-in-1 syringe as shown in the figure below, they were not constant with standard deviation of 3.28.

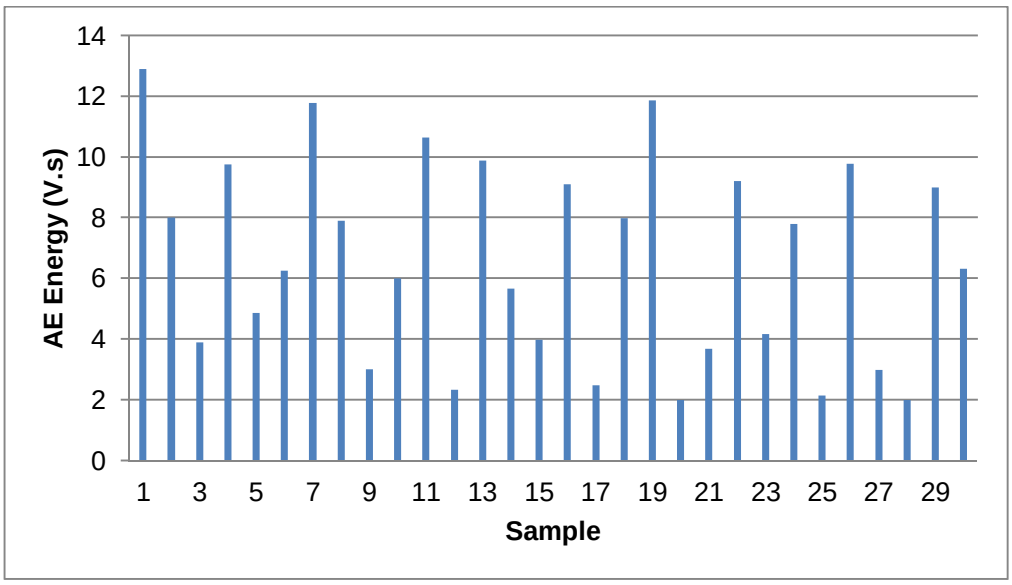

Figure 3.30: AE energy from 3-in-1 dental syringe on the metal plate

The factors that could affect the reproducibility of AE signals were:

a) Stability of the air source: as the syringe was hand-held by the investigator the distance and the position between the tip of 3-in-1 and the metal plate varied between each reading.

b) Air pressure: air pressure in the 3-in-1 syringe was set by the manufacturer, which was approximately 15 PSI. The amount of air released from the 3-in-1 syringe was dependent on the investigator's figure pressure on the release button and the stability of the air pressure produced by the compressor.

To overcome the above issues further investigations and developments took place.

3.3.10.2 Development and fabrication of the air nozzle

The simple feasibility test with the 3-in-1 syringe showed that the air pressure might be a potential non-invasive AE source as an alternative to the pencil lead fracture. The aims and objectives of this experiment are:

1. To stabilise the air nozzle position
2. To evaluate the influence of various diameters of the air nozzle on the production of the AE signals

3. To evaluate the influence of the distance between the air nozzle and the metal plate on the production of the AE signals

The following materials were used this test.

1. Stainless steel orthodontic tubes (K.C. Smith LTD, Hanley works, Cranborne Road, Potters Bar, Herts, EN6 3JL, UK) with different internal diameters (1.5mm, 1.2mm, 1mm, 0.8mm and 0.5mm).
2. Vice
3. Paladur® self curing acrylic resin (Heraeus Kulzer GmbH, Grůner weg 11, 63450 Hanau, Germany)
4. High Vacuum Grease (Dow Corning Corporation, MIDLAND, United States)
5. SDPC Air Regulator Model: FM-30-02-R (SDPC Pneumatic Machinery Co.,Ltd. Fenghua, Ningbo,China)
6. Metal plates 60X60X5mm (Click Metal Ltd, Hampshire, UK)
7. AE system (Heriot-Watt University, Edinburgh, UK)
8. Polyurethane tube (Duncan Rogers Engineering Ltd, Glasgow, UK)
9. Argen "750Y" gold solder (Argen ltd, Hergestellt, USA)
10. Soldering investment (Cendres+Métaux SA, Biel/Bienne, Switzerland)

The same metal plate as in Section 3.3.10.1 was mounted in a vice; orthodontic stainless steel tubes with diameters of 0.5mm, 0.8mm, 1.0mm, 1.2mm and 1.5mm were used to construct the air nozzles. Each of the nozzles was cut into a 20mm length and secured into a polyurethane pneumatic tube with self-curing acrylic orthodontic resin and clamps. The pneumatic tube was connected to the SDPC Air Regulator, which provided a continuous flow of air at constant pressure of 30 PSI. The air nozzles were mounted at right angles to the vice to produce a stable position and distance relative to the metal plate, as seen in Figure 3.31.

Each air nozzle was placed at distances away from the metal plate of 2mm, 4mm and 6mm. The AE sensor was mounted opposite the nozzle on the back of the metal plate with aid of customised magnetic clamps; high vacuum grease couplant was used. A total of ten AE recordings of one-second length data were made using each air nozzle

diameter at each distance. The AE data were transferred to a personal computer and analysed with MatLab software.

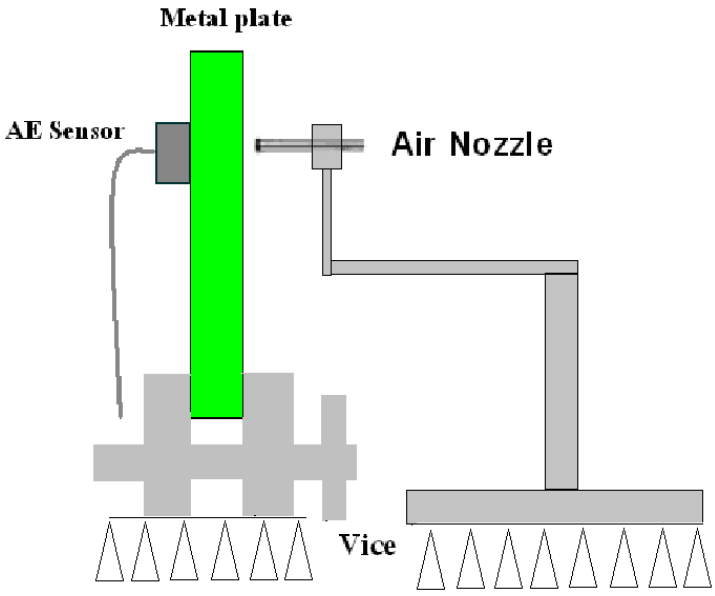

Figure 3.31: Schematic figure of mounting the air nozzle and metal plate in a vice

Figure 3.32 shows the summary of AE energy produced by nozzles with different internal diameters at different distances from the metal plate.

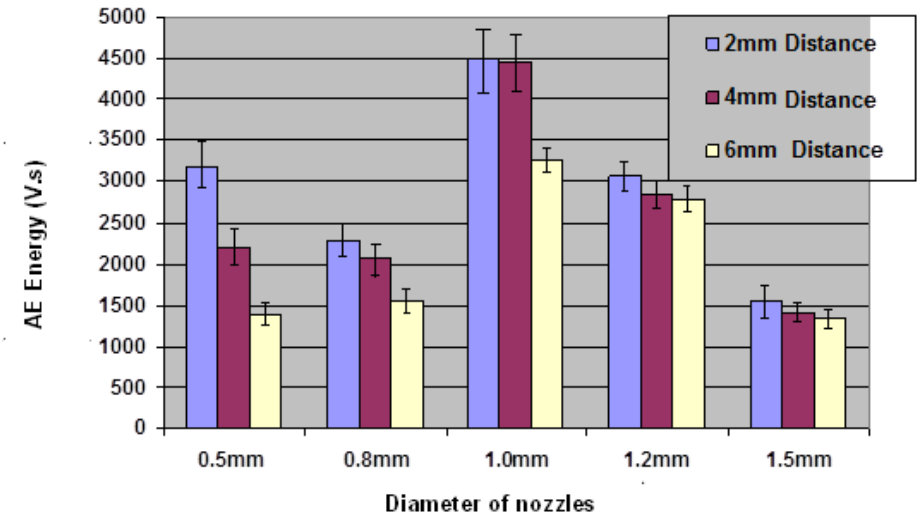

Figure 3.32: AE energy produced by nozzles with different diameters at different distances from the metal plate

Figure 3.33 (a – e) shows the degree of consistency of the AE signals produced with various air nozzle diameters at each distance. The data from air nozzles of 0.5mm, 0.8mm and 1.5mm diameter show that a distance of 2mm produces higher AE energy than a distance of 4mm whilst the 4mm distance produces higher AE energy than 6mm. The data from the air nozzle of 1mm diameter indicate that it produces the highest AE energy and there are marginal differences between distances of 2mm and 4mm.

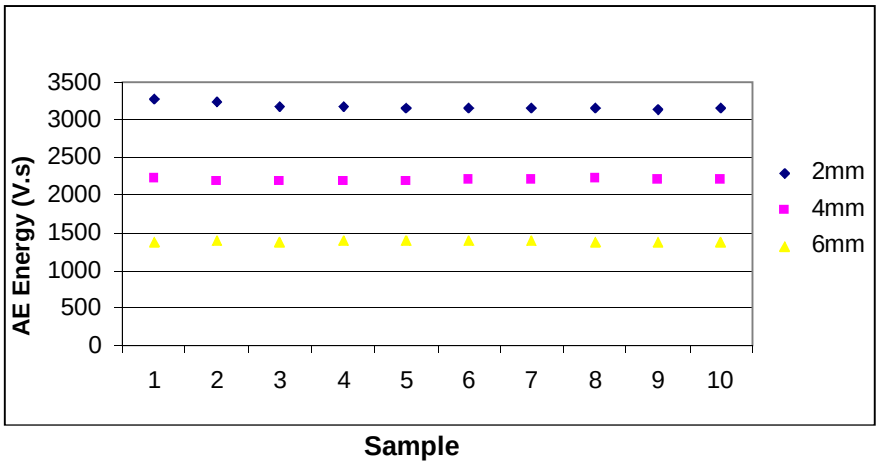

(a)

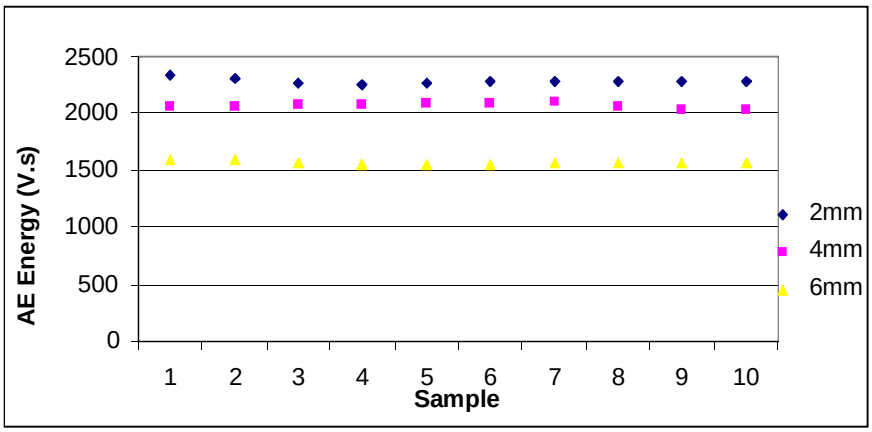

(b)

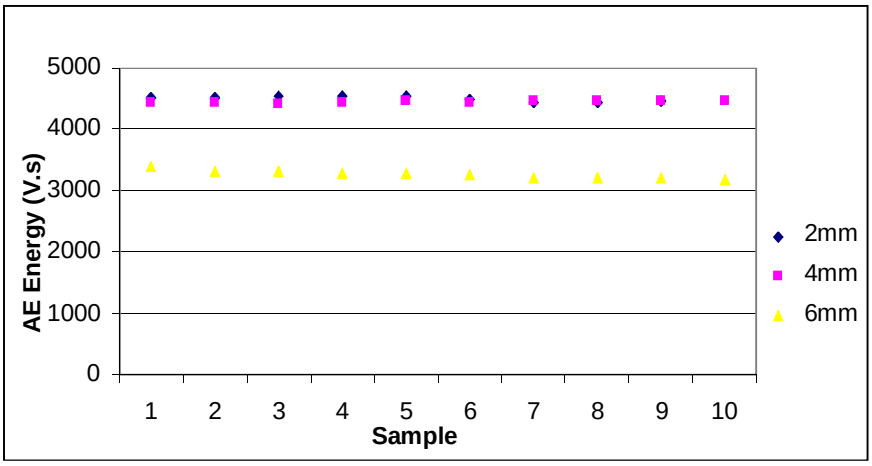

(c)

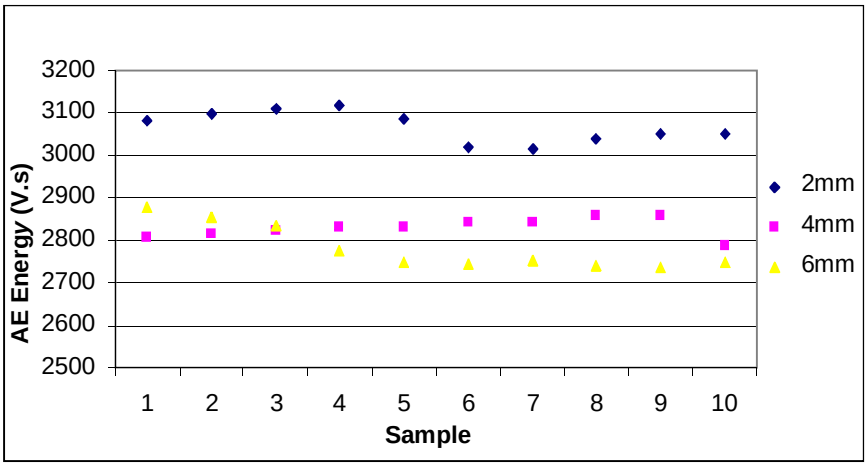

(d)

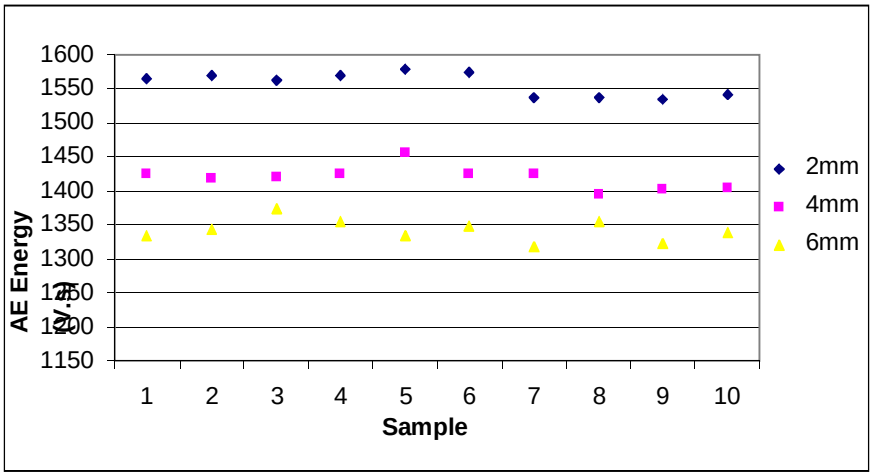

(e)

Figure 3.33: AE energy produced with different nozzle sizes at distances of 2, 4 and 6mm: nozzle diameter of (a) 0.5mm,(b) 0.8mm, (c) 1.0mm, (d) 1,2mm, (e) 1.5mm

The above figures indicate that the optimal nozzle diameter is 1mm and the optimal distance between the nozzle and the metal plate is 2mm.

3.3.10.3 Air pressure experiments on metal plate

Following the establishment of the appropriate parameters for the air jet nozzle, further investigation was required to determine the following:

- Reproducibility of the AE signals with air jet source
- Appropriate air pressure to generate AE signals

This experiment was set up as in Section 3.2.10.2, an air nozzle with 1mm diameter was positioned at right angles and at 2mm distance from the metal plate. The air pressure was controlled by the SDPC Air Regulator at 20, 30, 40, 50 and 60 PSI.

A total of one hundred AE readings of 0.01 second length data was collected. In order to examine the effect of duration of the air jet, the sensor was re-mounted and ten AE readings of 1 second length data were also collected.

Figures 3.34 and 3.35 show 0.01 and 1 second data of AE energy produced at the different air pressures. There is a clear correlation between air pressure and AE energy, with higher air pressures resulting in higher energy.

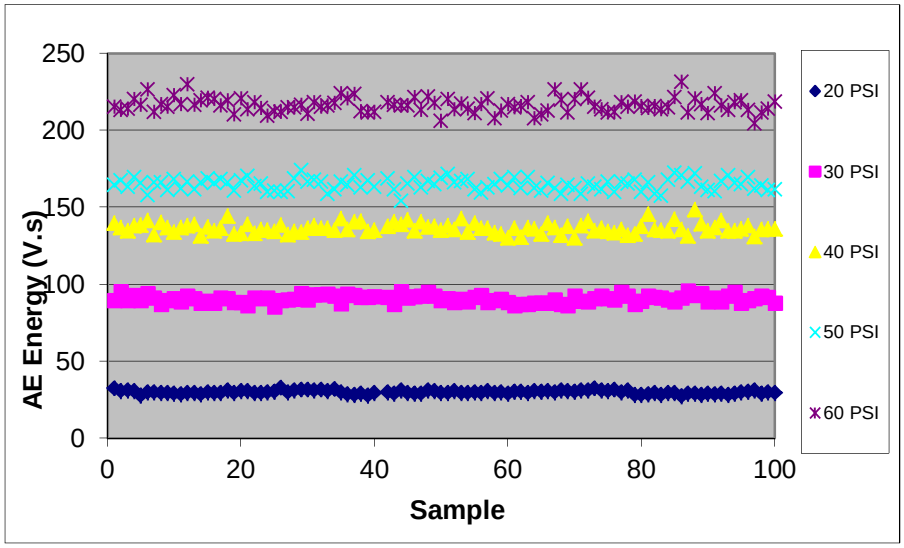

Figure 3.34: AE energy in 0.01 second of air jet on metal plate

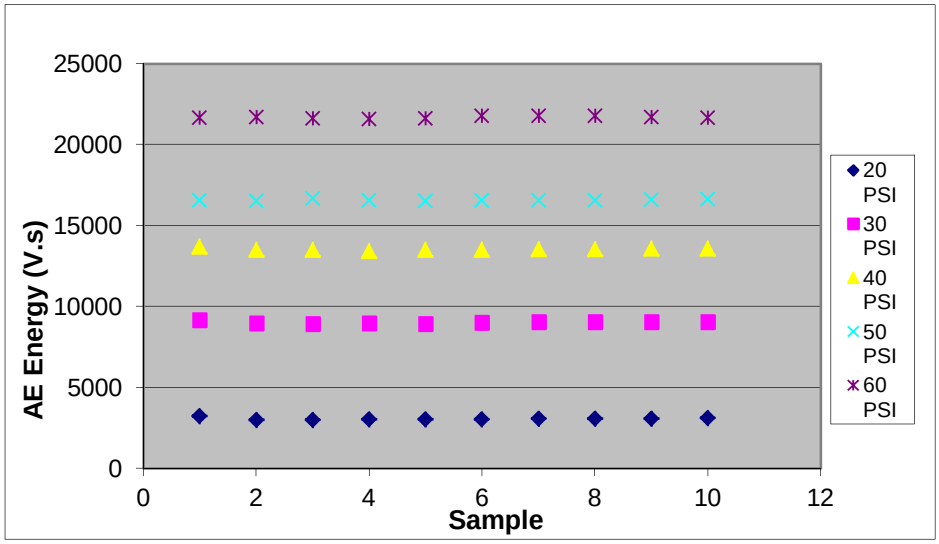

Figure 3.35: AE energy in 1 second of air jet on metal plate

In order to examine the effect of time on the AE energy and compare the 1 second data with the 0.01 second data, each of the 1 second data was split into 100 separate readings of 0.01 second, as shown in Figures 3.36 (a-b).

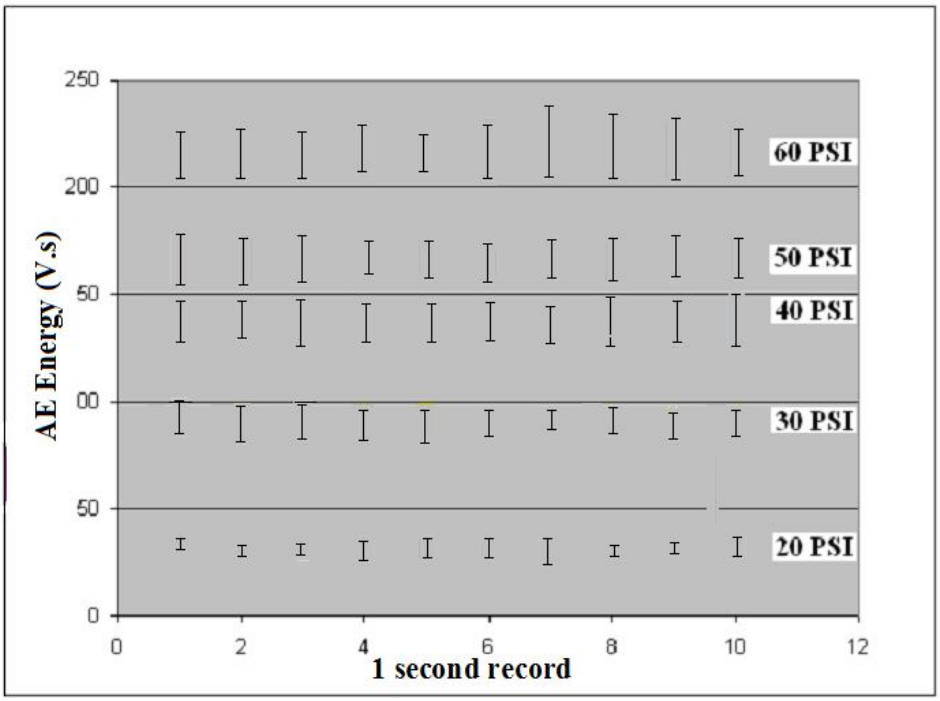

Figure 3.36: AE energy in split-1 second of air jet on metal plate

In addition to analysis of energy, high frequency data were examined by 0.01s and split-1s as shown in Figures 3.37 and 3.38.

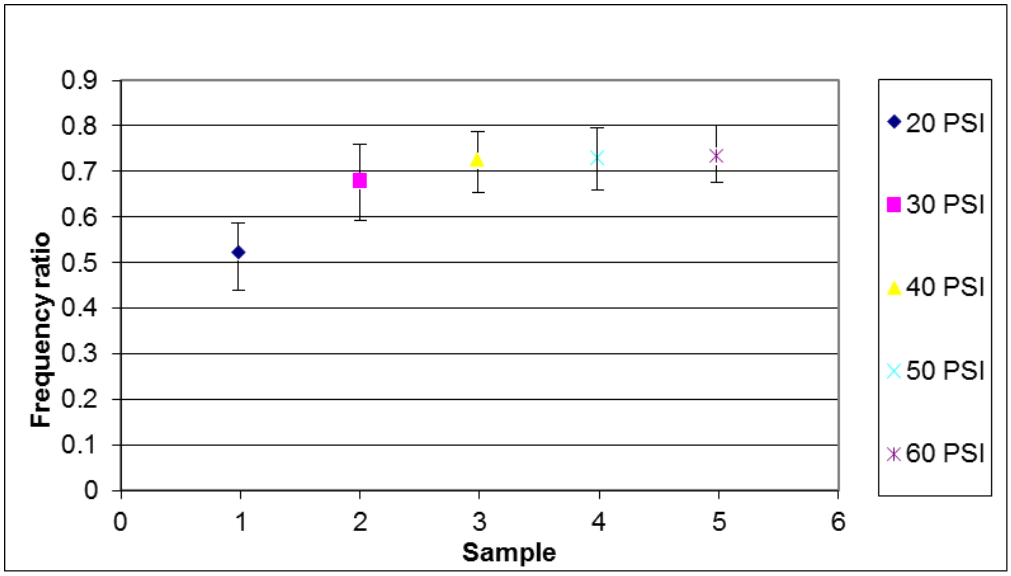

Figure 3.37: Frequency ratio of high frequency band in 0.01 second

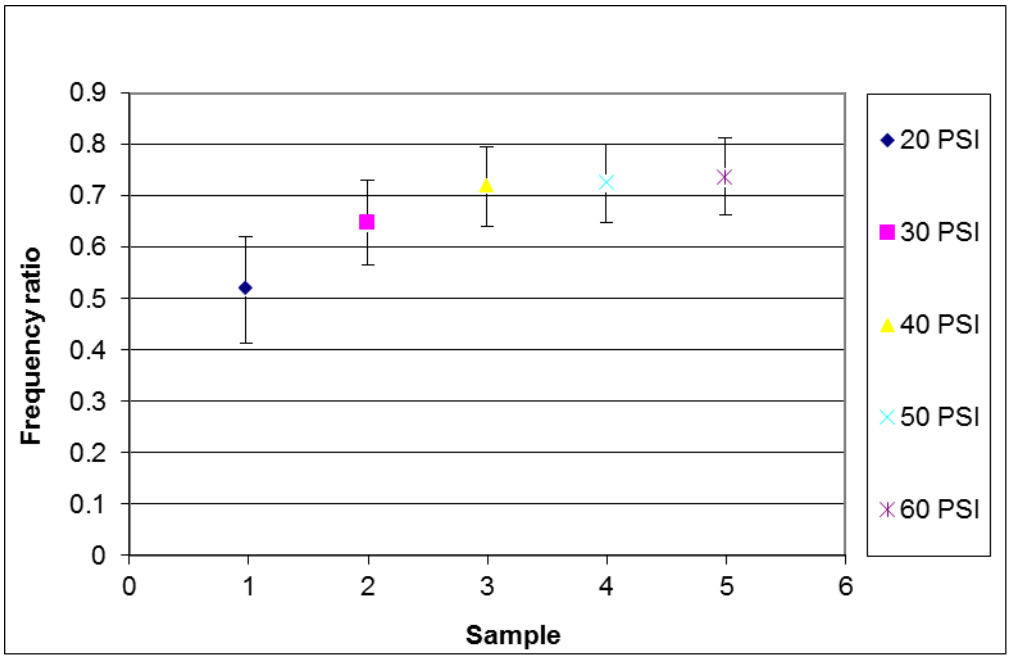

Figure 3.38: Frequency ratio of high frequency band in split-1 second

The means and standard deviations of the frequency ratio under each air pressure (0.01s and split-1s) are summarised in Table 3.2. These indicate that the higher the air pressure, the higher the frequency ratio and the smaller the standard deviation.

	Means		**Standard Deviations**	
	0.01s	**Split-1s**	**0.01s**	**Split-1s**
20PSI	0.505	0.507	0.0266	0.0270
30PSI	0.656	0.647	0.0246	0.0246
40PSI	0.725	0.724	0.0242	0.0207
50PSI	0.730	0.732	0.0193	0.0199
60PSI	0.737	0.737	0.0183	0.0198

Table 3.2: Means and standard deviations of frequency ratio of all air pressures in 0.01 second and split-1 second

ANOVA shows that there is no significant difference between the two sets of data since p-value is 0.98544, i.e. there is no significant time effect.

Following from the observations in Figure 3.37 and 3.38, the frequency structures of the transmitted air jet signals for both 0.01 and 1 second data (ten records were randomly selected from each air pressure group) were further analysed, by averaging the signals with a range of averaging times.

For the 0.01 second data, the frequencies lower than the filter cut-off of 50 kHz were revealed, by a technique known as demodulated resonance analysis. Two different averaging times were used to reveal frequencies in the mid-range (up to 50 kHz) and in the low range (up to 10 kHz). The resulting spectra were complex and, to simplify the analysis, each of the ranges was divided into bands and the heights of the significant spectral peaks within that band were added together as an indicator of the energy in the band. Figure 3.39 (a) shows the sum of peaks of 0.01 second data in the five frequency bands used for the mid-frequency range and, as can be seen, between 40 and 50% of the energy is in the band below 10 kHz. Figure 3.39 (b) shows a further breakdown of the low frequency range (below 10 kHz), between 35 and 45% of the energy is in the band below 2 kHz. Despite this clear frequency structure, there

seems to be little in these lower frequency bands to distinguish between the various air pressures. However, 20 PSI shows the highest energy level.

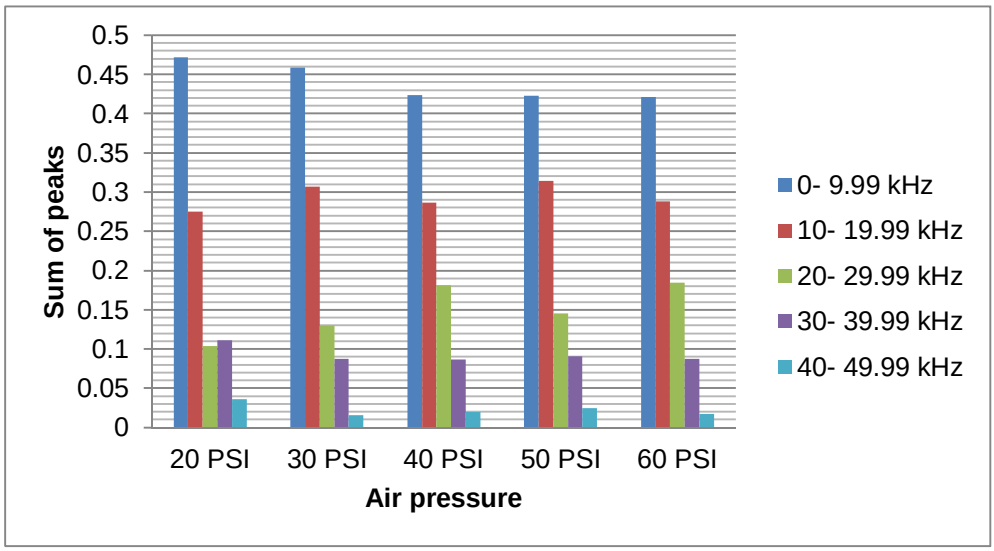

(a)

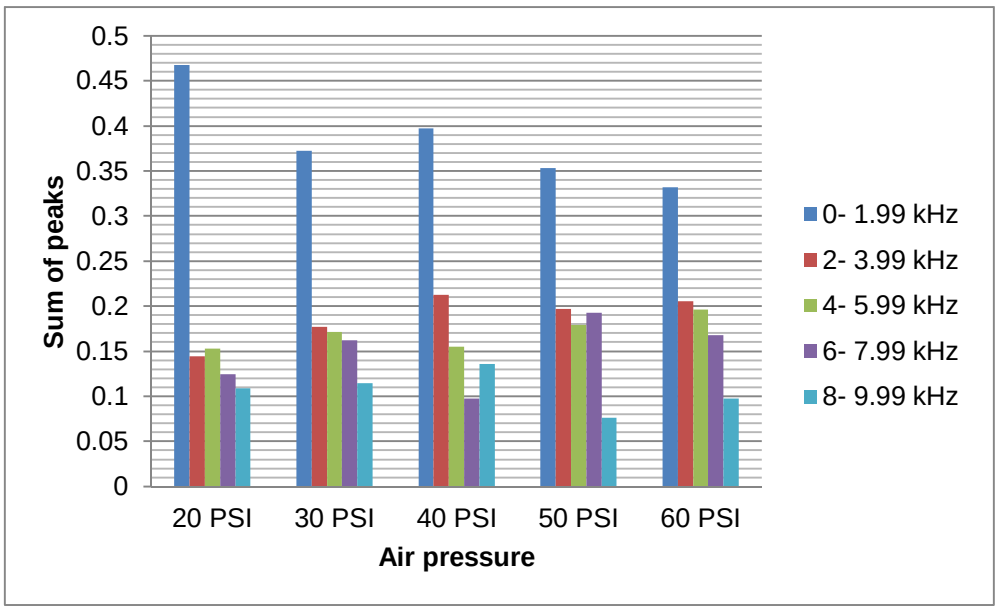

(b)

Figure 3.39: Demodulated analysis of transmitted air jet signal: (a) mid-range frequency bands 0 – 49.99 kHz, (b) low frequency bands 0 – 9.99 kHz (bar heights are cumulative over 10 – 20 records)

The data are regrouped by frequency band, ANOVA analysis was carried out to compare the signals between air pressures. The P-values are shown in Table 3.3 below; they are higher than 5% confidence level (except frequency bands 20 – 29.99 kHz). The sum of peaks cannot discriminate between the air pressures.

Med-range frequency bands					
	0 – 9.99 kHz	10 – 19.99 kHz	20 – 29.99 kHz	30 – 39.99 kHz	40 – 49.99 kHz
P-values	0.877162	0.647861	0.041222	0.87624	0.761828
Low frequency bands					
	0 – 1.99 kHz	2 – 3.99 kHz	4 – 5.99 kHz	6 – 7.99 kHz	8 – 9.99 kHz
P-values	0.702071	0.49747	0.821264	0.237451	0.627952

Table 3.3: Summary of ANOVA for sum of peaks of air jet on metal plate (0.01 second)

For the 1 second data, the demodulated resonance analysis revealed frequencies lower that the filter cut-off of 500 kHz. Two different averaging times were used to reveal frequencies in the mid-range (up to 500 kHz) and in the low range (up to 100 kHz). Each of the ranges was divided into bands and the heights of the significant spectral peaks within that band were added together as an indicator of the energy in the band. Figure 3.40 (a) shows the sum of peaks of 1 second data in the five frequency bands used for the mid-frequency range and between 30 and 45% of the energy is in the band below 100 kHz. Figure 3.40 (b) shows a further breakdown of the low frequency range (below 100 kHz), the energy is unevenly spread across the five frequency bands. The lower frequency bands 0 – 99.99 kHz show that the highest energy is observed in 20 PSI, and there is a slight decrease in energy with increase in the air pressure.

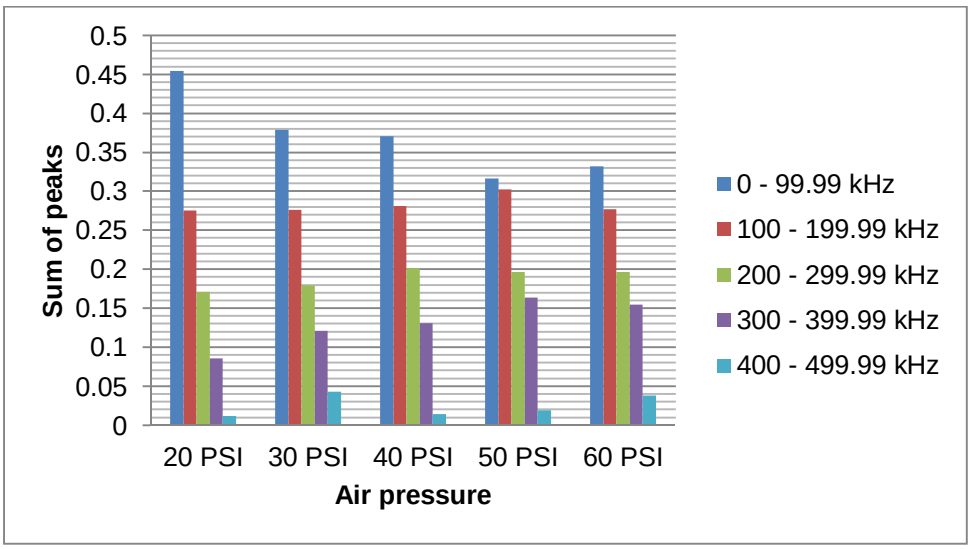

(a)

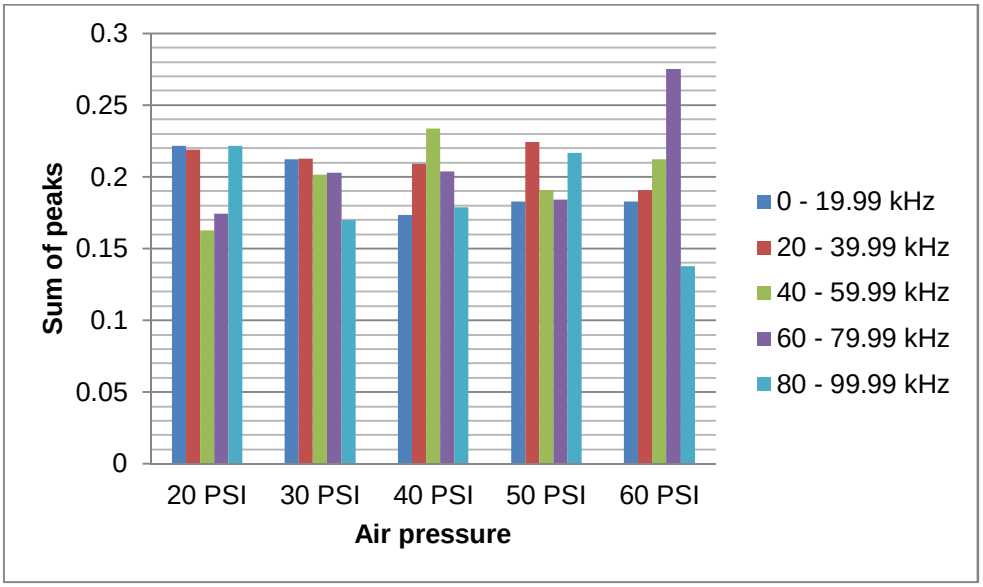

(b)

Figure 3.40: Demodulated analysis of transmitted air jet signal: (a) mid-range frequency bands 0 – 499.99 kHz, (b) low frequency bands 0 – 19.99 kHz. (Bar heights are cumulative over 10 – 20 records)

The 1 second data are regrouped by frequency bands the same as 0.01 data. The P-values in Table 3.4 show that sum of peaks is unable to discriminate between different air pressures.

Med-range frequency bands					
	0 – 9.99 kHz	10 – 19.99 kHz	20 – 29.99 kHz	30 – 39.99 kHz	40 – 49.99 kHz

P-values	0.036307	0.295643	0.399532	0.001686	0.582642
Low frequency bands					
	0 – 1.99 kHz	2 – 3.99 kHz	4 – 5.99 kHz	6 – 7.99 kHz	8 – 9.99 kHz
P-values	0.118886	0.53045	0.284073	0.236168	0.034084

Table 3.4: Summary of ANOVA for sum of peaks of air jet on metal plate (1 second)

This experiment was conducted to evaluate the effects of air pressure on the AE signals and determine the appropriate air pressure for the investigations to follow. Air pressures of 20, 30, 40, 50 and 60 PSI were applied as they were within the range of pressures used in dental units.

The AE energy data from both 0.01 and 1 second sampling show that the air jet source is reproducible at all air pressures, evidenced by the R^2 values of the AE energy linear functions as discussed earlier. They are summarised in Table 3.5.

	20PSI	**30PSI**	**40PSI**	**50PSI**	**60PSI**
R^2 0.01s	0.0294	0.0004	0.0035	0.0025	0.0087
R^2 Split-1s	0.0066	0.0107	0.0005	0.0342	0.1763

Table 3.5: R^2 of AE energy in 0.01s and split-1s

	20PSI	**30PSI**	**40PSI**	**50PSI**	**60PSI**
STDEV 0.01s	1.060085	2.376206	3.371578	3.835096	4.742258
STDEV Split-1s	1.083393	2.259998	3.163123	3.415112	4.540562

Table 3.6: STDEV of AE energy in 0.01s and split-1s

The standard deviations increase with increase in air pressure, it means that lower air pressure generate more consistent energy. Although 20PSI shows the lowest standard deviation, it also produces the lowest amount of AE energy; it is considered that low energy levels may not have been suitable for *in vitro* studies.

Frequency ratio analysis also indicates the reproducibility of AE signal; higher values for air pressure produce higher frequency ratios and greater consistency.

In order to generate sufficient AE signals without compromising the reproducibility, the medium range of air pressure of 30-40PSI is found to be the most appropriate.

3.3.11 Fabrication of air jet device

Following the establishment of the key features of an air jet source, e.g. the appropriate air nozzle diameters and the distance between the nozzle and the specimen, it was necessary to construct a device to accommodate the implant abutment and the nozzle housing. A cast-to U-Impl (U-Impl Implant System, Aarbergstrasse, Switzerland) abutment was used to fabricate the gold abutment for this study, and a wax pattern was constructed around it (Plastodent®-Set, DeguDent GmbH, Germany). The wax patterns were carved to provide a tube-shape of 7mm height and 4mm diameter. Carving wax and orthodontic stainless steel of 1mm tube were used to construct the housing for the nozzle (Figure 3.41 and Figure 3.42). Both parts were sprued separately, invested and a casting was made in Type IV gold as described in the Section 3.3.3. Locating grooves and dots were carved on the housing nozzle and the implant abutment. Both parts of the air jet device were positioned and mounting in soldering investment (Cendres+Métaux SA, Biel/Bienne, Switzerland) and soldered together using gold solder (Argen ltd, Hergestellt, USA). The device was then finished and polished as described in Section 3.3.3.

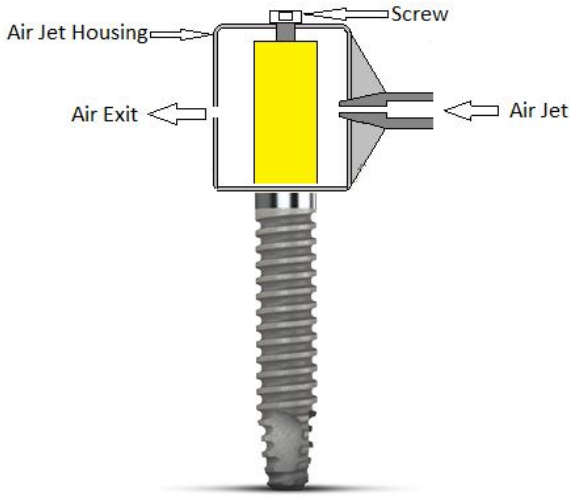

Figure 3.41: Air jet device fixed on implant

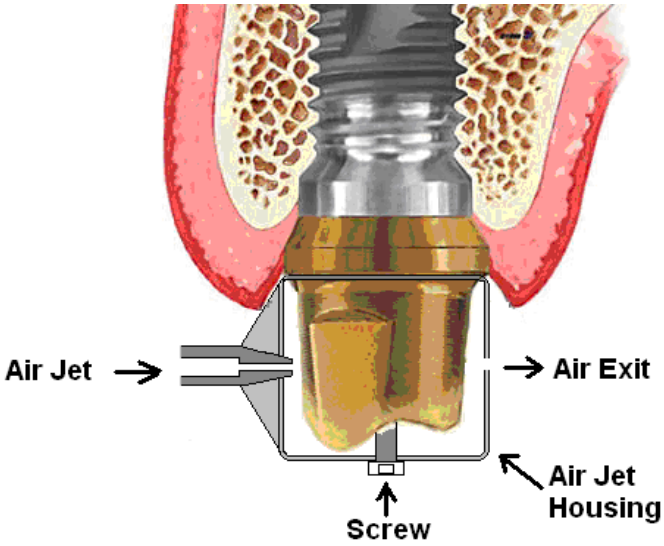

Figure 3.42: Schematic view of air jet source

3.4. Experimental procedures

This section describes the procedures of all experiments in this study.

3.4.1 Initial feasibility: *in vivo* transmission of AE

The objective of this experiment is to assess the transmission of AE signals from the oral cavity to the skin of the face, by biting on various types of food with an AE

sensor mounted on the face. Almonds, peanuts and carrots were selected for this experiment; they were purchased from a Lidl food store.

1. Almonds: one can of 150g Alesto Californian roasted and salted almonds (Alestro, Harmsen & Utescher, Germany) as shown in Figure 3.43(a).
2. Peanuts: one bag of 150g Alesto Californian roasted and salted peanuts (Alesto, Harmsen & Utescher, Germany) as shown in Figure 3.43(b).
3. Carrots: one 1 kg bag of raw Oaklands Scottish Carrots (Scottish Borders, Scotland) as shown in Figure 3.43(c). The carrots were cleaned and chopped into thirty 1cm cubes.

(a)

(b)

(c)

Figure 3.43: Food used in initial feasibility test: (a) almonds, (b) peanuts, (c) carrots

The test was performed by the investigator using himself as the subject. He had a complete natural dentition with four small and medium size restorations (amalgam and composite). There was no history of orthodontic treatment, jaw injuries, nor of medication that could have affected mastication or salivation. There was mild tooth surface loss affecting the maxillary anterior teeth.

Different anatomical areas such as the skin overlying the zygoma, temporomandibular joint (TMJ) and body of the mandible at the area of mental foramen were investigated for optimal position for placement of the AE sensor as shown in Figure 3.44. These positions were chosen because they had minimum soft tissue between the bone and the sensor.

Fixation and stabilisation of the sensor were essential for reproducible readings. Sticky plaster was proposed to stabilise it and a coupling agent (GEL-KAM FluoriGard, Colgate-Palmolive Manufacturing (UK) LtD, Surrey, UK) was used to ensure intimate contact with the skin, as shown in Figure 3.45.

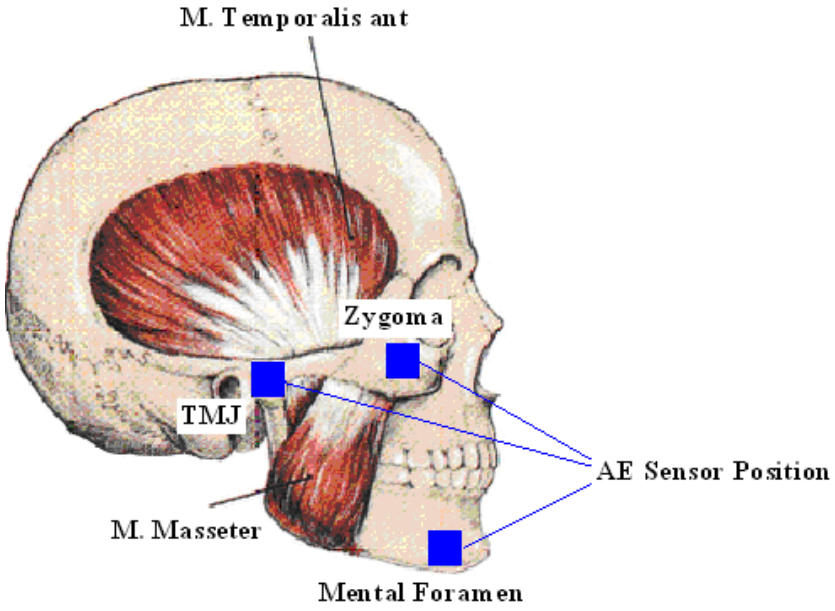

Figure 3.44: Schematic illustration of AE sensor positioning

Figure 3.45: Extra-oral placement of AE sensor using sticky plaster

A single bite of one piece of each type of food was made between the molars with the sensor mounted on the same side. A total of fifteen AE recordings were made from each mounting position for each of the three types of food.

3.4.2 Transmission tests on dental materials and bones

The aim of these experiments is to assess any differences in transmission between various dental materials and bovine rib bones with various degrees of hydration. The first test is to assess the surface propagation on various synthetic materials compared with fresh bovine rib bone. The second test is a transmission tests on fresh bones and dried bones each with implants with various degrees of fixity.

3.4.3 Surface transmission on synthetic materials and bone

The limitation of the *in vitro* experiments is the difficulty in reproducing the osseo-integration between the implant and the bone. Therefore basic transmission tests were carried out to search for a medium between implant/bone interfaces to replicate the osseo-integration *in vitro.* Materials with various structure and density were used, such as dental plaster of Paris (MIC Global (UK) Limited), acrylic orthodontic resin (Heraeus, Heraeus Holding GmbH, Heraeusstraße 12-14, D-63450 Hanau, Germany), glass ionomer cement (3M, Maplewood, Minnesota) and dental stone type IV.

An impression of a fresh bovine rib with dimensions of 12x2x4 cm^3 was made using silicone putty (Aquasil, DENTSPLY Caulk, 38 West Clarke Avenue, Milford, DE 19963) and replicas of the bone were made of the materials described above. An AE sensor was fixed on one side of the materials, and the Hsu Neilson source was applied on the materials at distances of 30mm, 40mm, 50mm and 60mm from the sensor, as shown in Figure 3.46.

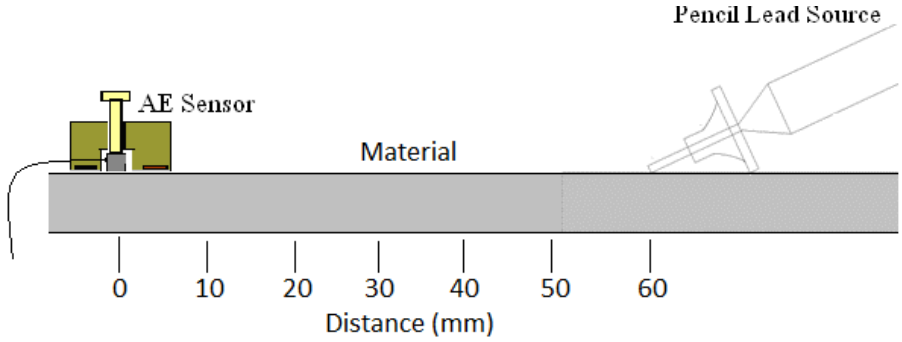

Figure 3.46: Materials testing set up

3.4.4 Effect of hydration of the bone on transmission

The aim of these experiments is to study the effect of moisture level on the transmission of AE signals. The first stage is to examine the effect of continuous drying of the bone on the transmission of AE signals. Four bone-level U-Impl titanium dental implants were placed in a fresh bovine rib as per Section 3.3.5 and the AE sensor was placed as per Section 3.3.6. The Hsu-Nielson source was applied as described in Section 3.3.8, data were collected and stored as per Section 3.3.7. Then the bone was subjected to 100˚C for 6 days in Humboldt furnace oven (Humboldt Scientific, Inc. 551-D Pylon Drive, Raleigh, NC 27606-1487). The first test was performed when the bone was fresh, and it was repeated every 24-hour. In each test, a total of sixty AE recordings was made for each implant at the coronal edge of the customised abutment which was retained on the implant by an implant abutment screw tightened to 15 N.cm.

The second set of tests was to apply water through the bones as described in Section 3.3.9, to examine the effect on the AE transmission when the moisture level is high.

3.4.5 Use of standard source to test interface

This test was conducted to determine whether difference in implant sizes and degree of contact with bone could be detected using a standard AE source. Forty bone-level U-Impl titanium dental implants were placed in the ten fresh bovine ribs as per Section 3.3.5. The Hsu-Nielsen source was applied to produce AE signals as per Section 3.3.8. The signals were collected by a sensor mounted on the side of the rib as described in Section 3.3.6. A total of thirty AE recordings was made for each implant at the coronal edge of the customised abutment (Section 3.3.3) which was retained on the implant by an implant abutment screw tightened to a torque of 15 N.cm. Data were stored and analysed as in Section 3.3.7.

3.4.6 *In vitro* monitoring of interface using the air jet source

The aim of this experiment is to assess the feasibility of using an air jet source to replace the pencil lead break for assessing the implant interface. Forty bone-level U-

Impl titanium dental implants were placed in the ten fresh bovine ribs as per Section 3.3.5. The custom made air jet source was applied to produce AE signals as per Section 3.3.11. The signals were collected by a sensor mounted on the side of the rib as described in Section 3.3.6. A total of thirty AE recordings was made for each implant with 30 PSI air pressure. Data were stored and analysed as per Section 3.3.7.

3.4.7 Deployability of the air jet source *in vivo*

This was an initial experiment to apply the newly developed air jet source on selected participants, with the aims of identifying:

1. Whether AE transmission was feasible from an implant to the skin surface
2. Characteristics of the AE signals to assess the variability between participants
3. The correlation between the AE signals and the implant sizes
4. Any other variables

Ethical approval for this experiment was granted by the NHS Lothian Research & Development Department, Queen's Medical Research Institute (Project Number: 2010/R/DEN/01), on 07th October 2010. The certificate is shown in Appendix C. The participants had received Astra Tech dental implants, therefore Astra Tech provided cast-to abutments as a form of grant to conduct the study, PO Box 14, SE-431 21 Molndal, Sweden (Reference: D-2010-029), in order to facilitate the experiments.

Patients who had received dental implant treatment at the Edinburgh Dental Institute were included in this experiment: Patients who had their implants for number of years and where treatment was considered to be successful were selected for the following reasons:

1. The healing period was completed;
2. The outcome of implant therapy was known as the implants had been in function for some years;
3. Our intervention would not affect the osseo-integration;
4. The test would be more acceptable to this group of patients

These patients were divided into four groups according to the type of restoration on those implants:

Group 1 - Single implant retaining a single crown

Group 2 - Two or more implants retaining a bridge

Group 3 - Two mandibular implants retaining a mandibular complete removable prosthesis

Group 4 - Four mandibular or maxillary dental implants retaining a maxillary or mandibular complete removable prosthesis

Group 3 patients were selected to participate in this experiment for the following reasons.

1. The implants were well integrated and the risk of damaging them or their osseo-integration was small
2. There were no crowns or bridges attached to the implants, usually the implants were located in the area of the mandibular canines and were at least 20mm apart
3. The implants were located in the anterior area of the mandible giving relatively easy access to mount the air nozzle on the implant
4. The implants were usually restored by a ball attachment or locator abutment which could be easily removed and replaced without damaging the restorations or implants
5. Availability of this type of patient was high as it was a common treatment option to stabilise a complete mandibular denture.

45 participants of Group 3 patients (49-72 years old) were present on the Edinburgh Dental Institute database. Only five participants were able to attend, the rest were either unwell or had difficulty with mobility. Informed consent was obtained from each participant. The dimensions of implants of the five participants are shown in Table 3.7.

Participants Initials	**1**	**2**	**3**	**4**	**5**
Length (mm)	15.00	11.00	9.00	9.00	9.00
Diameter (mm)	4.00	3.50	3.50	3.50	3.50

Table 3.7: Participants' information

The tests were performed in the Restorative Dentistry Department of the Edinburgh Dental Institute, with the participants sitting upright in a dental chair. The denture and only one ball attachment abutment were removed first, and the air jet housing was directly mounted on the dental implant and secured with the standard abutment screw at a torque of 15Ncm. The air was supplied to the air jet device from the dental chair through tubing connected to the air regulator as shown in the schematic view in Figure 3.47.

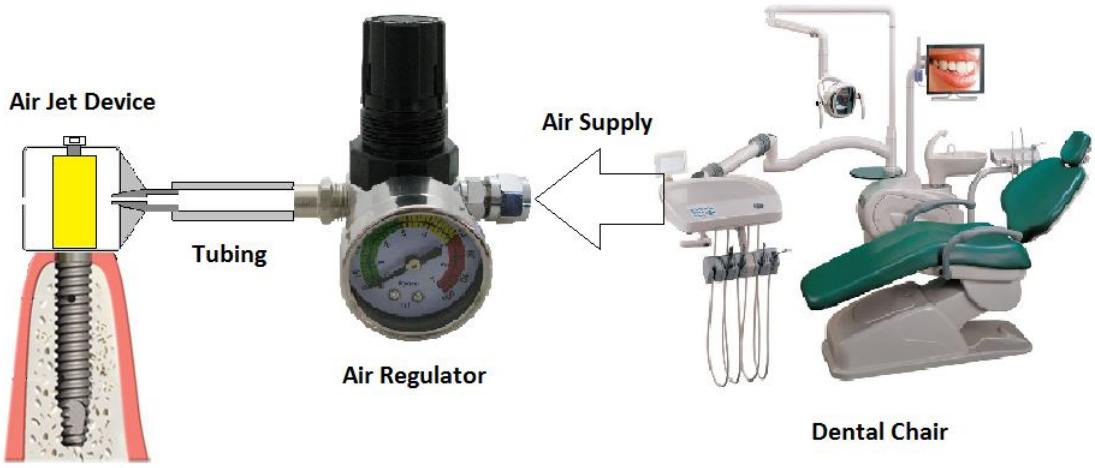

Figure 3.47: *In vivo* experimental setup

The AE sensor was mounted on the participant's face by the mounting device (Figure 3.24), Fluoragard Acquas gel was used as a couplant agent (Section 3.3.6). A continuous flow of compressed air of 30 PSI was released from the dental unit, 30 AE signals each of 1 second length of time were collected, and the air supply was then switched off. The AE sensor was re-mounted, and the same test was carried out with another 30 AE signals collected. The data were stored and analysed following the method described in Section 3.3.7.

Chapter 4

EXPERIMENTAL RESULTS, ANALYSIS AND DISCUSSION

This chapter presents, analyses and interprets the results of all of the experiments, with emphasis on the main systematic tests which investigate the influence of bone/implant interface on AE transmission.

First, general observations are made from the basic transmission test on a living subject with an AE sensor mounted on the face. The second series of experiments were focused on the degree of transmission of AE over various dental materials compared with fresh bovine ribs and also through-transmission (via implants) for bovine ribs in various states of hydration. The third and fourth sets of tests studied systematically the characteristics of AE signals transmitted through bone-implant interfaces, first using a standard source of AE and then using the specially-developed air jet source. Finally, the *in vivo* study focused on the deployment of the new AE source, specifically on the effect of patient-related and uncontrolled variation on AE transmission.

4.1 Analysis techniques

In all experiments, the raw AE signals were acquired at a sampling rate of 5 MHz for two fixed periods of 1 second and 0.01 second (5 million and 50000 points respectively), the longer periods being used to assess the consistency of the continuous (air jet) source.

All records were subjected to a similar analysis approach. The simplest analysis consisted of determining the total energy of the raw AE, essentially by adding the absolute values of each of the five million or 50,000 points in each record. The resulting value is a relative energy in V.s and allows comparison between records of the same length assuming that the input energy (e.g. from breaking a pencil lead or a given time length of the air jet) is the same for all records. One disadvantage of this measure is that it is not absolutely calibrated, since the measured voltage depends on the sensor sensitivity and the amplifier gain, and so a second measure was also used

for raw AE. This consisted of casting the signal into the frequency domain, essentially producing a spectrum of signal. By inspection, it was decided that the spectrum could be divided into two bands, from 0.1-0.2 MHz and from 0.2-0.4 MHz. the ratio of the energy (the sum of the spectral points) in the high frequency band to the low frequency band provided an indication which is absolutely calibrated, since the ratio removes energy calibration. Other frequency domain processing was applied to the longer records (air jet) and this is described later.

4.2 Initial feasibility: *in vivo* transmission of AE

In this experiment, the AE signals generated from biting on various types of food in the oral cavity were examined. Also, data was collected with the sensor placed in various locations on the face to determine if AE is transmitted sufficiently and also to find out if there was a preferable mounting location for the sensor. Figure 4.1 (a – c) shows typical raw AE signals in the time domain captured from the area of the mental foramen from biting on the three types of food. It can be seen that biting on almond produced higher amplitude over a shorter period of time.

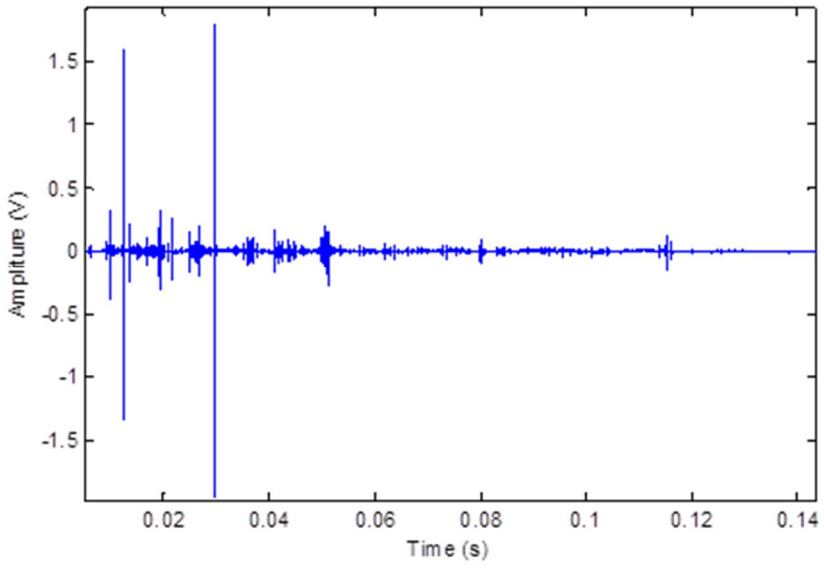

(a)

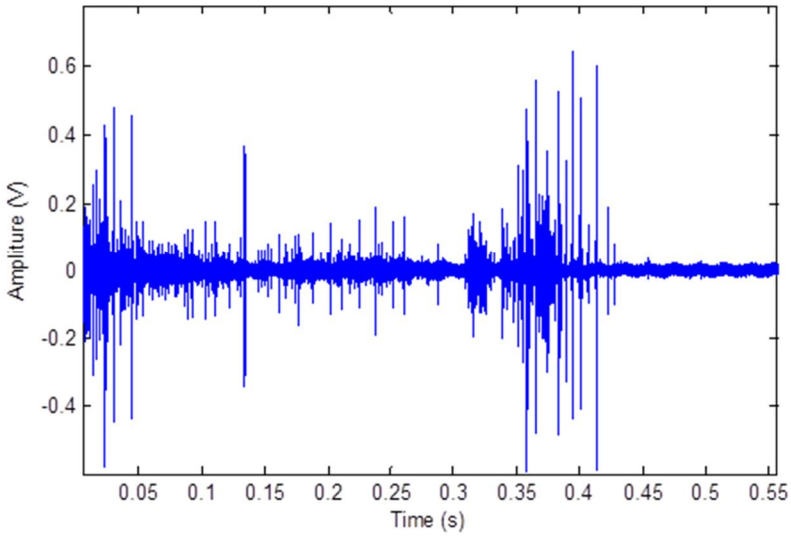

(b)

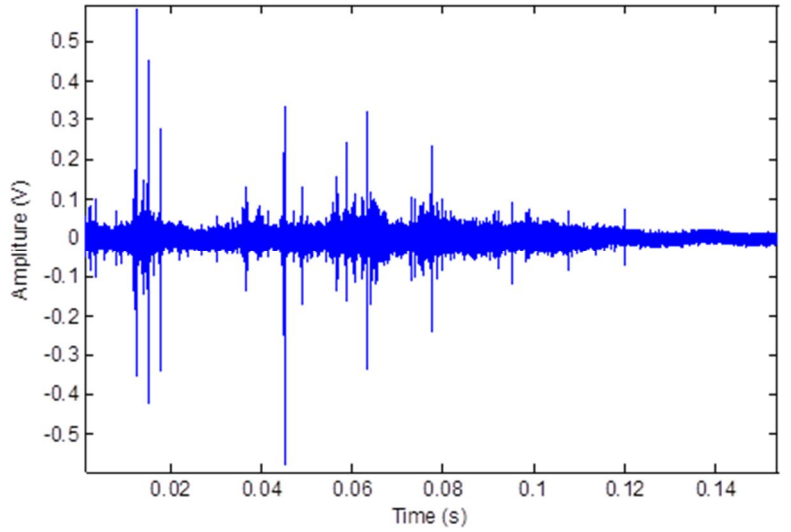

(c)

Figure 4.1: Typical AE signal structure (amplitude and frequency) acquired with sensor positioned in the area of mental foramen and biting three types of food: (a) almond, (b) carrot, (c) peanut

Figures 4.2 summarises the AE energy produced by the three types of food collected from the three locations on the face (the detailed figures are shown in Appendix D). The energy produced by biting on almonds is the highest of the three food types. Also, the energy transmitted through the mandible in the area of the mental foramen was the highest compared with the sensor being positioned on the skin over the zygoma bone or the temporo-mandibular joint.

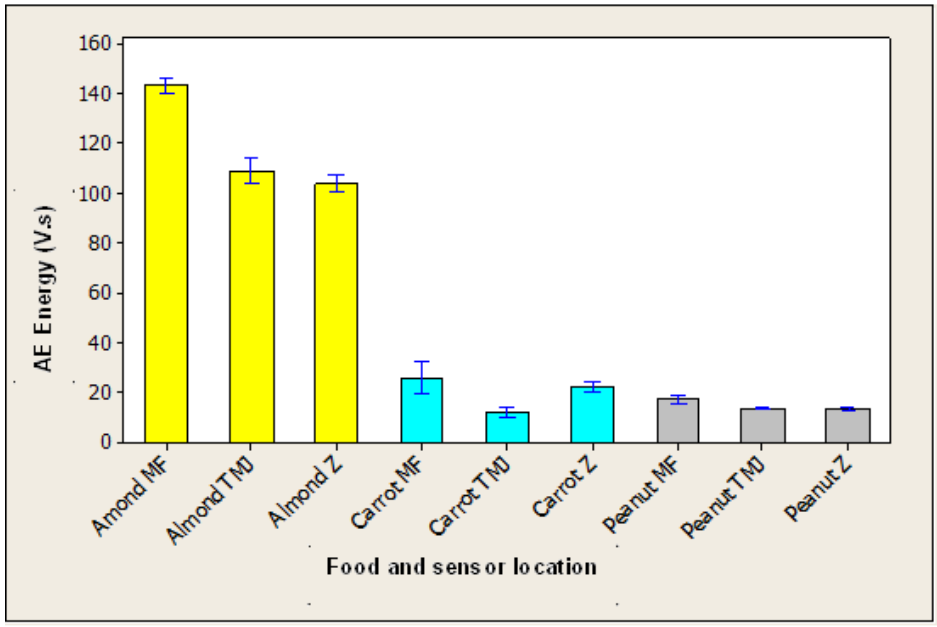

Figure 4.2: AE energy produced by biting on different foods collected from different AE sensor positions; mental foramen (MF), tempro-mandibular joint(TMJ) and zygomatic bone (Z)

First, and most importantly, the above results demonstrated that AE could be transmitted from the masticating surface to a sensor mounted on the face of a living subject, essentially through "normal" tissue. The variation in transmitted energy was largest for carrot, and smallest for peanut, an observation that suggests that this variation is more attributable to the source than to the transmission (including sensor coupling). For almond, the variation was about 10% of the transmitted energy, whereas it was almost 50% for carrot. Together, these two observations are of considerable importance since they suggest that transmission paths on a given real subject vary by no more than 10%, even when the sensor is removed and replaced.

Mounting the AE sensor in the area of the mental foramen was found to be more stable than the other locations. The results also demonstrated that AE transmission was better to this location, which was closest to the source. It is unclear which of the other two locations shows the better transmission. Unknown as the source intensity is, those tests are the first to assess AE transmission *in vivo*. The only published *in vivo* work that could be found on ultrasound transmission in the jaw was in the assessment of jaw bone quality using ultrasonic wave speed (at 1.25MHz) (Klein *et al.* 2008). However, whereas ultrasonic wave speed could discriminate bone quality,

it was not a strong indicator, showing about a 15% variation between subjects with osteoporosis from “healthy” subjects, against an individual variation of around 5% and a variation in the healthy sub-collective of about 50%. The transmission tests on the dental materials and the bone-implant systems (and, indeed in all of the tests in the current work) used a mechanical source, so it was not possible to use ultrasonic speed measurements as the time of injection of the pulse is not recorded. However, it was possible to determine the degree of attenuation of the source, on the assumption that the source intensity is fixed.

4.3 Transmission tests on dental materials and bones

The primary aim of these experiments was to assess any differences in transmission between various dental materials and bovine rib bones with various degrees of hydration. First the results of the tests for surface propagation on various synthetic materials compared with fresh bovine rib bone will be presented followed by the through-transmission tests on fresh bones and dried bones each with implants with various degrees of fixity.

4.3.1 Surface transmission on synthetic materials and bone

In these tests, the transmitted energy was measured as a function of the distance in order to obtain values of the effective material damping, which can usually be expressed by an exponential absorption law: $E = E_0 e^{-kx}$.

where E_0 is the effective source energy (energy at $x = 0$), E is the energy at a distance x from the source, and k is the attenuation coefficient, characterisation of the material.

In order to determine k, the exponential absorption law can be re-written:

$$\ln E = \ln E_0 - kx$$

So that a plot of $\ln E$ vs. x should yield at straight line of slope $-k$ and with a common intercept for all the materials. The resulting plots are shown in Figure 4.3, where it can be seen that the attenuation follows the exponential law reasonable closely given the relatively long extrapolation (60mm), the relatively short observation distance

(30mm) and the scatter of the results. The apparent values of k vary between the materials, being greatest for the glass ionomer cement and least for the stone. The fresh bone behaved slightly anomalously in that its apparent attenuation coefficient was between bone and plaster, although the transmitted energy in the 30 – 60mm experimental range was lowest of all the materials tested and closest to the glass ionomer cement. This anomaly may be attributable to the experimental scatter, although it is more likely that the injection of AE energy into the bone from the pencil lead break was less efficient than for the drier, synthetic materials. It might be noted, however, that the indicative values of E_0 also vary considerably between the materials.

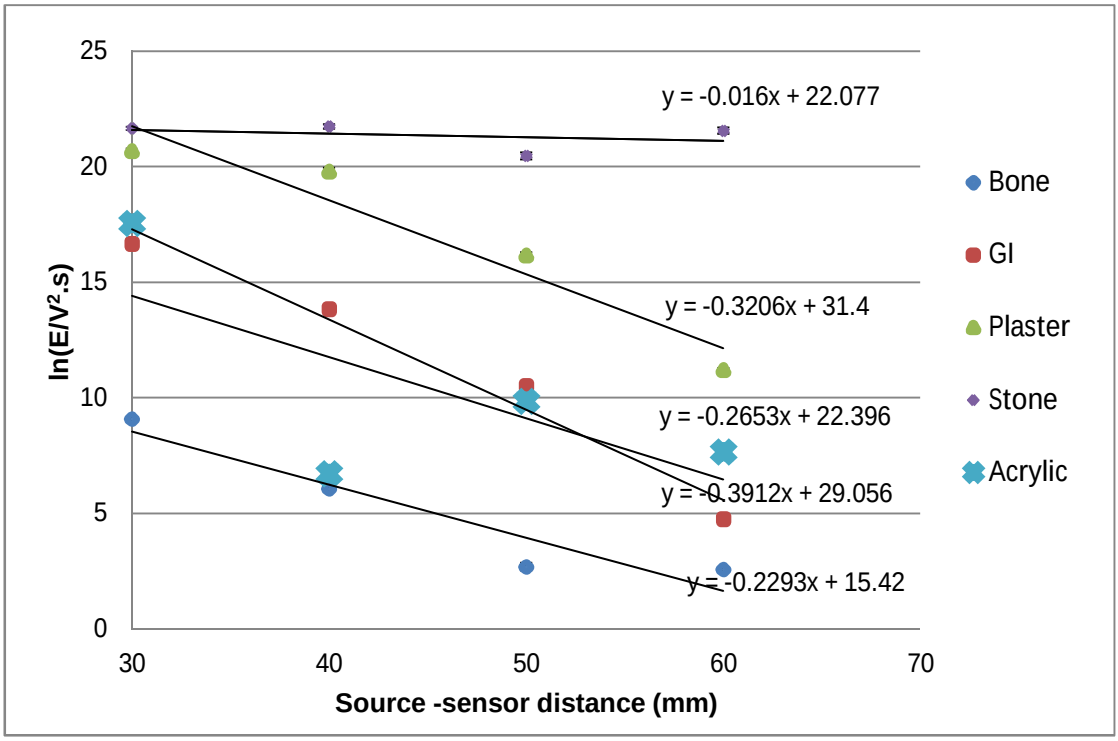

Figure 4.3: Material absorption plots for surface AE transmission

It was also of interest to examine the extent to which the materials exhibited "structural filtering", i.e. preferential transmission of one frequency band over another. Figure 4.4 shows the frequency ratio plotted against distance from the source for each of the materials over the 30 – 60 mm measurement range. As can be seen, the glass ionomer and the bone behave in a similar fashion, with low values of

frequency ratio, which appear to decrease with distance. The minerals (stone and plaster) also show a decrease in frequency ratio with distance, but have generally higher frequency ratios. The acrylic behaves rather anomalously with an erratic range in frequency ratio but one which appears to increase with distance from the source.

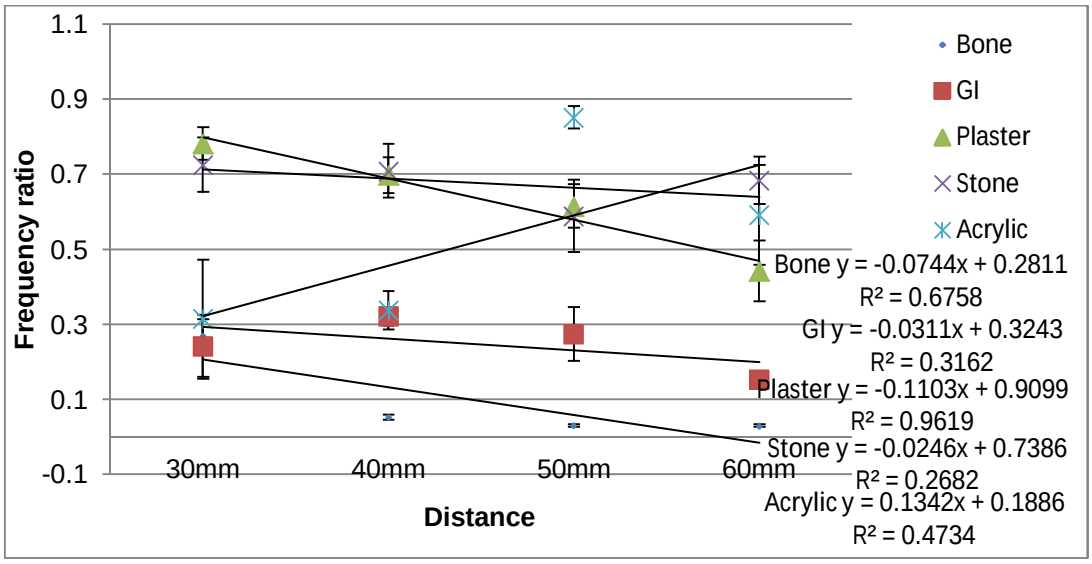

Figure 4.4: Average frequency ratios of materials tested

4.3.2 Bone samples

Figure 4.5 (a – d) shows the energy transmitted through the bones for each of the implant conditions as the bones were dried. It is clear that there is a substantial decrease in transmission between the fresh and dried bones tending to decrease most between fresh and 24 hours of drying.

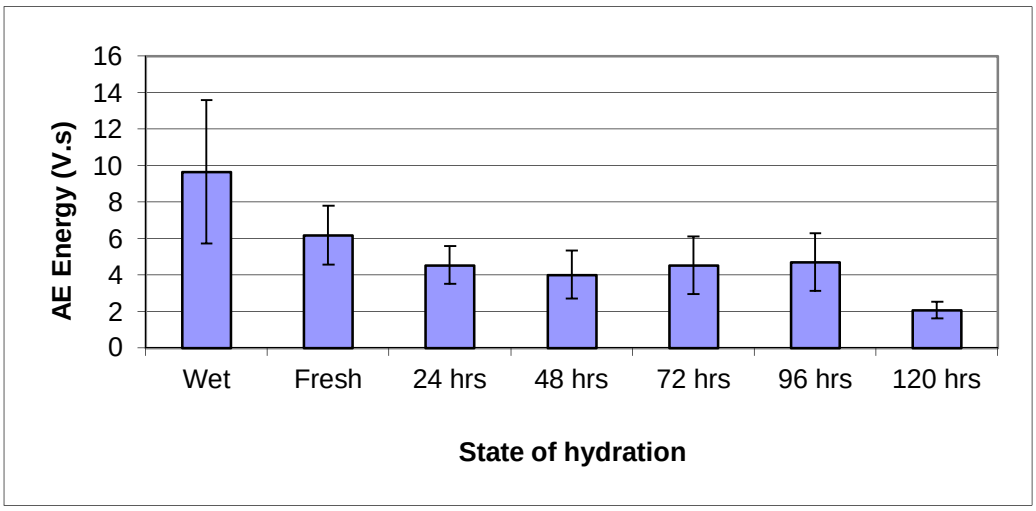
16
14
12
10
8
6
4
2
0
AE Energy (V.s)
Wet
Fresh
24 hrs
48 hrs
72 hrs
96 hrs
120 hrs
State of hydration

(a)

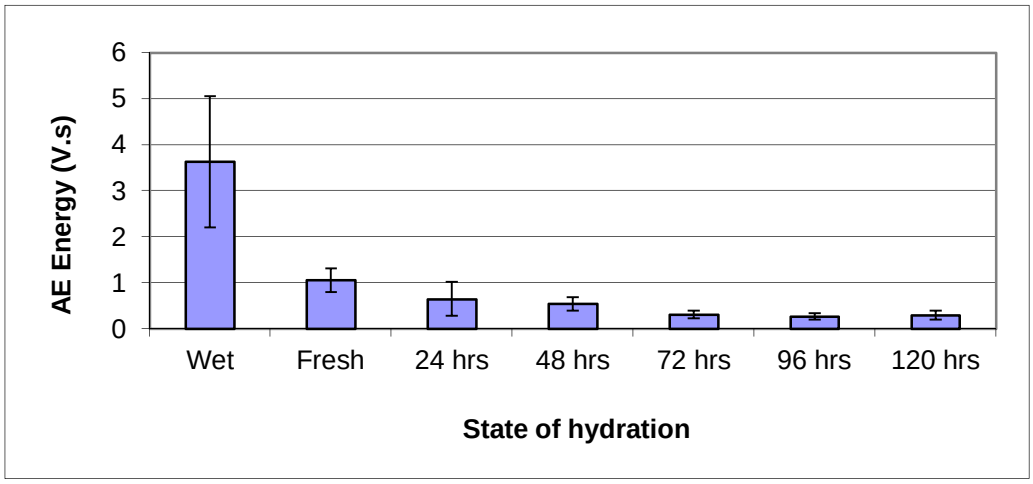
6
5
4
3
2
1
0
AE Energy (V.s)
Wet
Fresh
24 hrs
48 hrs
72 hrs
96 hrs
120 hrs
State of hydration

(b)

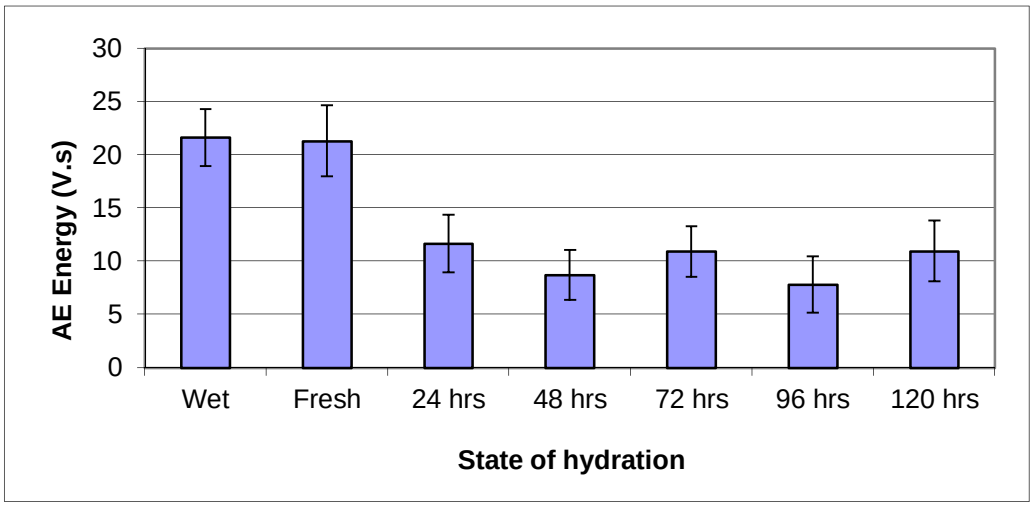
30
25
20
15
10
5
0
AE Energy (V.s)
Wet
Fresh
24 hrs
48 hrs
72 hrs
96 hrs
120 hrs
State of hydration

(c)

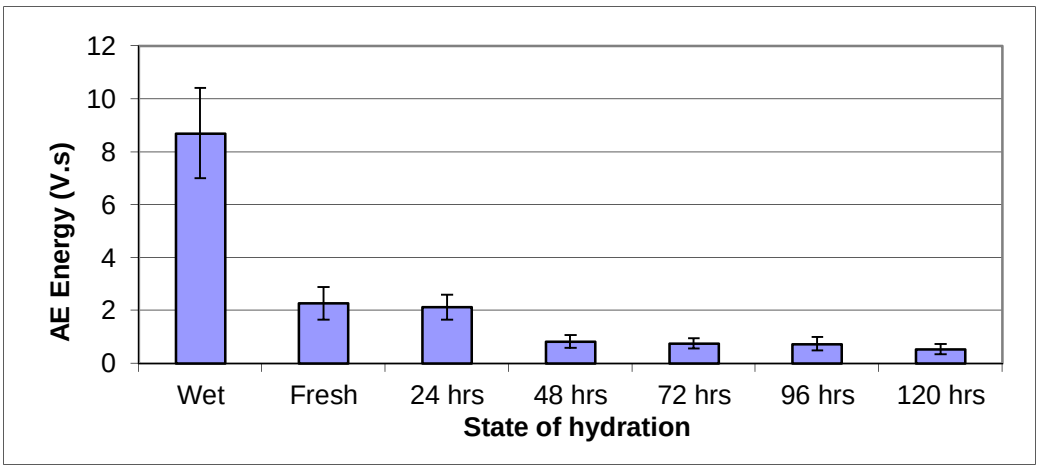

(d)

Figure 4.5: Transmitted energy with bone hydration level for each of the implant fixities: (a) 8.5mm implant in tight fitting condition, (b) 8.5mm implant in loose fitting condition, (c) 13mm implant in tight fitting condition, (d) 13mm implant in loose fitting condition

Figures 4.6 (a-b) show the frequency ratio, again plotted to highlight any changes which might be attributed to the hydration level in the bones. These graphs seem to indicate little or no effect of hydration of the frequency ratio of the transmitted AE.

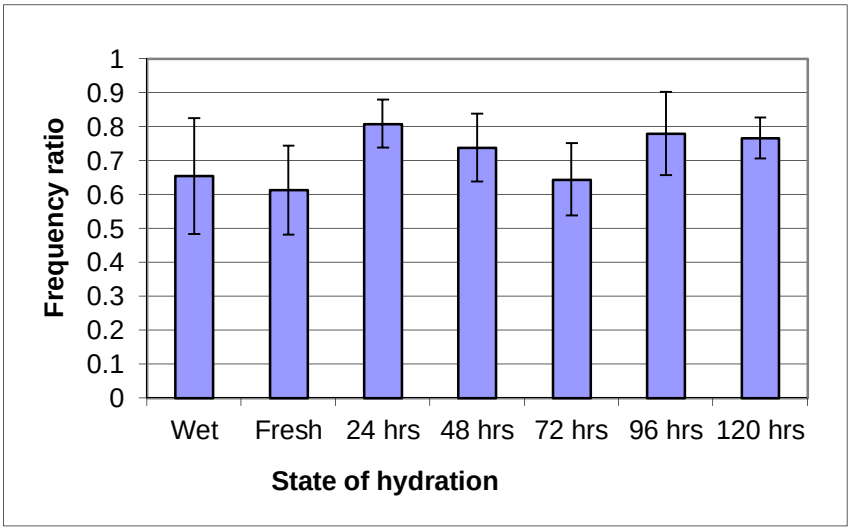

(a)

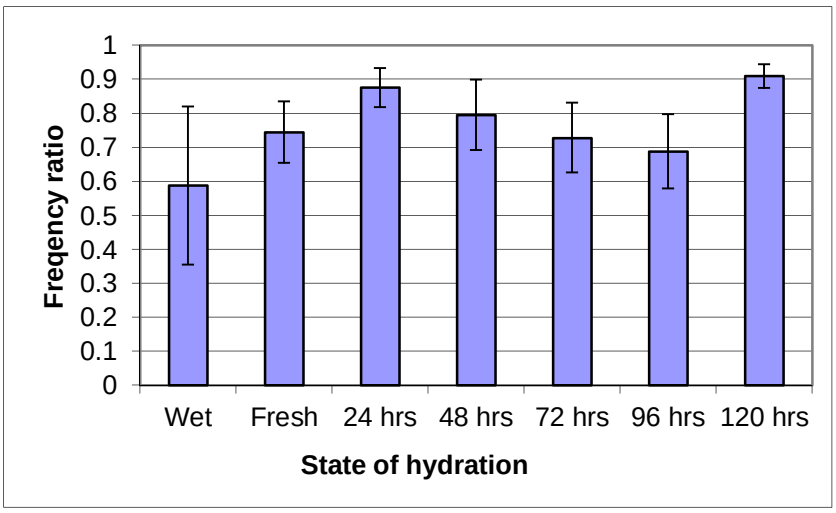

(b)

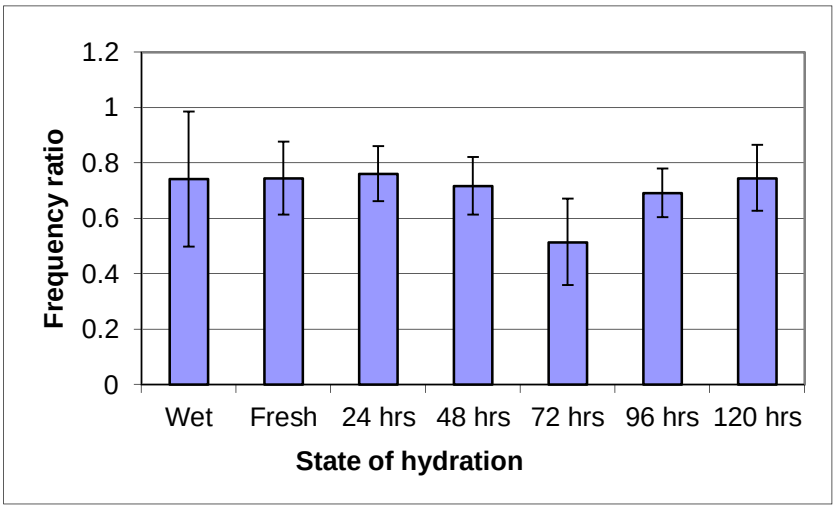

(c)

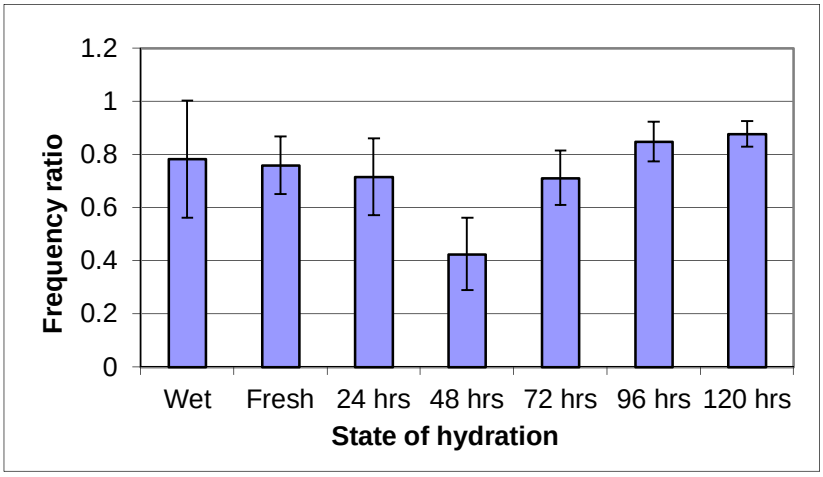

(d)

Figure 4.6: Effect of hydration level on frequency ratio: (a) 8.5mm implant in tight fitting condition, (b) 8.5mm implant in loose fitting condition, (c) 13mm implant in tight fitting condition, (d) 13mm implant in loose fitting condition

The tests with fresh, wet and dried bones with the implant interface included showed the importance of water, not only in transmission through the bone, but also in transmission across the interface, as summarised in Figure 4.7. When the interfaces were tight, overall transmission is improved by having a larger interface area (13mm vs. 8.5mm length). This increase is almost directly in proportion to the nominal surface contact area (93.5mm^2 for the smaller implants and 184mm^2 for the larger ones). For a given implant size in the tight condition in a fresh bone the amount of transmission is increased by 30 – 40% by hydrating the bone and is decreased by a similar amount by desiccating the bone. The tests do not discriminate between the interface and bone transmission effects but it seems likely that the difference between wet and fresh is largely associated with the condition of the interface, whereas the difference between the fresh and dry bones is largely due to bone transmission.

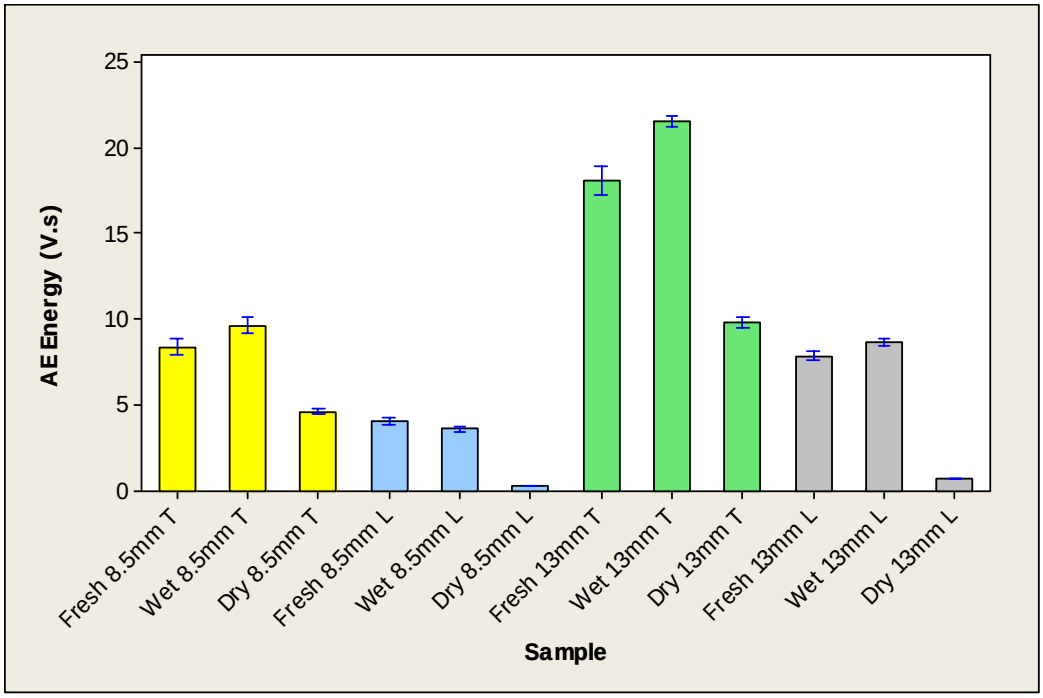

Figure 4.7: Average transmitted AE energy in fresh, wet and dried bones

Figure 4.8 shows the evolution of bone weight versus drying time. As with the transmitted energy, it can be seen that the weight drops most between fresh bone and 24 hours of drying, eventually flattening by the time it reaches 5 days.

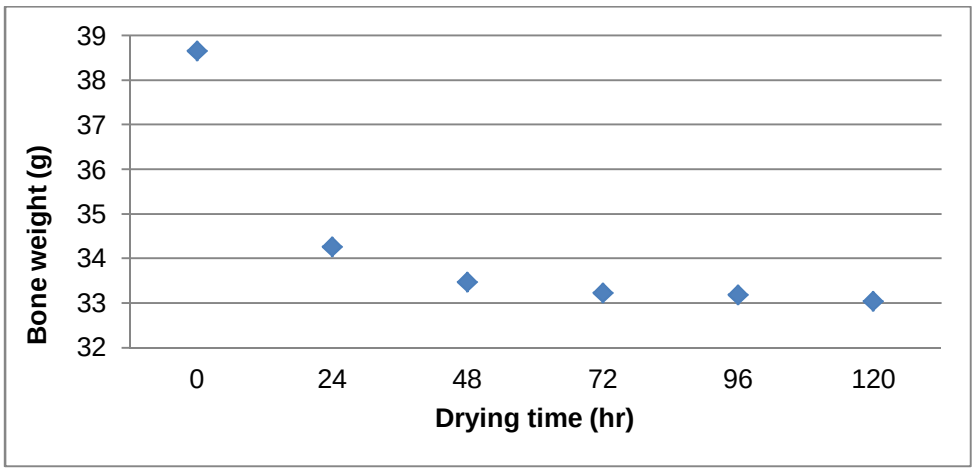

Figure 4.8: Effect of drying time on bone weight

Figure 4.9 shows the date from Figure 4.8 for the variation in moisture content (grammes above the driest weight of 33g) with time in the oven, plotted on a log-linear scale. Although drying is a complex phenomenon, practical weight loss curves can often be treated as an exponential decay (e.g. Kemp *et al.*, 2001). As can be seen, the weight loss data suggest a moisture content exponential decay time constant of around 0.03 hr^{-1}.

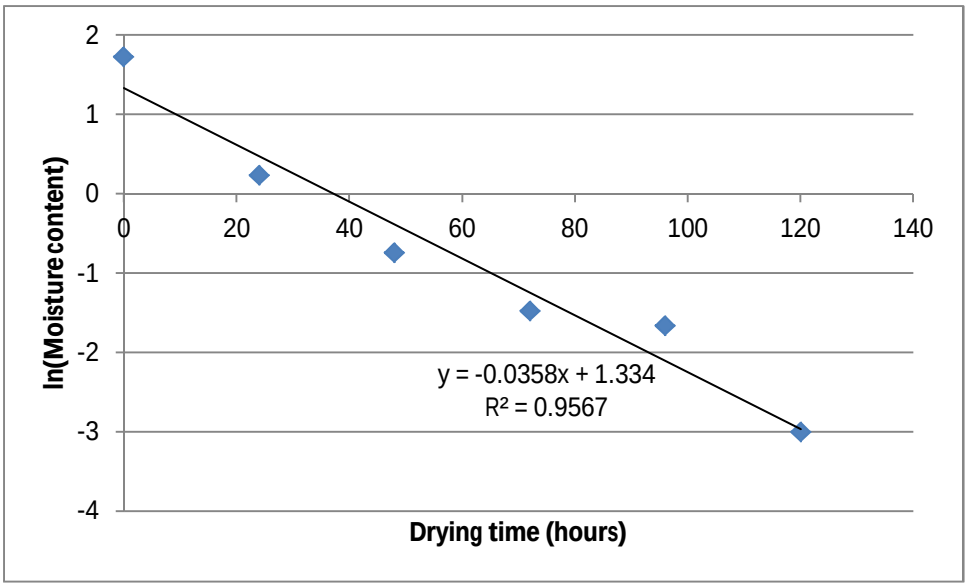

Figure 4.9: Weight loss in bone during drying (re-plotted from Figure 4.8)

Figure 4.10 compares the transmitted AE energy for the wet and fresh bones per sample and Table 4.1 summarises the analysis of variance for each of the fitting

conditions. Clearly, flooding of the bone leads to a significant increase in transmitted AE energy for each of the fitting conditions, but also the effect of wetness is much greater for the loose fitting implants.

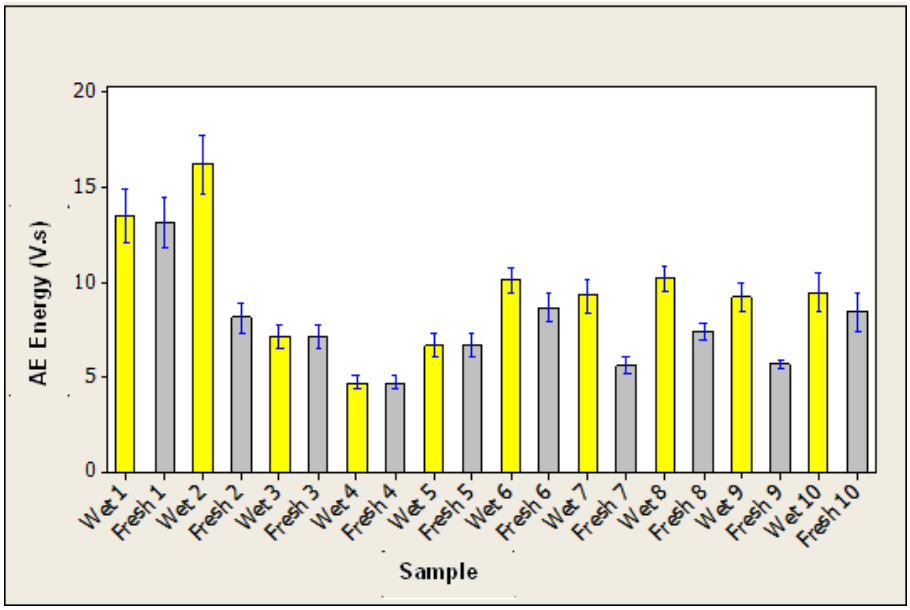

(a)

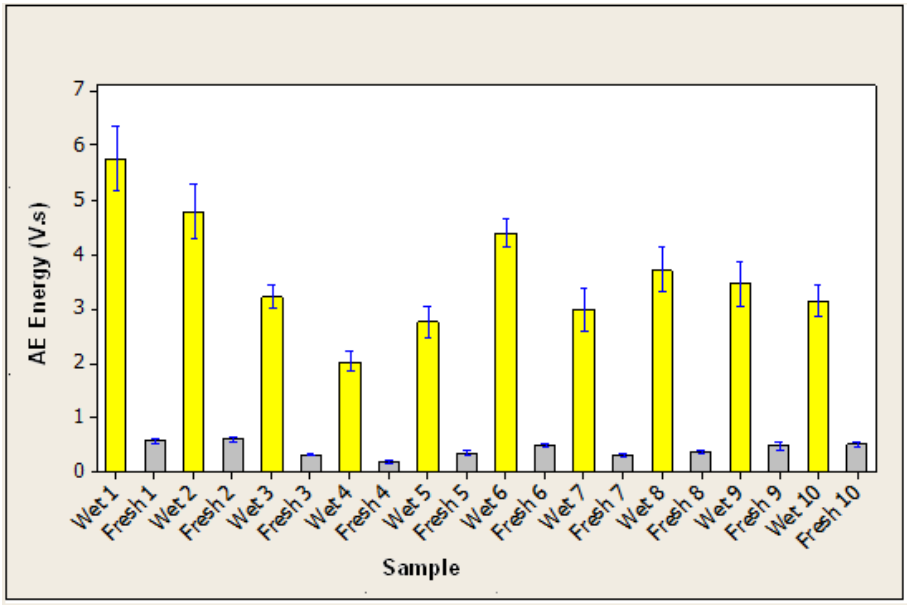

(b)

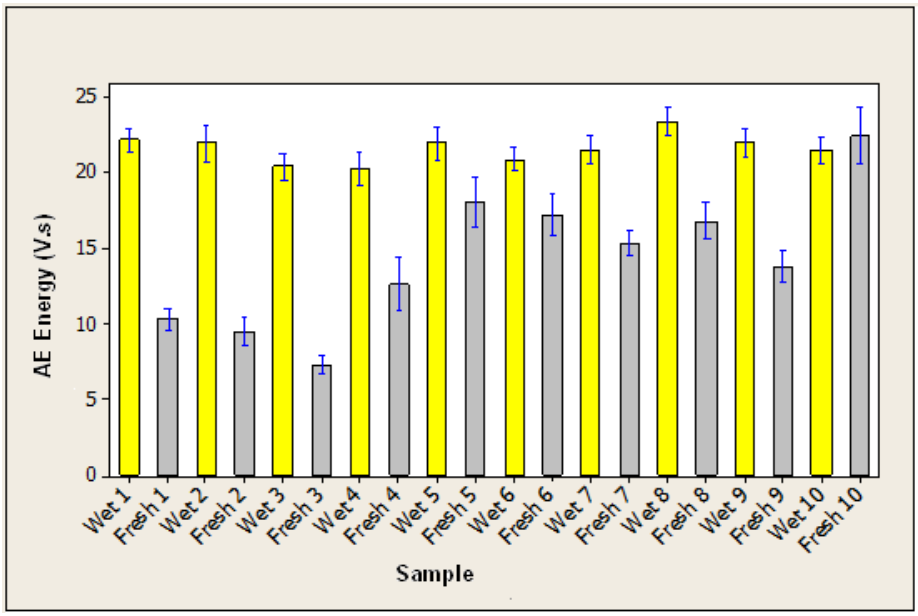

(c)

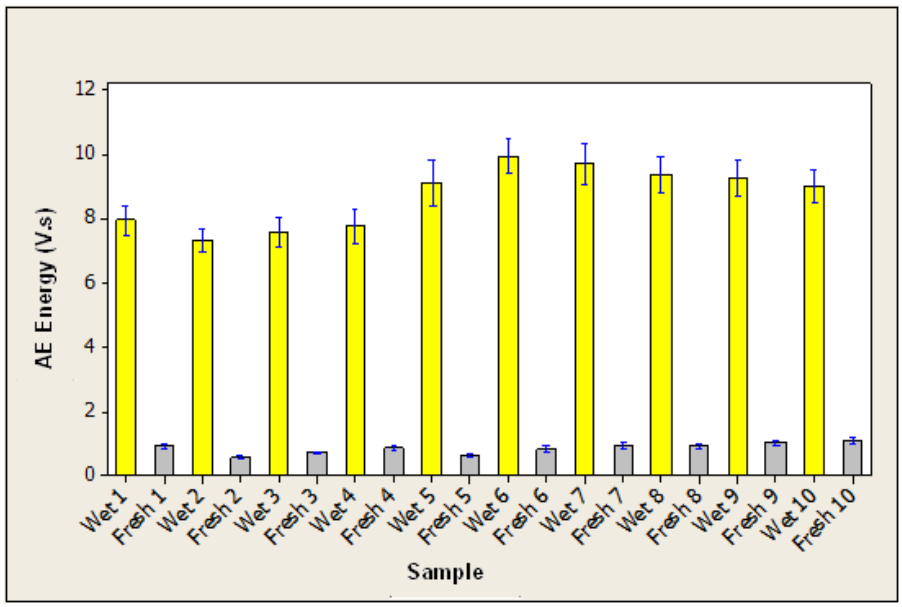

(d)

Figure 4.10: Comparison of transmitted AE energy for wet and fresh bones: (a) 8.5mm implants in tight fitting condition, (b) 8.5mm implants in loose fitting condition, (c) 13mm implants in tight fitting condition, (d) 13mm implants in loose fitting condition

	8.5mm Tight	**8.5mm Loose**	**13mm Tight**	**13mm Loose**
P Value	4.12E-13	1.03E-164	8.70E-72	5.23E-62

Table 4.1 ANOVA for wet vs. fresh bones

Figure 4.11 shows the decay in transmitted energy for each of the fitting conditions as the bone goes from its non-dried (fresh) state to what is assumed to be the desiccated state after 120hr. The data have been treated to subtract the lowest recorded energy (lowest mean-SD) so that no negative results are displayed, but the curves decay essentially to zero. With this presentation, it is possible to fit an exponential decay to the effect of drying. As can be seen, the decay constants vary between 0.01 and 0.02hr-1, the lower values being associated with the tighter fitting conditions. It might also be noted that the scatter means that the section of the curve closest to zero has an abnormally large effect of the decay constant, and this is almost certainly underestimated. Given this limitation, it is reasonable to conclude that the processes leading to drying weight loss and those leading to reduction in transmitted energy are the same. This lends further credence to the suggestion that drying affects the bone transmission whereas flooding has an effect which is more to do with the interface condition.

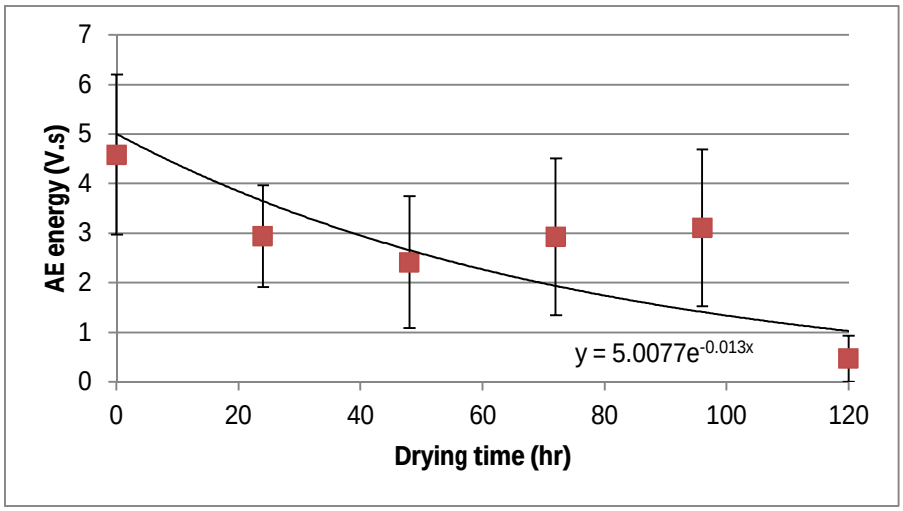

(a)

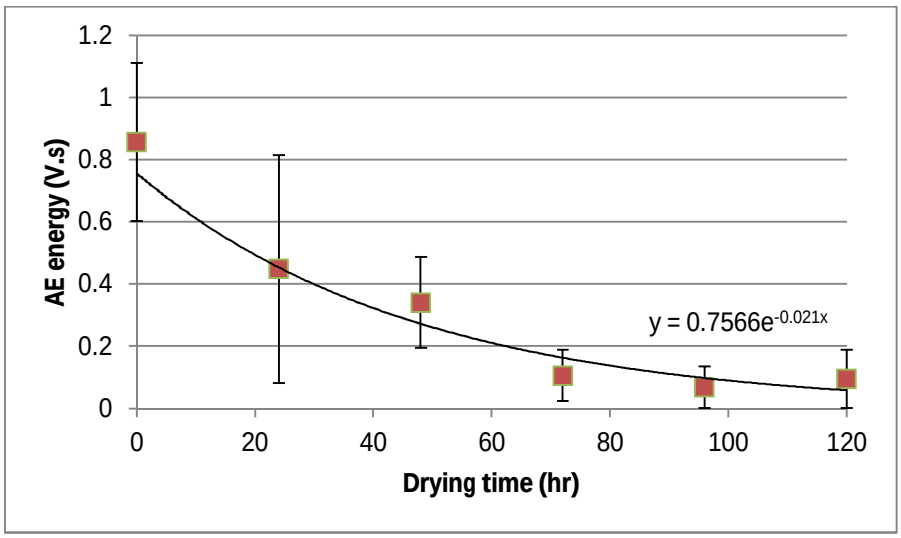
AE energy (V.s)
1.2
1
0.8
0.6
0.4
0.2
0
0
20
40
60
80
100
120
Drying time (hr)
y = 0.7566e-0.021x

(b)

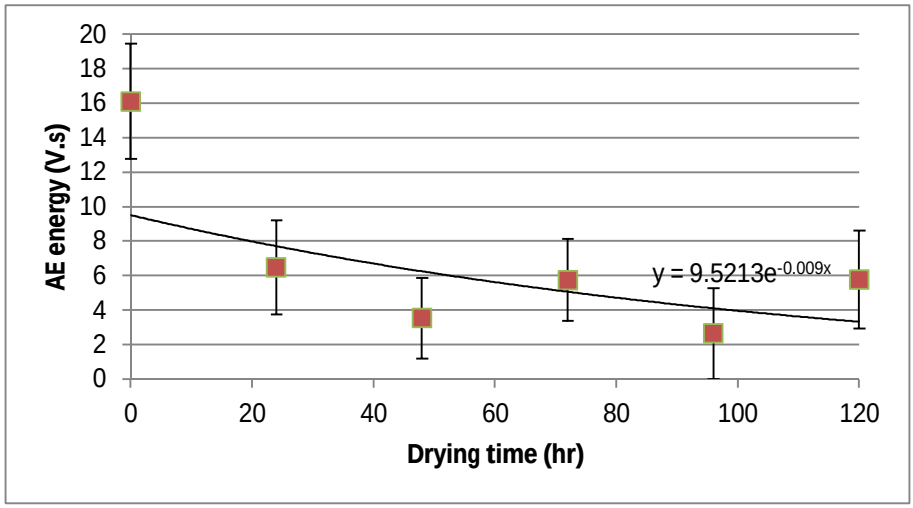
AE energy (V.s)
20
18
16
14
12
10
8
6
4
2
0
0
20
40
60
80
100
120
Drying time (hr)
y = 9.5213e-0.009x

(c)

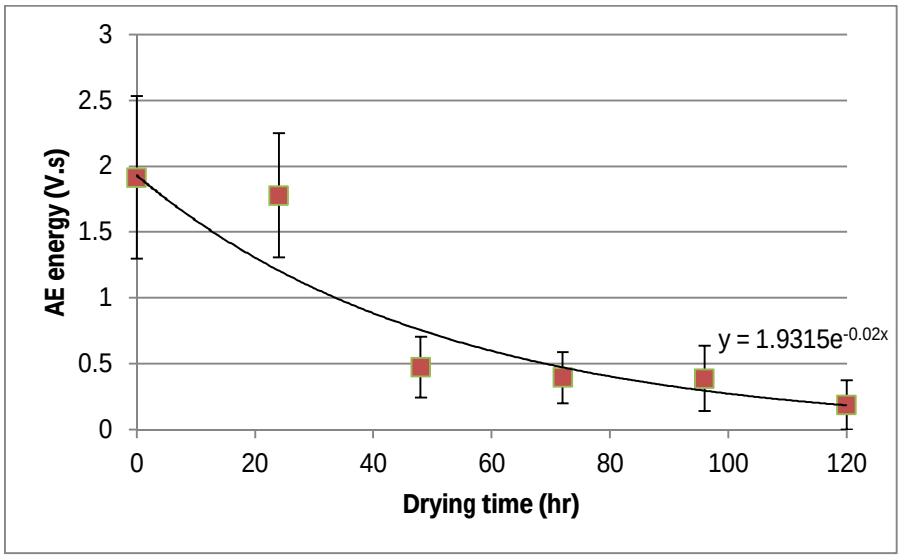
AE energy (V.s)
3
2.5
2
1.5
1
0.5
0
0
20
40
60
80
100
120
Drying time (hr)
y = 1.9315e-0.02x

(d)

Figure 4.11: Effect of drying on transmission of AE in pencil-lead tests for each of the fitting conditions: (a) 8.5 mm, tight, (b) 8.5 mm, loose, (c) 13 mm, tight, (d) 13 mm, loose.

4.4 Use of standard source for systematic interface tests

In this section, AE energy and frequency analysis are carried out on signals transmitted from the standard AE source applied to implants with various diameters and lengths inserted into bovine bones in tight and loose fitting conditions. The focus in this set of tests was to assess the interface, and bones in a fresh condition were used throughout.

Figures 4.12 (a-d) show typical pencil lead break signals in the time and frequency domains captured from the AE sensor mounted on the side of the bovine ribs. The signals are of a typical "burst" type, rising rapidly to maximum amplitude and falling less rapidly. The duration of the signal was determined by setting a threshold of ±0.2V, chosen to be safely above the background noise, and setting the signal duration as being between the first and last crossings of the threshold. It can be seen immediately that larger implants inserted in tight fitting conditions produced higher amplitudes, and that there are some changes in the spectra for different conditions.

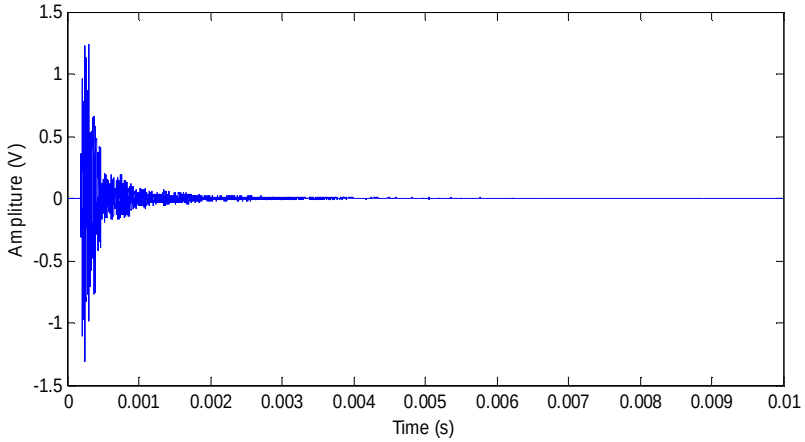

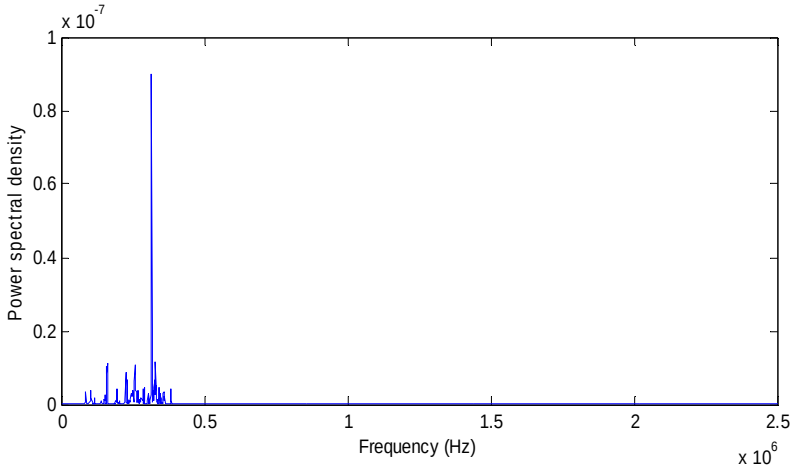
x 10^-7
Power spectral density
Frequency (Hz)
x 10^6

(a)

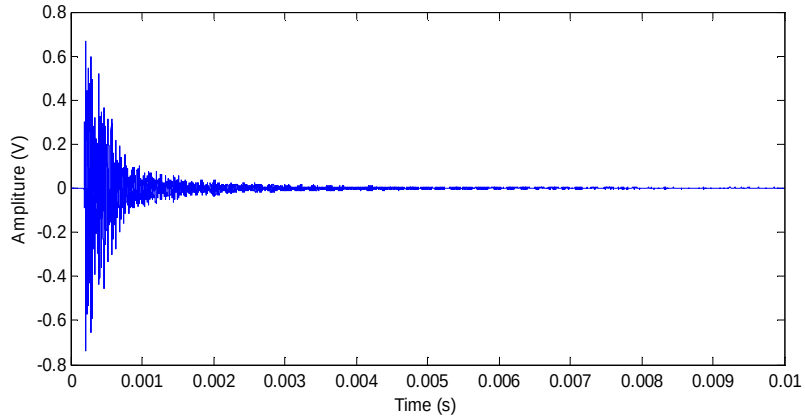
Ampliture (V)
Time (s)

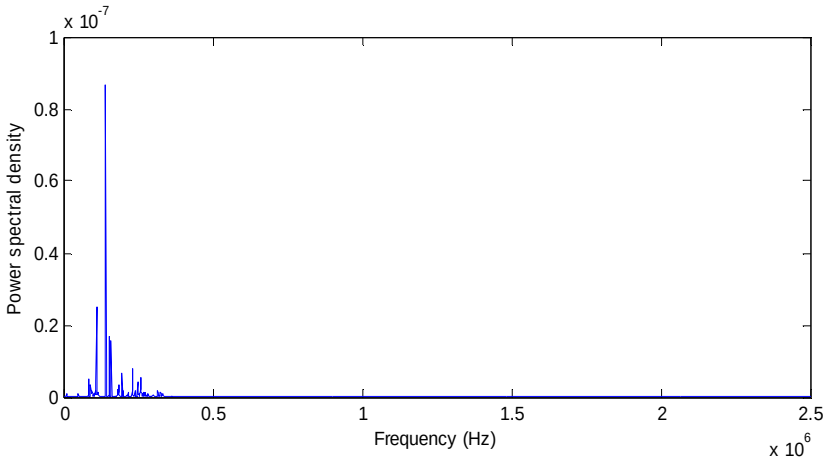
x 10^-7
Power spectral density
Frequency (Hz)
x 10^6

(b)

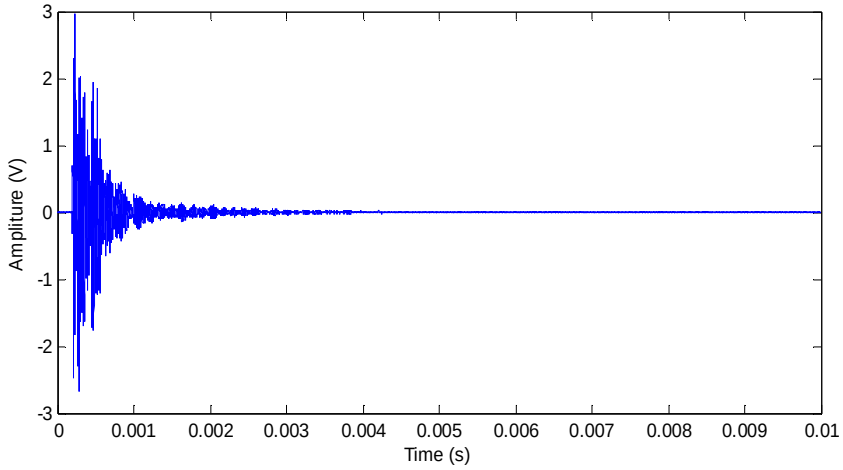
Ampliture (V)
Time (s)

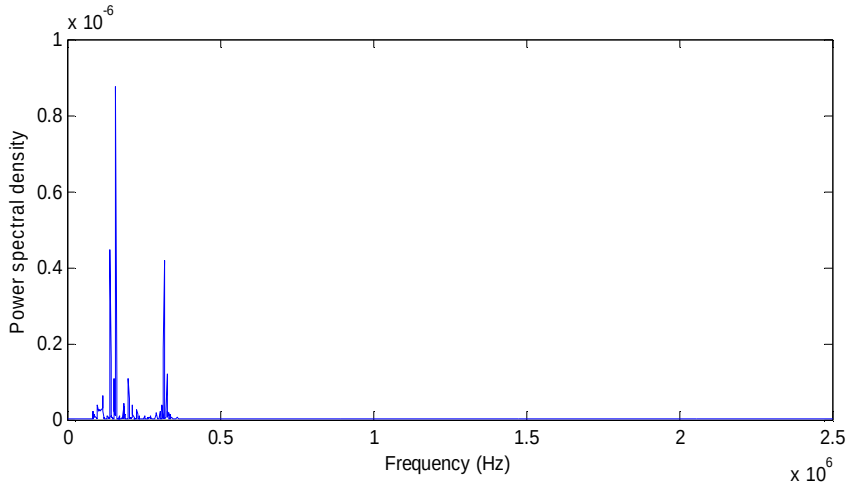
x 10^-6
Power spectral density
Frequency (Hz)
x 10^6

(c)

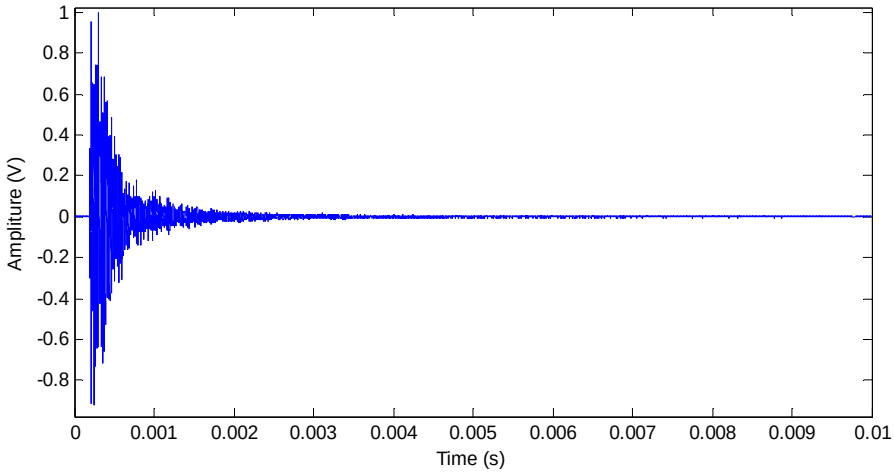
Ampliture (V)
Time (s)

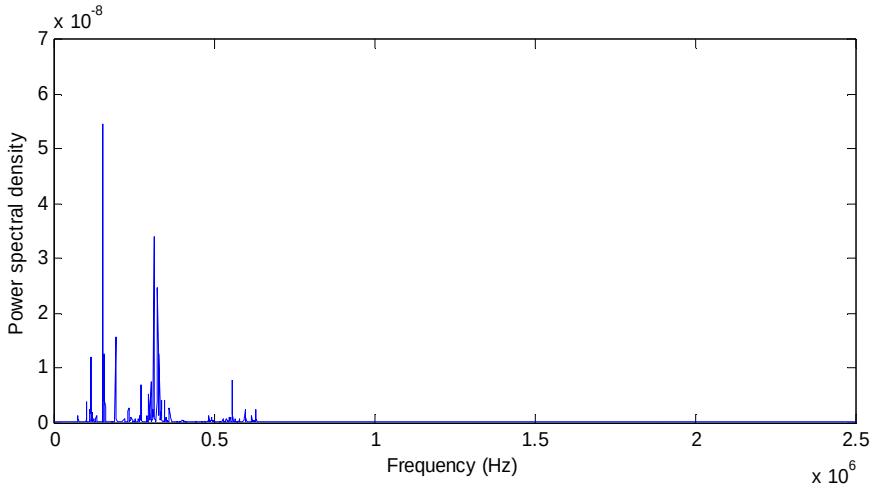

(d)

Figure 4.12: Typical AE signal structure (amplitude and frequency) from various implant sizes and fitting conditions: (a) 8.5mm implants in tight fitting condition, (b) 8.5mm implants in loose fitting condition, (c) 13mm implants in tight fitting condition, (d) 13mm implants in loose fitting condition

Figures 4.13 (a-d) show the energy values, plotted to highlight the effects of tightness of fitting (a and b) and size (c and d) for each of the 10 bone samples used. The graphs show the mean values (bar height) plus the standard deviations (error bars) of the 30 repeats with the contrasting data sets. For a given bone, the expected result (better transmission with a larger and/or tighter interface) is clearly shown, although there is considerable variation between the different bones.

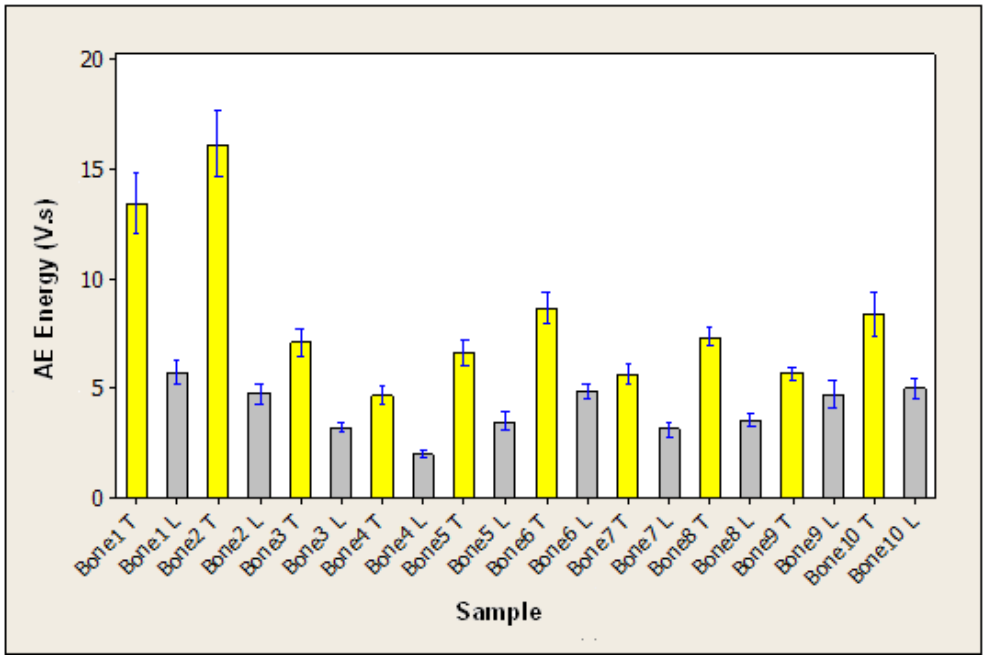
AE Energy (V.s)
20
15
10
5
0
Bone1 T
Bone1 L
Bone2 T
Bone2 L
Bone3 T
Bone3 L
Bone4 T
Bone4 L
Bone5 T
Bone5 L
Bone6 T
Bone6 L
Bone7 T
Bone7 L
Bone8 T
Bone8 L
Bone9 T
Bone9 L
Bone10 T
Bone10 L
Sample

(a)

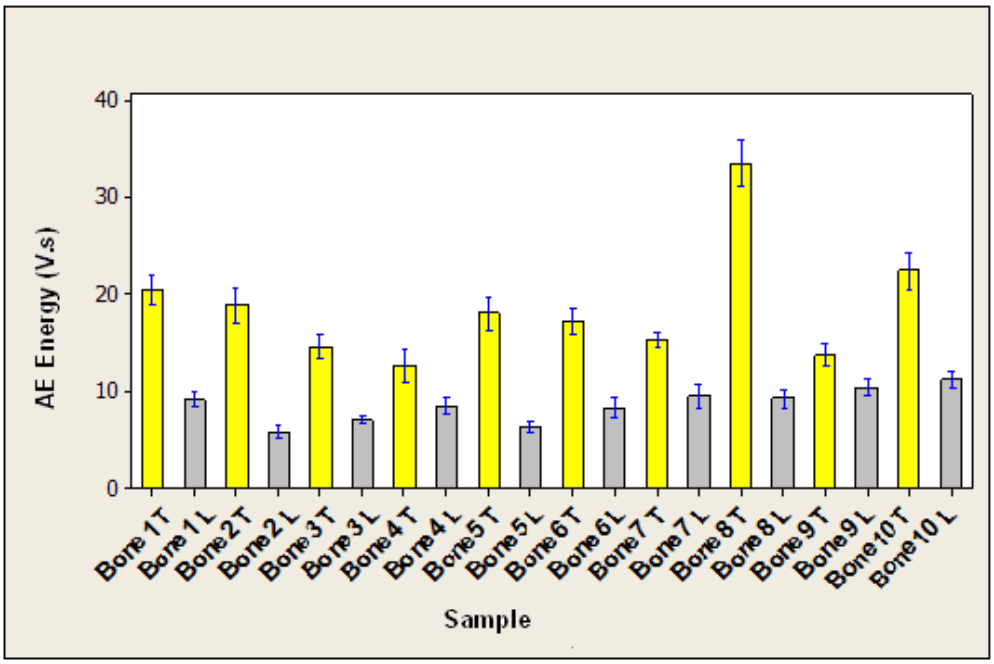
AE Energy (V.s)
40
30
20
10
0
Bone 1T
Bone 1L
Bone 2T
Bone 2L
Bone 3T
Bone 3L
Bone 4T
Bone 4L
Bone 5T
Bone 5L
Bone 6T
Bone 6L
Bone 7T
Bone 7L
Bone 8T
Bone 8L
Bone 9T
Bone 9L
Bone 10T
Bone 10L
Sample

(b)

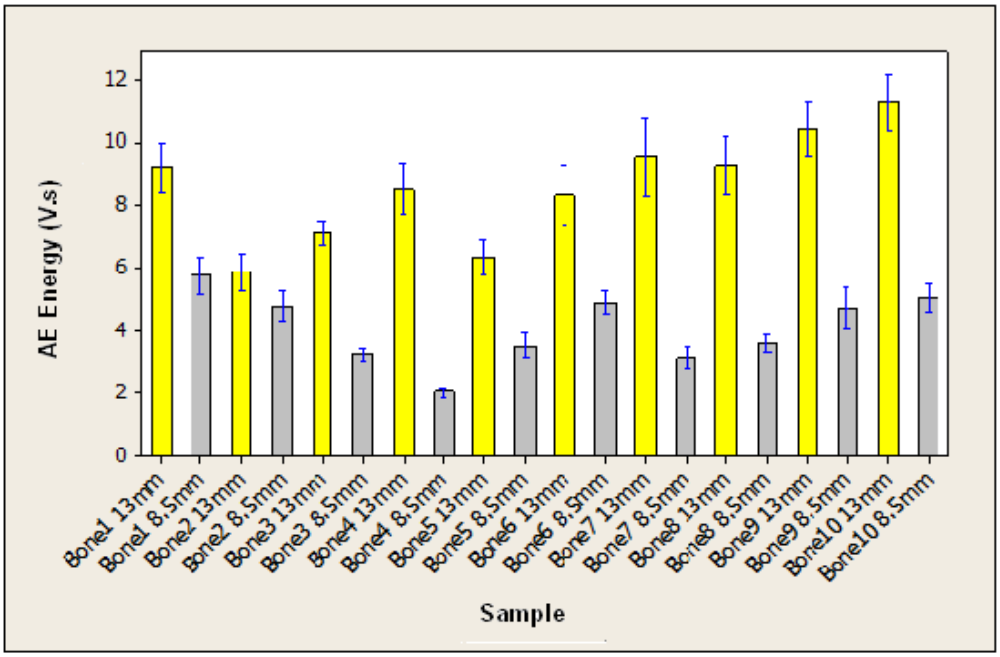

(c)

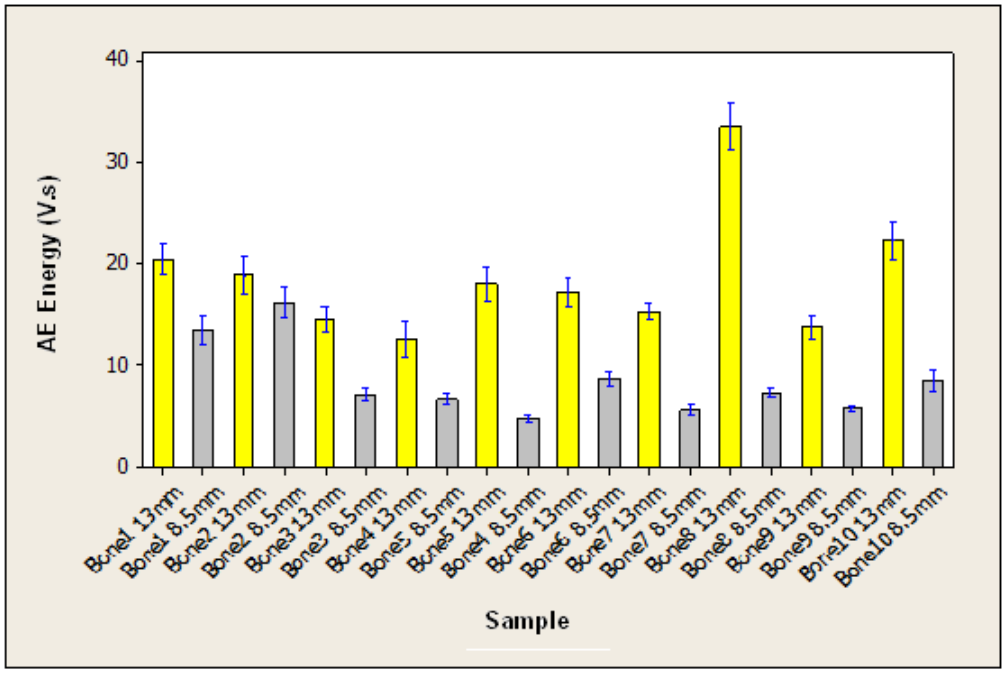

(d)

Figure 4.13: Effect of implant interface on transmitted AE energy of pencil lead fracture on fresh bone: (a) 8.5mm implant - Tight vs. Loose fitting, (b) 13mm implant - Tight vs. Loose fitting, (c) Loose fitting condition - 13mm vs. 8.5mm implants, (d) Tight fitting condition - 13mm vs. 8.5mm implants

Table 4.2 shows an example of an analysis of variance (ANOVA) for the effect of tightness for the 8.5mm implant in Bone 1 on AE energy. The 30 pencil lead breaks were grouped according to tight or loose fitting and tested at the 5% confidence level. The P-value was 10^{-15}, indicating a very clear discrimination in energy between the two conditions for this bone.

Anova: Single Factor

SUMMARY						
Groups	*Count*	*Sum*	*Average*	*Variance*		
8.5mm Tight-fitting condition	30	405.0882	13.50294	13.93457		
8.5mm Loose-fitting condition	30	172.4798	5.749327	2.551331		
ANOVA						
Source of Variation	*SS*	*df*	*MS*	*F*	*P-value*	*F crit*
Between Groups	901.7778	1	901.7778	109.3999	5.72E-15	4.006873
Within Groups	478.0912	58	8.242952			
Total	1379.869	59				

Table 4.2: Example of ANOVA on the effect of tightness for the smaller implant installed in Bone 1

Table 4.3 shows an analysis of variance (ANOVA) for the effect of sensor placement for each bone. The sensor was placed on each bone 4 times in the area of each implant while 30 AE recordings were collected per implant. Tested at the 5% confidence level, the P-value was 10^{-19} indicating a clear discrimination in energy between the two conditions for each bone which was not affected by the location of the sensor.

Anova: Single Factor

SUMMARY

Groups	*Count*	*Sum*	*Average*	*Variance*
Bone 1	120	1469.46	12.2455	39.60087
Bone 2	120	1372.747	11.43956	50.05286
Bone 3	120	960.9253	8.007711	20.7138

Bone 4	120	836.1759	6.968133	22.72923		
Bone 5	120	1037.382	8.644846	37.53612		
Bone 6	120	1173.574	9.779784	26.72534		
Bone 7	120	1008.506	8.404219	25.72415		
Bone 8	120	1613.154	13.44295	151.9556		
Bone 9	120	1038.574	8.654782	17.80689		
Bone 10	120	1414.673	11.78894	52.34826		
ANOVA						
Source of Variation	*SS*	*df*	*MS*	*F*	*P-value*	*F crit*
Between Groups	4983.892	9	553.7658	12.43878	5.2E-19	1.887733
Within Groups	52977.98	1190	44.51931			
Total	57961.87	1199				

Table 4.3: Summary ANOVA for the effect of sensor placement for individual bones

Finally, the same statistical tests were applied to all of the bones together and a summary of the results is shown in Table 4.4. The discrimination between tight and loose and large and small implants was more significant than for the bones treated individually, largely because of the increase in the number of degrees of freedom.

Data grouping	**Null hypothesis**	**P value**
1. All data by bone (10 groups × 120 observations)	That variation between bones was less than the variation due to changes in length and tightness	5.2×10^{-19}
2. Small by tightness (2 groups × 300 observations)	That variation due to tightness was less than variation due to bone and/or sensor placement for small implants	3.8×10^{-53}
3. Large by tightness (2 groups × 300 observations)	That variation due to tightness was less than variation due to bone and/or sensor placement for large implants	2.2×10^{-83}
4. Tight by length (2 groups × 300 observations)	That variation due to length was less than variation due to bone and/or sensor placement for tight installation	1.9×10^{-76}
5. Loose by length (2 groups × 300 observations)	That variation due to length was less than variation due to bone and/or sensor placement for loose installation	1.3×10^{-92}

Table 4.4: Summary ANOVA for all data grouped in various ways

Figure 4.14 (a-d) shows the frequency ratio for each of the fitting conditions and implant sizes. On average 60% of the signals indicate that the larger implants have higher frequency ratios than the smaller ones, and tight conditions have higher frequency ratios than loose ones.

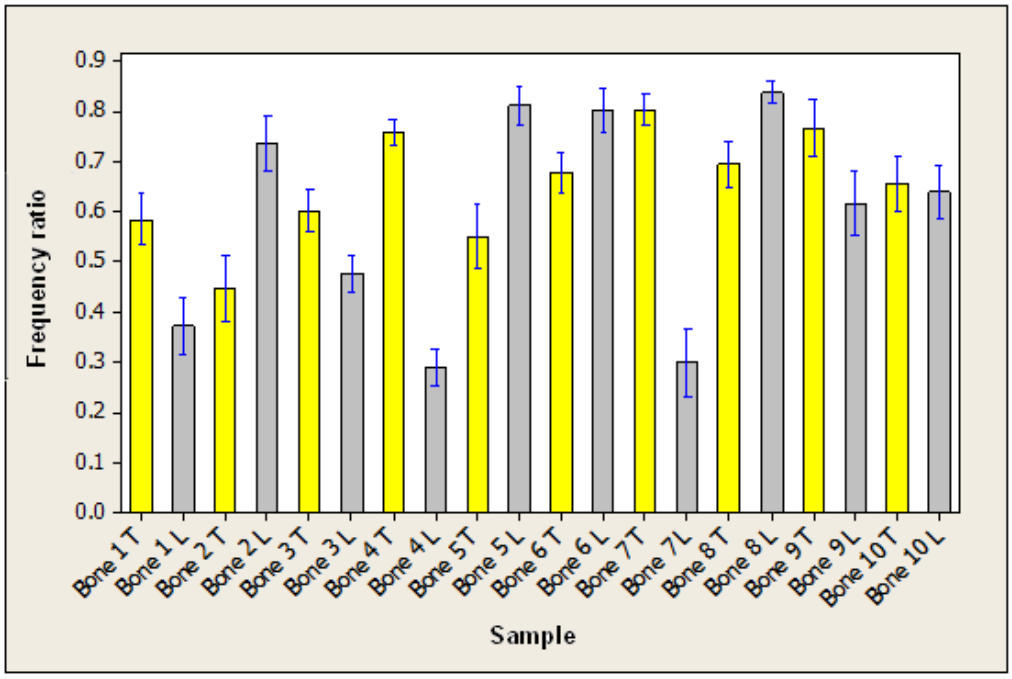

(a)

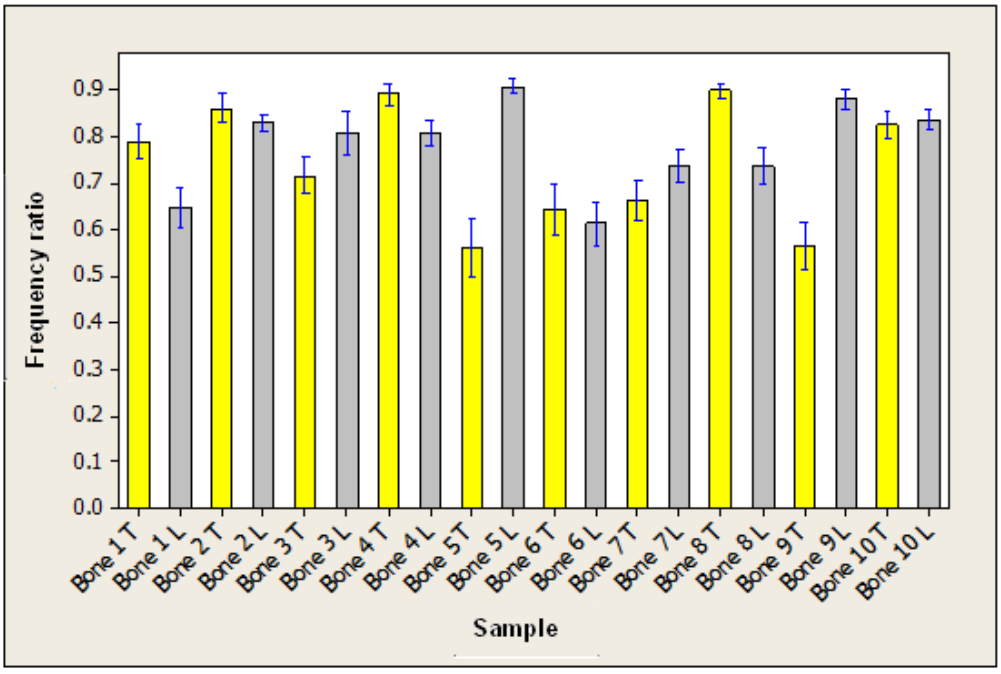

(b)

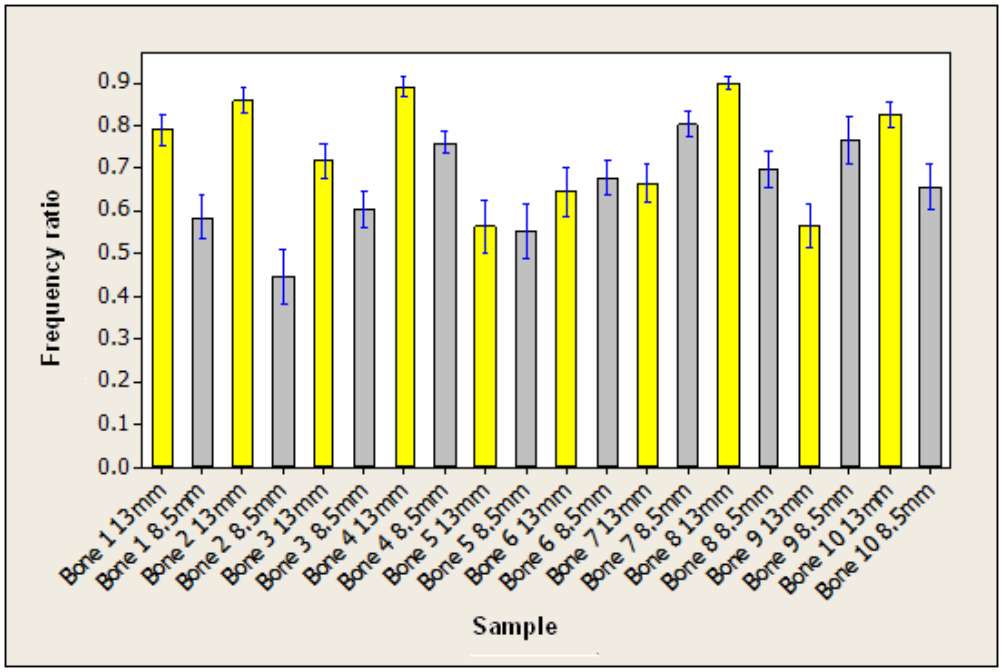

(c)

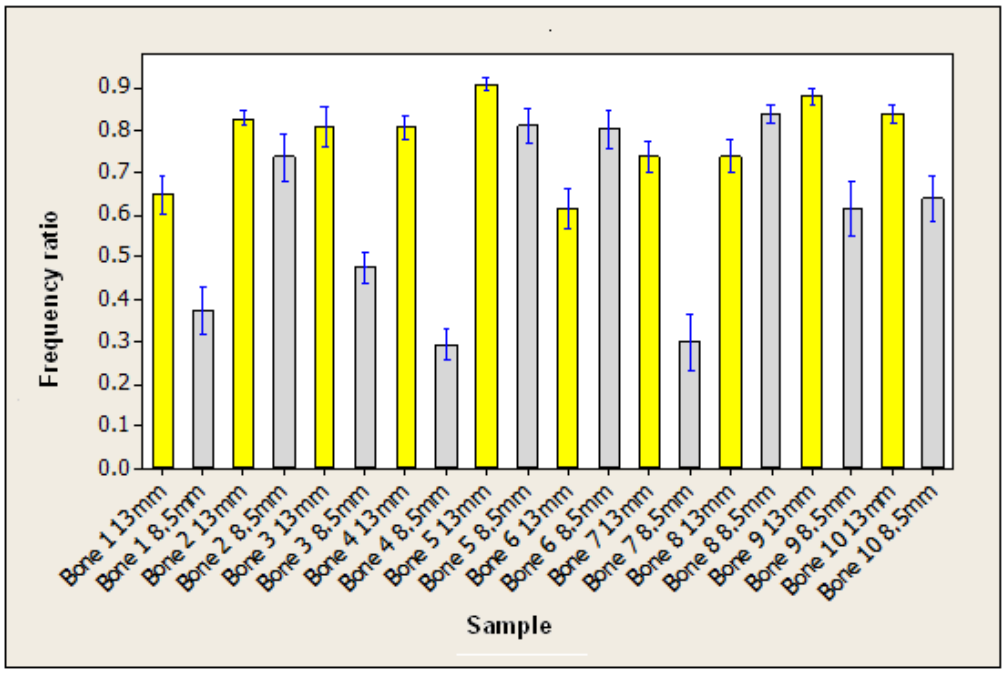

(d)

Figure 4.14: Effect of input interface condition on the frequency ratio of transmitted AE on fresh bone: (a) 8.5mm implants - tight vs. loose fitting, (b) 13mm implants - tight vs. loose fitting, (c) Tight fitting condition - 13mm vs. 8.5mm implants, (d) Loose fitting condition - 13mm vs. 8.5mm implant

P-values of the ANOVA are shown in Table 4.5, and can be seen to be larger than 0.05 except for 8.5mm vs. 13mm in the loose fitting condition. The frequency ratio

analysis did not therefore show clear discrimination between implant sizes and fitting conditions.

	8.5mm *vs* 13mm T	**8.5mm *vs* 13mm L**	**8.5mm T *vs* L**	**13mm T *vs* L**
P-value	0.117745	0.018169	0.397532	0.452449

Table 4.5: P-values of ANOVA analysis on AE energy with fresh bone

4.5 *In vitro* monitoring of interface using the air jet source

The objective of this experiment was to assess the feasibility of using an air jet source to replace the pencil lead break for assessing the implant interface. The air jet source is a continuous release of air at a constant pressure, which produces continuous AE signals. This offered a potentially more sophisticated probe and so some additional analysis was carried out over and above that used for the pencil lead in the previous section. Figure 4.15 shows typical raw AE signals captured per 0.01 second with the air jet source from 8.5mm and 13mm implants inserted under both tight and loose fitting conditions. Comparison of the vertical axes shows the tight fitting implants to have around 3 times the amplitude of the loose ones for a given size. Also, the amplitudes of the larger implants are around twice those of the smaller ones.

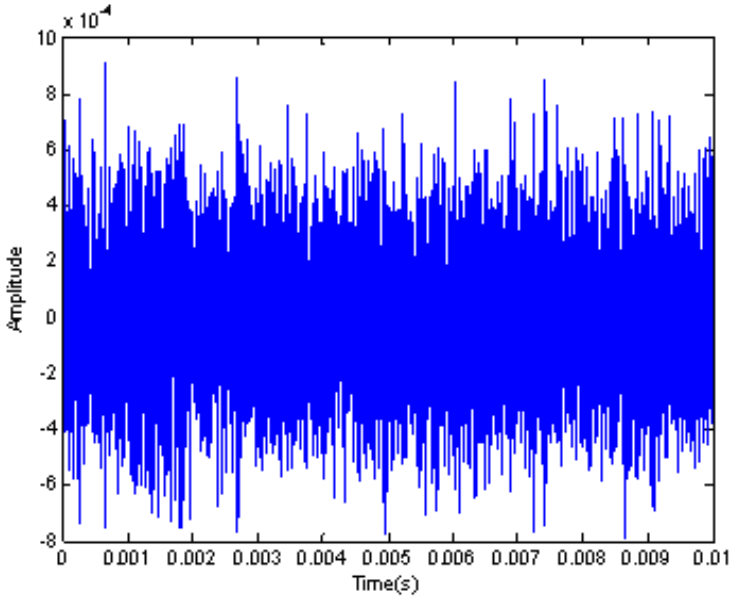

(a)

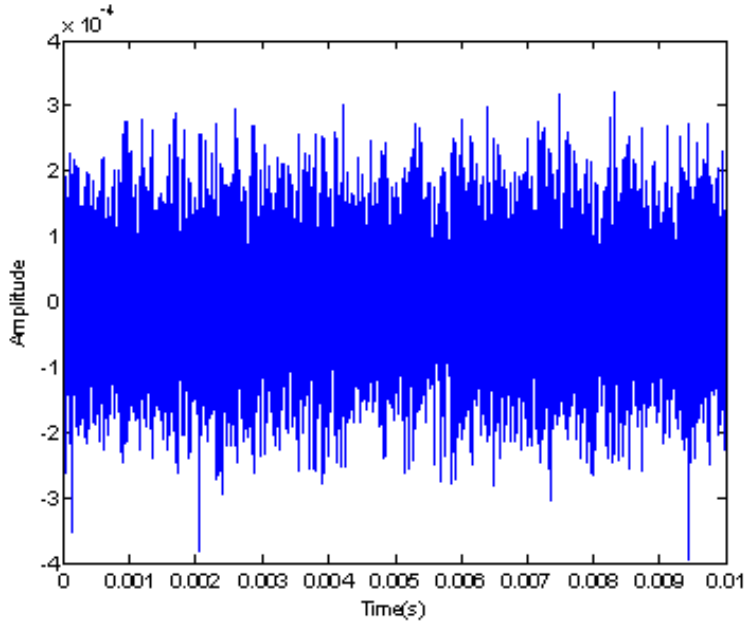
x 10^-4
4
3
2
1
0
-1
-2
-3
-4
Amplitude
0
0.001
0.002
0.003
0.004
0.005
0.006
0.007
0.008
0.009
0.01
Time(s)

(b)

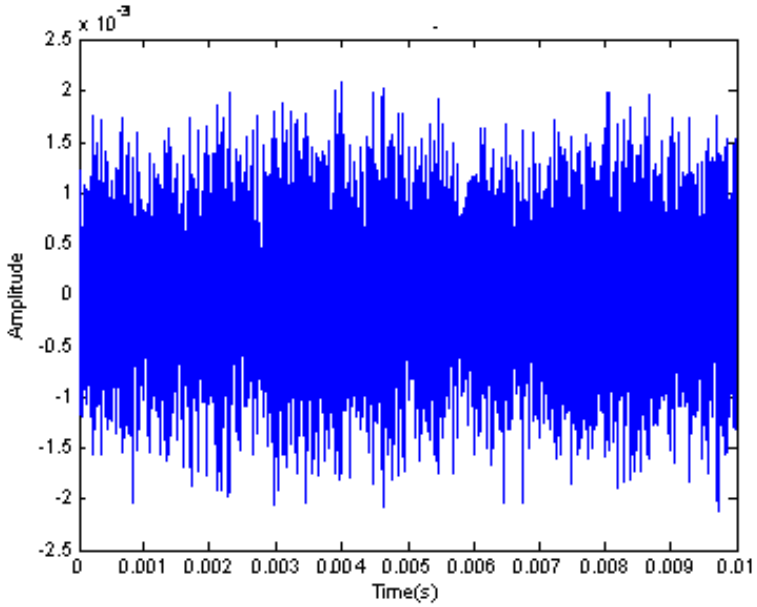
x 10^-3
2.5
2
1.5
1
0.5
0
-0.5
-1
-1.5
-2
-2.5
Amplitude
0
0.001
0.002
0.003
0.004
0.005
0.006
0.007
0.008
0.009
0.01
Time(s)

(c)

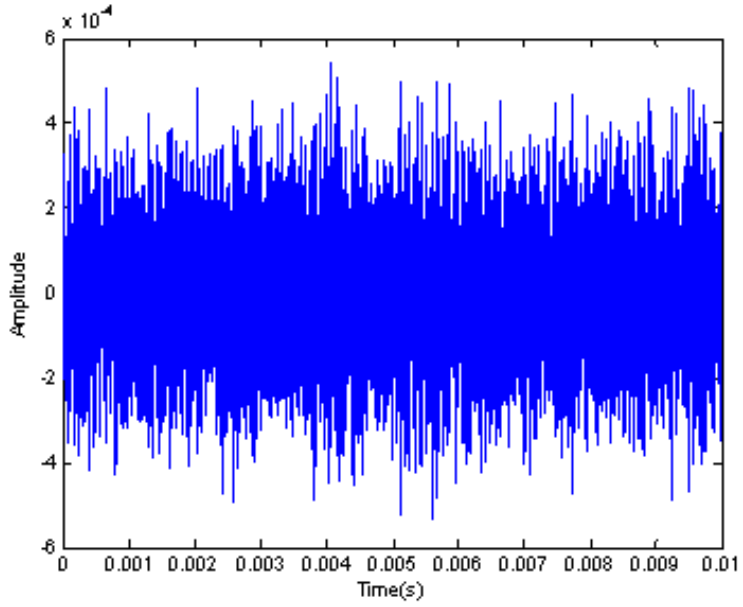

(d)

Figure 4.15: Typical raw AE signals from the air jet transmission test: (a) 8.5mm implant in tight condition, (b) 8.5mm implant in loose condition, (c) 13mm implant in tight condition, (d) 13mm implant in loose condition

Figure 4.16 (a – d) shows the transmitted AE energy for each of the 10 bone samples for each of the fitting conditions. A cursory comparison with Figure 4.13 for the pencil lead source shows that the air jet source leads to significantly less variation within a given sample and also to better discrimination between the tight and loose and the large and small implants.

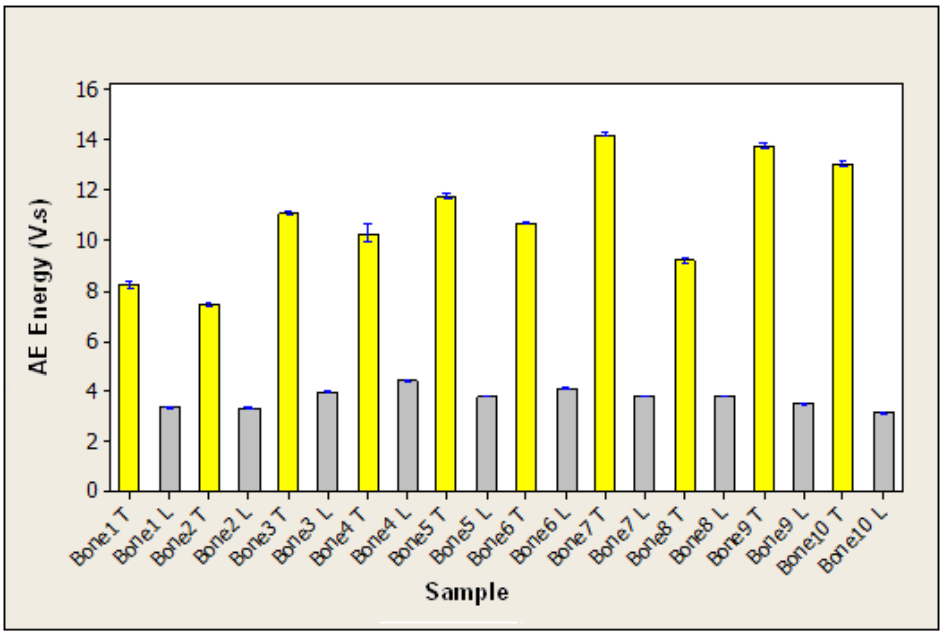

(a)

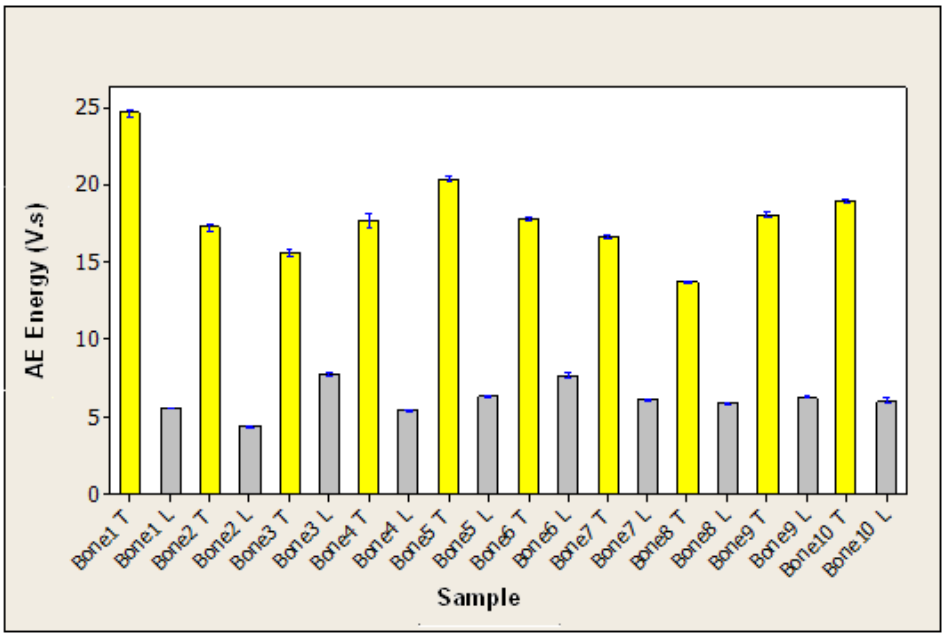
AE Energy (V.s)
25
20
15
10
5
0
Bone1 T
Bone1 L
Bone2 T
Bone2 L
Bone3 T
Bone3 L
Bone4 T
Bone4 L
Bone5 T
Bone5 L
Bone6 T
Bone6 L
Bone7 T
Bone7 L
Bone8 T
Bone8 L
Bone9 T
Bone9 L
Bone10 T
Bone10 L
Sample

(b)

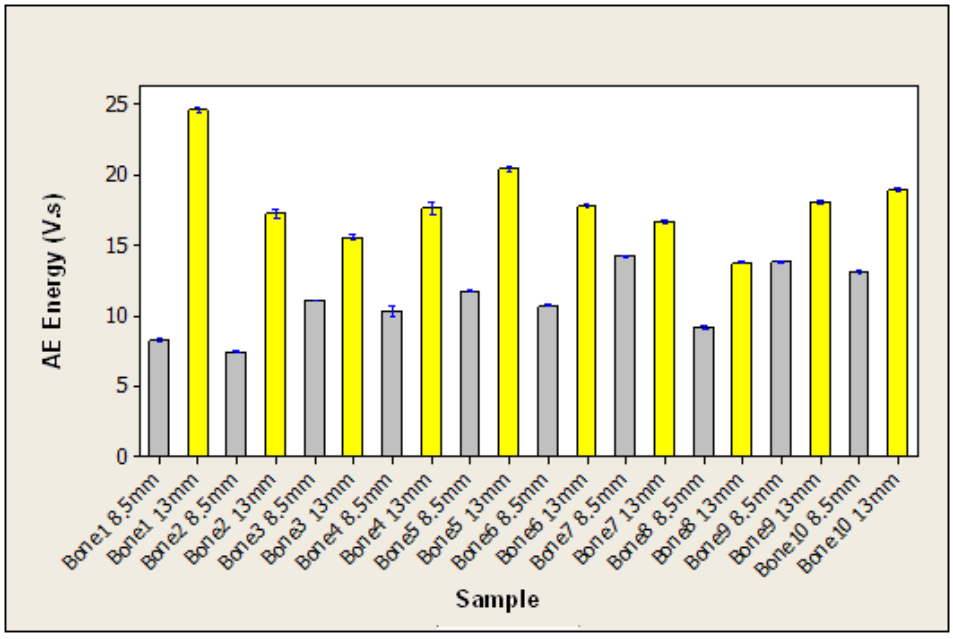
AE Energy (V.s)
25
20
15
10
5
0
Bone1 8.5mm
Bone1 13mm
Bone2 8.5mm
Bone2 13mm
Bone3 8.5mm
Bone3 13mm
Bone4 8.5mm
Bone4 13mm
Bone5 8.5mm
Bone5 13mm
Bone6 8.5mm
Bone6 13mm
Bone7 8.5mm
Bone7 13mm
Bone8 8.5mm
Bone8 13mm
Bone9 8.5mm
Bone9 13mm
Bone10 8.5mm
Bone10 13mm
Sample

(c)

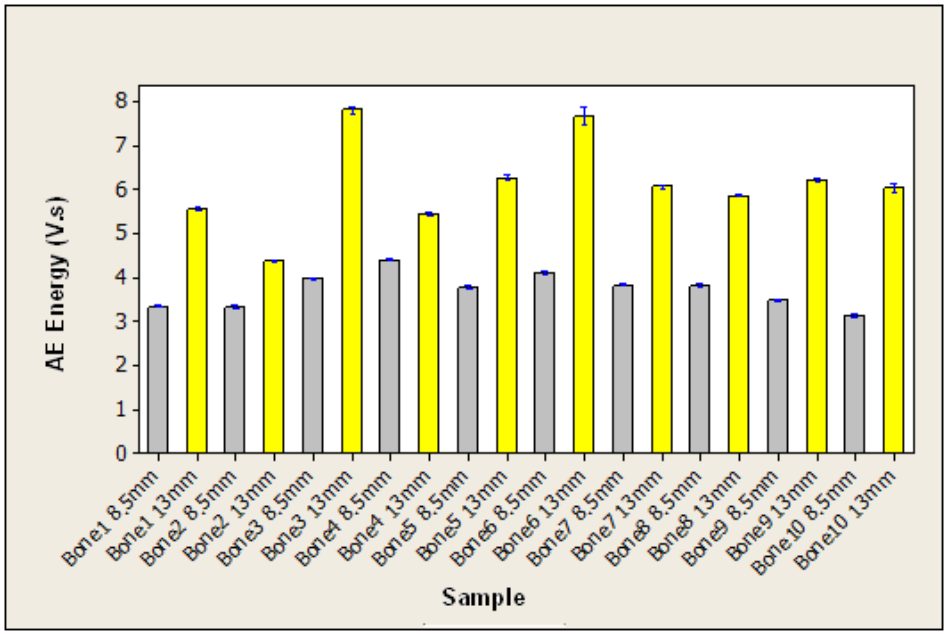

(d)

Figure 4.16: AE energy with air jet source: (a) 8.5mm implants tight vs. loose fitting, (b) 13mm implants tight vs. loose fitting, (c) 8.5mm vs. 13mm implants in tight fitting, (d) 8.5mm vs. 13mm implants in loose fitting

An analysis of variance (ANOVA) was performed for the effect of tightness for the 8.5mm implant in Bone 1 (Table 4.6). The 50 air jet readings were grouped according to tight or loose fitting and tested at the 5% confidence level. The P value was 6.26×10^{-92}, indicating a clear discrimination in energy between the two conditions for this bone. The same ANOVA applied to the remaining bones for both sizes (tight vs. loose) and for both fittings (large vs. small) showed P values in all cases to be less than 0.05. Table 4.7 summarises the ANOVA for all of the data grouped in different ways to test a range of hypotheses.

Anova: Single Factor Bone 1

SUMMARY

Groups	*Count*	*Sum*	*Average*	*Variance*
8.5 T	50	412.849	8.25698	0.176222
8.5 L	50	167.4825	3.34965	0.004397

ANOVA

Source of Variation	*SS*	*df*	*MS*	*F*	*P-value*	*F crit*
Between Groups	602.0472	1	602.0472	6666.505	6.26E-92	3.938111
Within Groups	8.850309	98	0.090309			
Total	610.8975	99				

Table 4.6: Example of ANOVA on the effect of tightness for the 8.5mm implant installed in bone 1

Data grouping	**Null hypothesis**	**P value**
1. All data, by bone (10 groups × 200 observations)	That variation between bones was less than the variation due to changes in length and tightness	9.6×10^{-262}
2. Small, by tightness (2 groups × 500 observations)	That variation due to tightness was less than variation due to bone and/or sensor placement for small implants	2.5×10^{-267}
3. Large, by tightness (2 groups × 500 observations)	That variation due to tightness was less than variation due to bone and/or sensor placement for large implants	7.1×10^{-279}
4. Tight by length (2 groups × 500 observations)	That variation due to length was less than variation due to bone and/or sensor placement for tight installation	2.4×10^{-231}
5. Loose by length (2 groups × 500 observations)	That variation due to length was less than variation due to bone and/or sensor placement for loose installation	4.3×10^{-267}

Table 4.7: Summary ANOVA for all data grouped in various ways

In order to examine the consistency of the air jet source the individual 0.01s averages were plotted in order as shown in Figure 4.17. Although the ordinate is not a precise indicator of time, the space between each record is approximately 3 seconds so that Figure 4.17 is essentially a time extension. The R^2 and the slope a of the regression lines ($y = ax + b$) were determined to assess any systematic drift in energy and the

majority of *a* values were close to 0 (Appendix E), showing that any such drift was small.

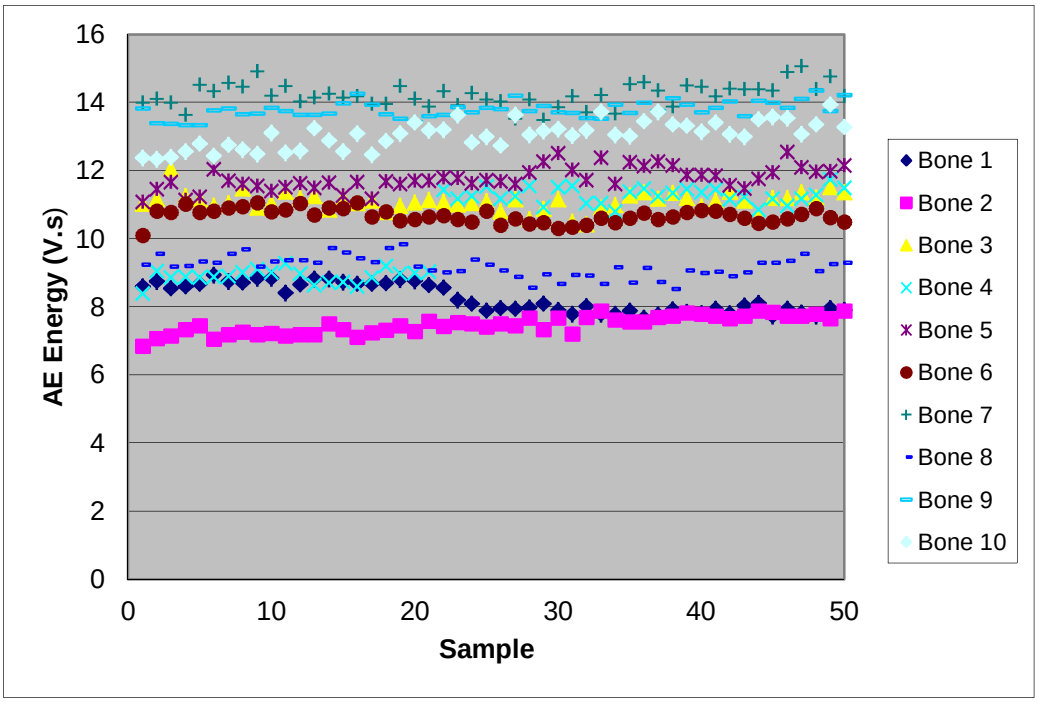

(a)

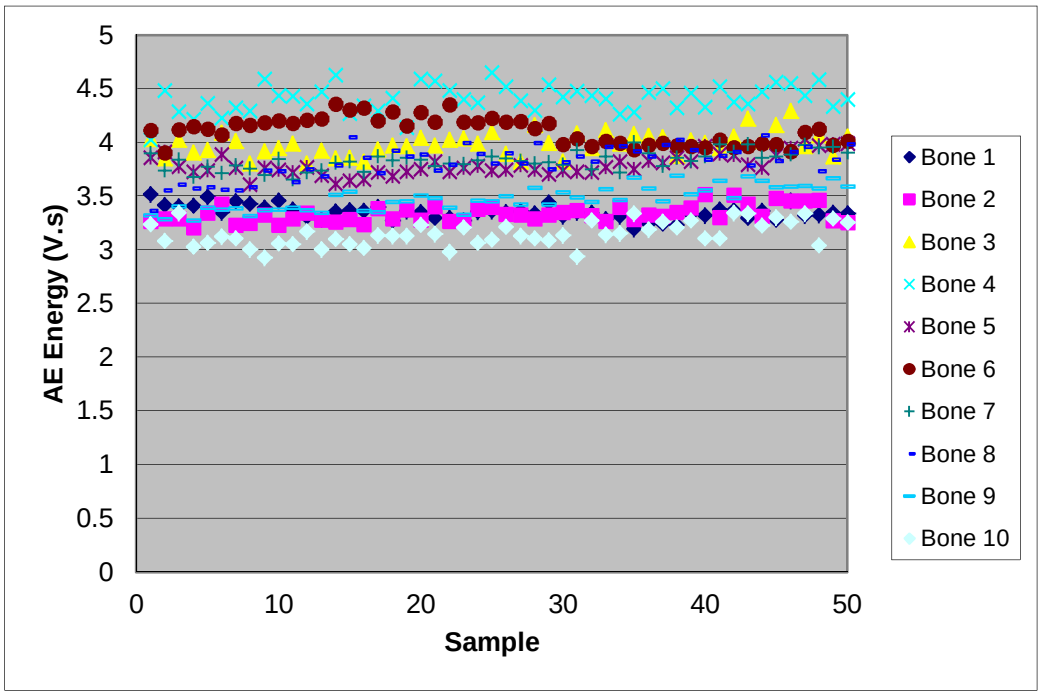

(b)

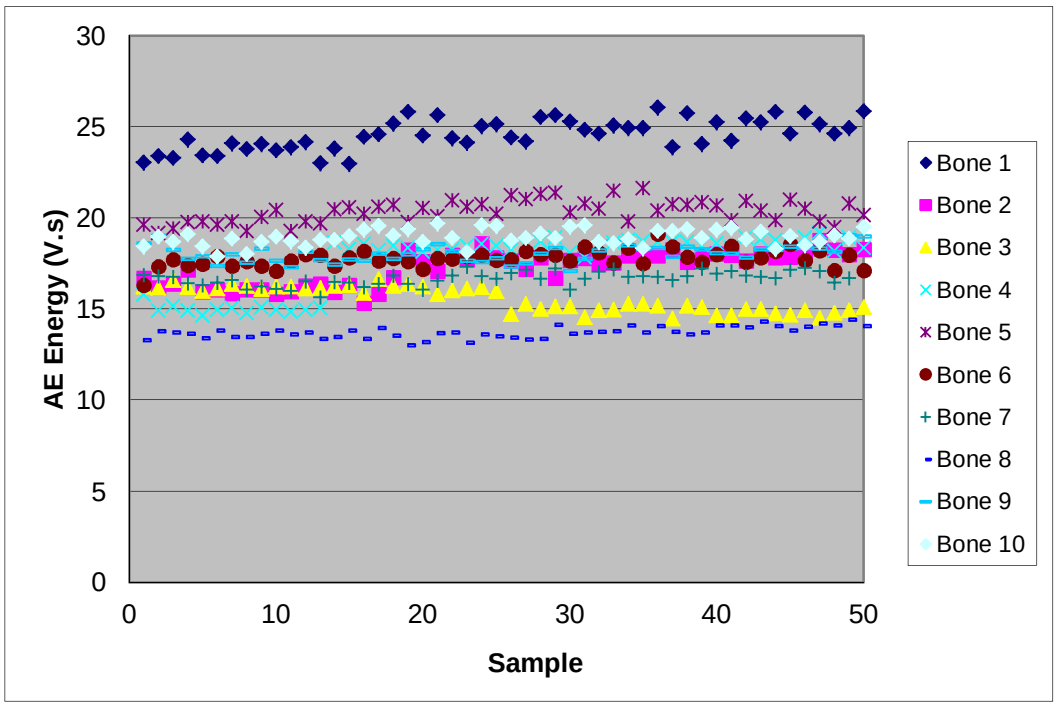

(c)

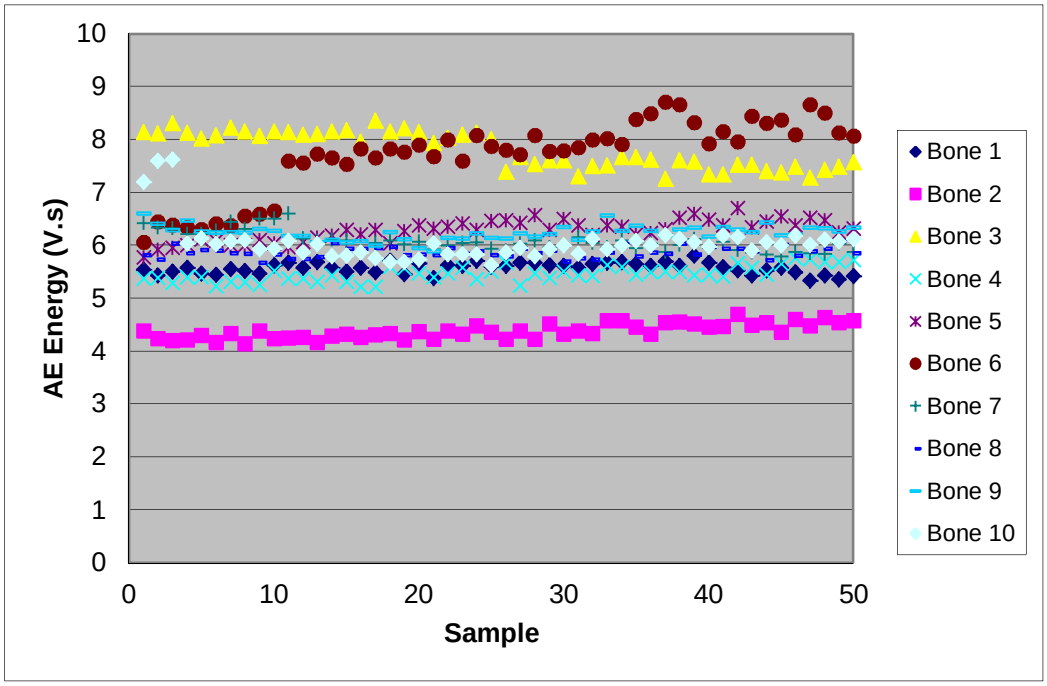

(d)

Figure 4.17: Variation in transmitted energy with time for air jet source: (a) 8.5mm implant in tight fitting conditoin, (b) 8.5mm implant in loose fitting condition, (c) 13mm implant in tight fitting condition, (d) 13mm implant in loose fitting condition

Figure 4.18 shows the frequency ratios, arranged to highlight the differences between tight and loose and large and small fittings. Comparison with Figure 4.14 for the pencil lead source shows the air jet to give rise to 2% variation within a given bone sample although the variation between samples with the same fitting condition remains large. Unlike the case for the pencil lead, the air jet source seems to be able to discriminate between tight and loose fittings for both sizes, but was less clearly able to discriminate between sizes for either tight or loose fittings.

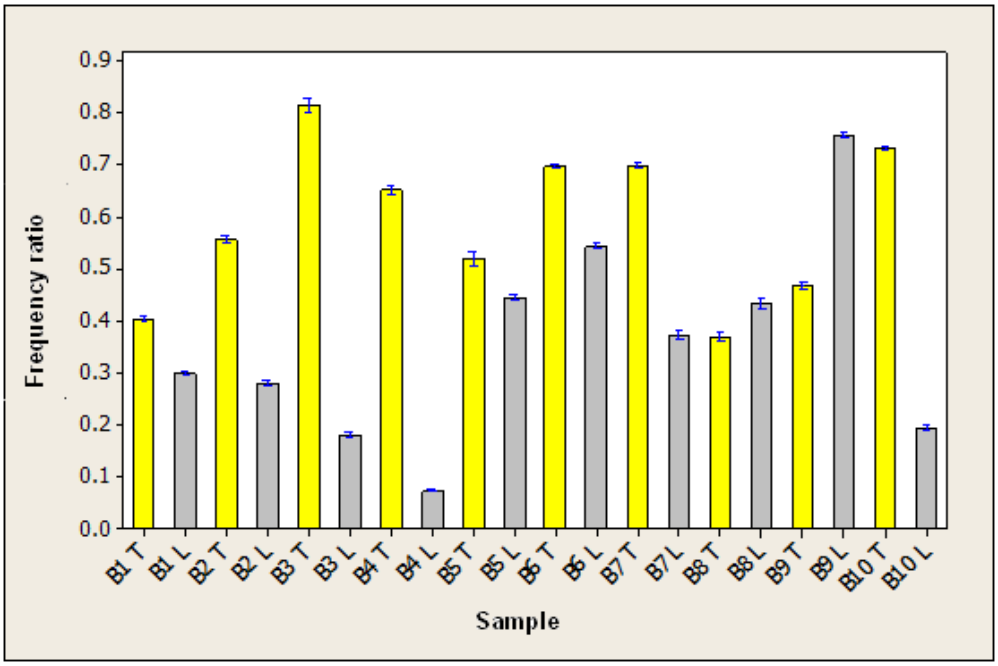

(a)

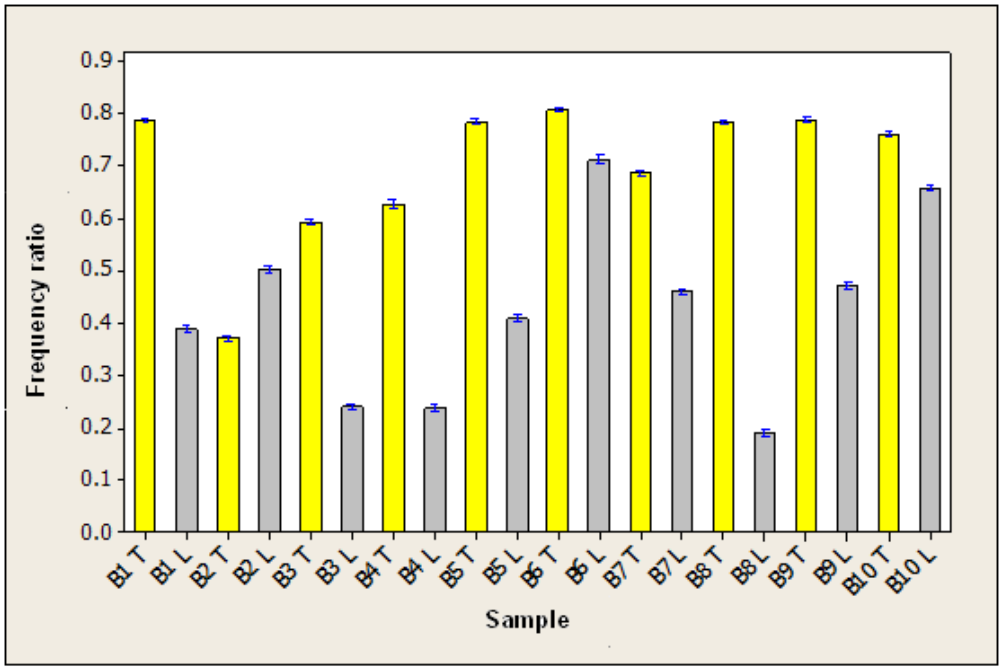
Frequency ratio
0.0
0.1
0.2
0.3
0.4
0.5
0.6
0.7
0.8
0.9
B1 T
B1 L
B2 T
B2 L
B3 T
B3 L
B4 T
B4 L
B5 T
B5 L
B6 T
B6 L
B7 T
B7 L
B8 T
B8 L
B9 T
B9 L
B10 T
B10 L
Sample

(b)

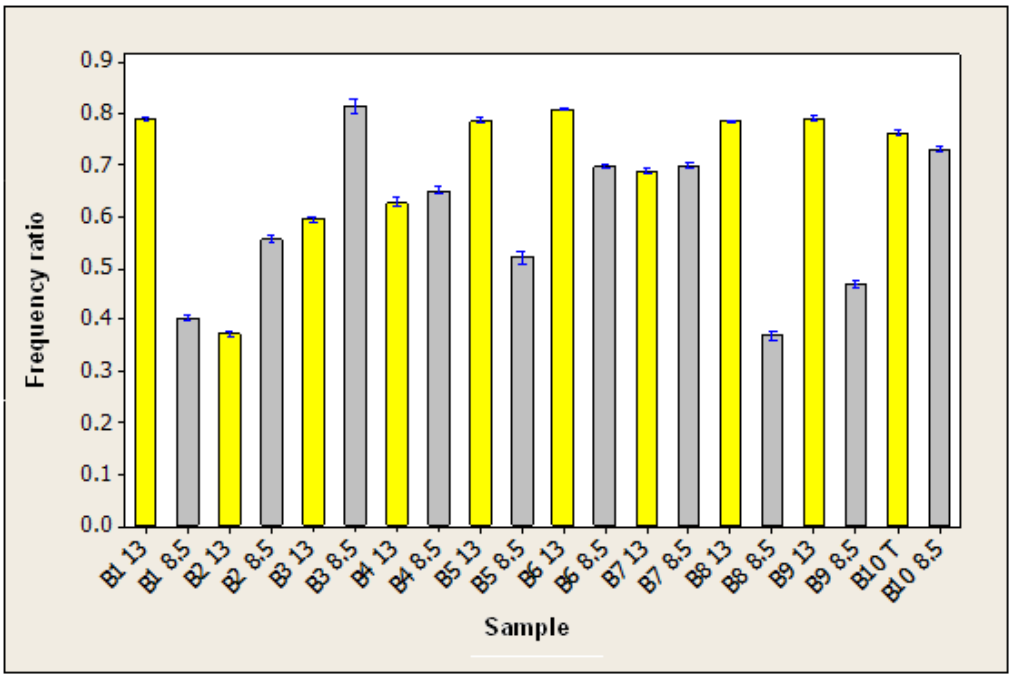
Frequency ratio
0.0
0.1
0.2
0.3
0.4
0.5
0.6
0.7
0.8
0.9
B1 13
B1 8.5
B2 13
B2 8.5
B3 13
B3 8.5
B4 13
B4 8.5
B5 13
B5 8.5
B6 13
B6 8.5
B7 13
B7 8.5
B8 13
B8 8.5
B9 13
B9 8.5
B10 T
B10 8.5
Sample

(c)

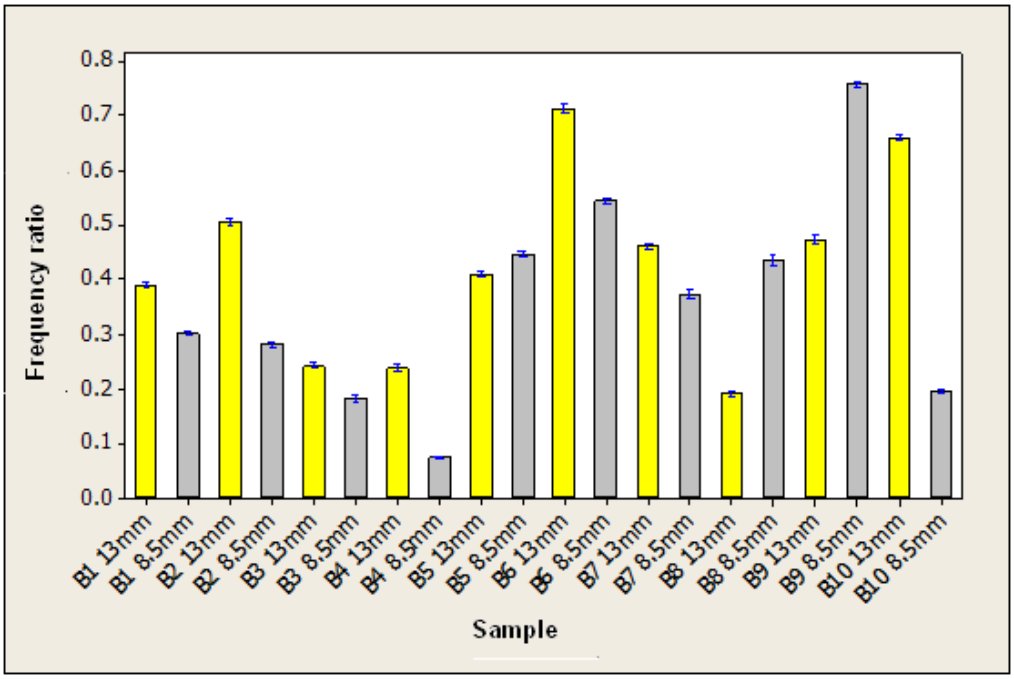

(d)

Figure 4.18: Frequency ratios with air jet source: (a) 8.5mm implant in tight vs. loose fitting condition, (b) 13mm implant in tight vs. loose fitting condition, (c) 8.5mm vs. 13mm implants in tight fitting condition, (d) 8.5mm vs. 13mm implants in loose fitting condition (B = Bone)

ANOVA showed the P values for comparison between sizes and fitting conditions were less than 0.05 confidence level in all cases, showing that there was discrimination between tight and loose fittings and also between large and small fittings (Table 4.8).

	8.5mm T vs. L	**13mm T vs. L**	**T 8.5mm vs. 13mm**	**L 8.5mm vs. 13mm**
P Value	3.53×10^{-86}	3.8×10^{-130}	6.89×10^{-33}	7.51×10^{-10}

Table 4.8: Summary of ANOVA for frequency ratios of high frequency bands with air jet source

Again, in order to assess the consistency of the air jet source over time, the individual 0.01s values are plotted in temporal order in Figure 4.19. As for the energy (Figure 4.17), the R^2 and the slope a of the regression lines ($y = ax + b$) were determined (summarized in Appendix F) and, again, the majority of a and R^2 values were close to zero, indicating that the time effect was small. However, examination of Figure

4.17 shows the value of the frequency ratio to be oscillating over time, which suggests that some other frequencies are present.

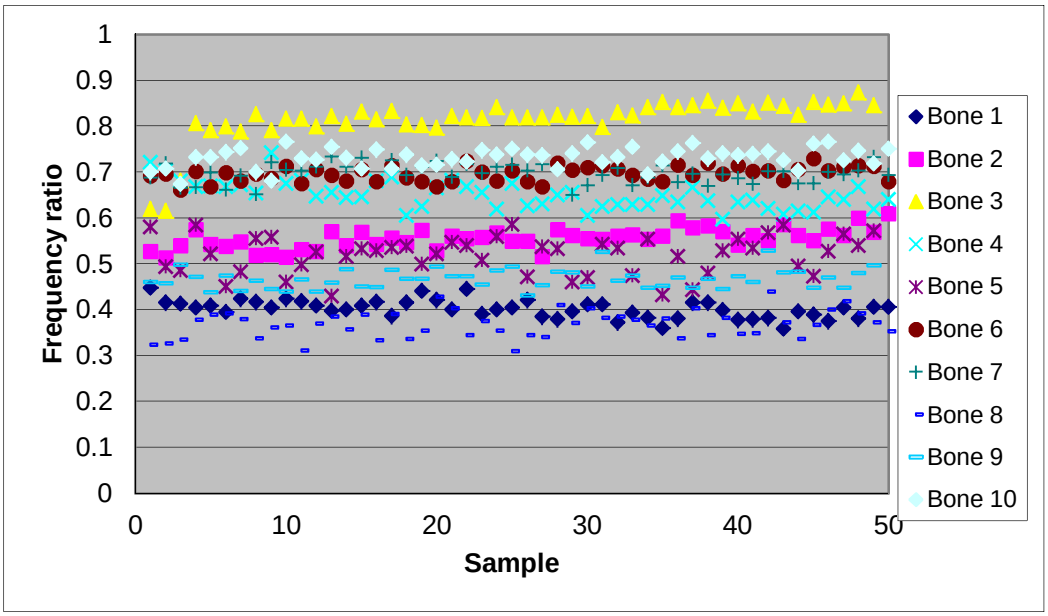

(a)

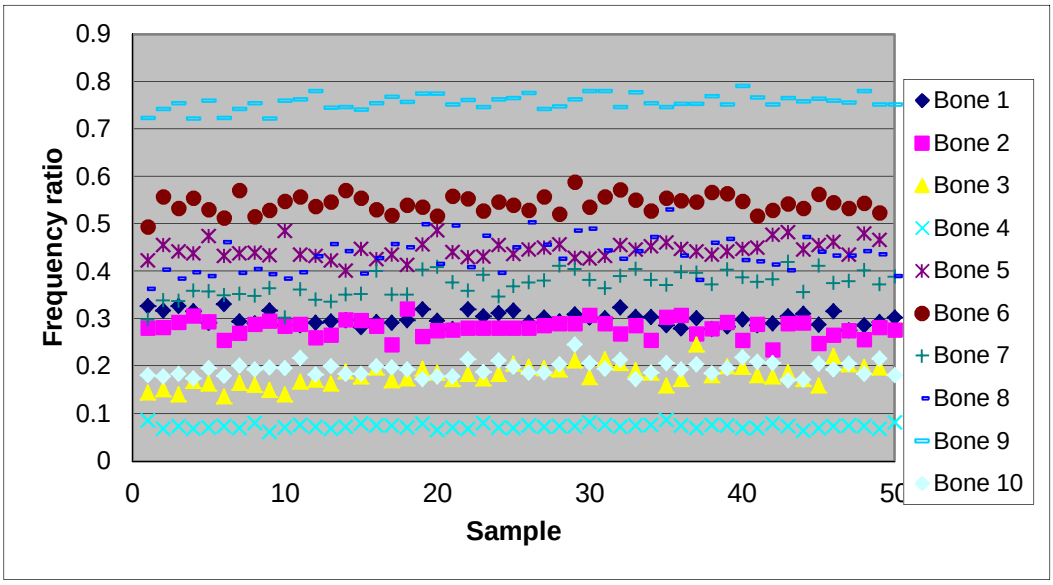

(b)

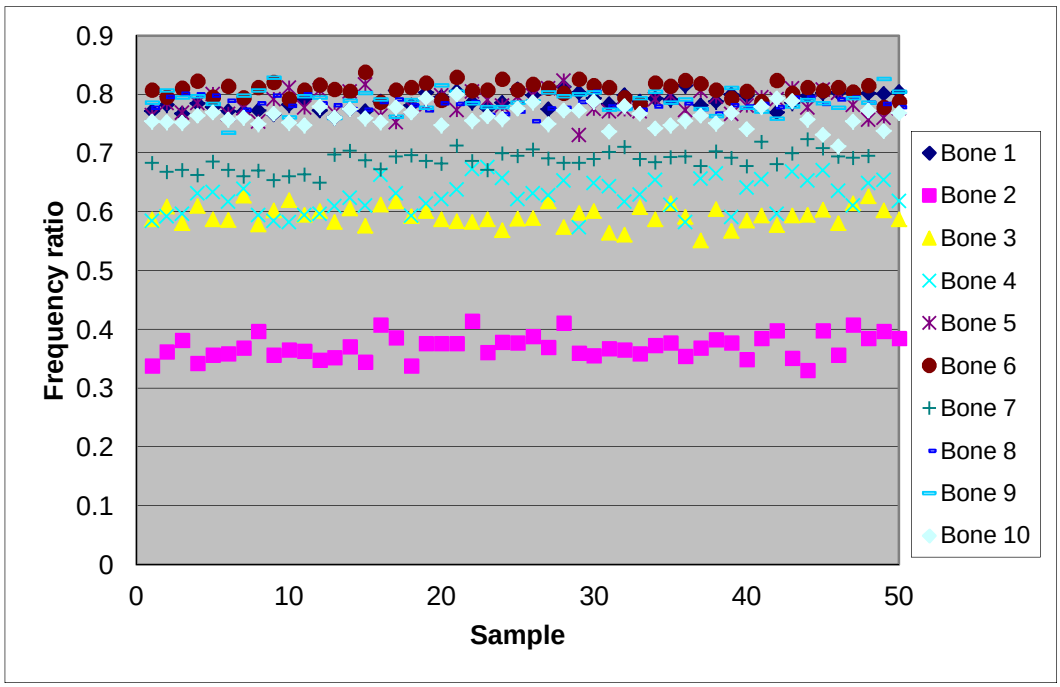

(c)

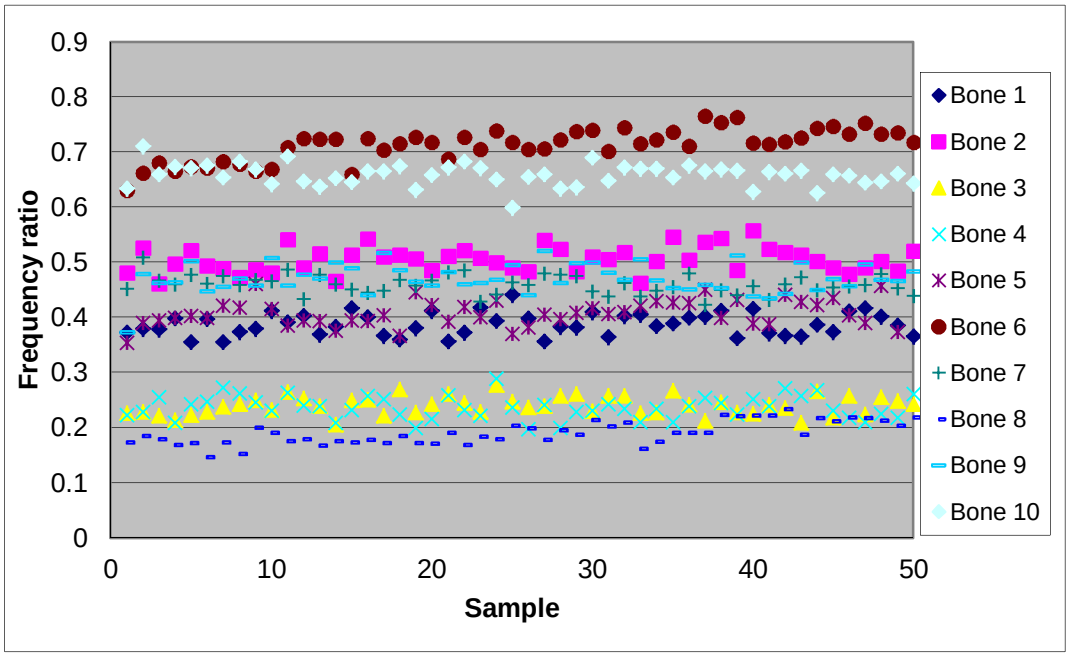

(d)

Figure 4.19: Variation in frequency ratio with time for of air jet source: (a) 8.5mm implant in tight fitting condition, (b) 8.5mm implant in loose fitting condition, (c) 13mm implant in tight fitting condition, (d) 13mm implant in loose fitting condition

Following from the observations in Figure 4.19, the frequency structures of the transmitted air jet signals were further analysed, by averaging the signals with a range of averaging times. This has the effect of revealing frequencies lower that the

filter cut-off of 100 kHz, a technique known as demodulated resonance analysis. Two different averaging times were used to reveal frequencies in the mid-range (up to 50 kHz and in the low range (up to 10 kHz). The resulting spectra were complex and, to simplify the analysis, each of the ranges was divided into bands and the heights of the significant spectral peaks within that band was added together as an indicator of the energy in the band. Figure 4.20(a) shows the sum of peaks in the five frequency bands used for the mid-frequency range and, as can be seen, between 60 and 70% of the energy is in the band below 10 kHz. Figure 4.20(b) shows a further breakdown of the low frequency range (below 10 kHz), showing the energy to be fairly evenly spread across the three lower bands. Despite this clear frequency structure, there seems to be little in these lower frequency bands to distinguish between the various fitting conditions, the only possible indication being that the loose fitting showed a higher proportion of mid-frequency energy in the band below 10 kHz.

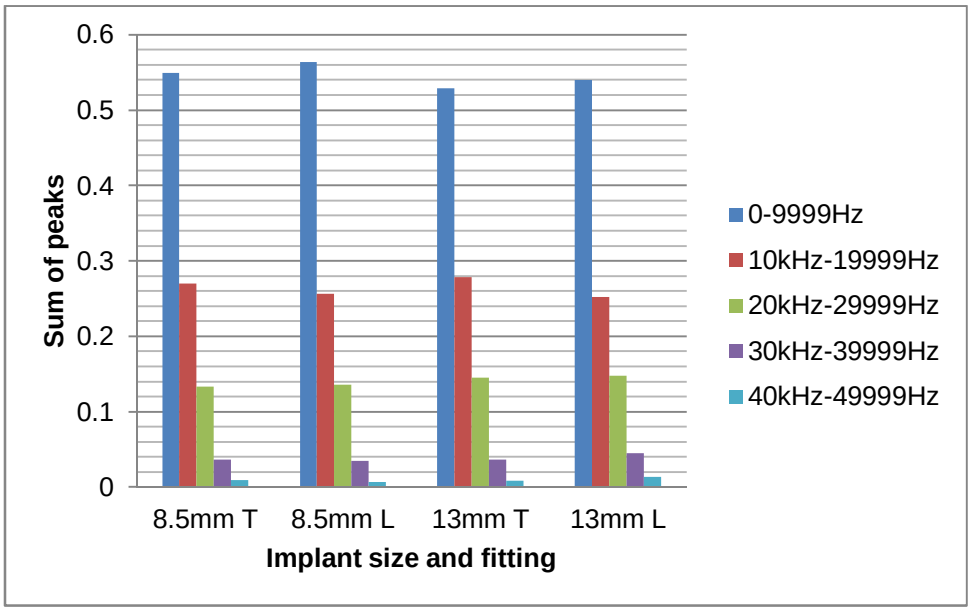

(a)

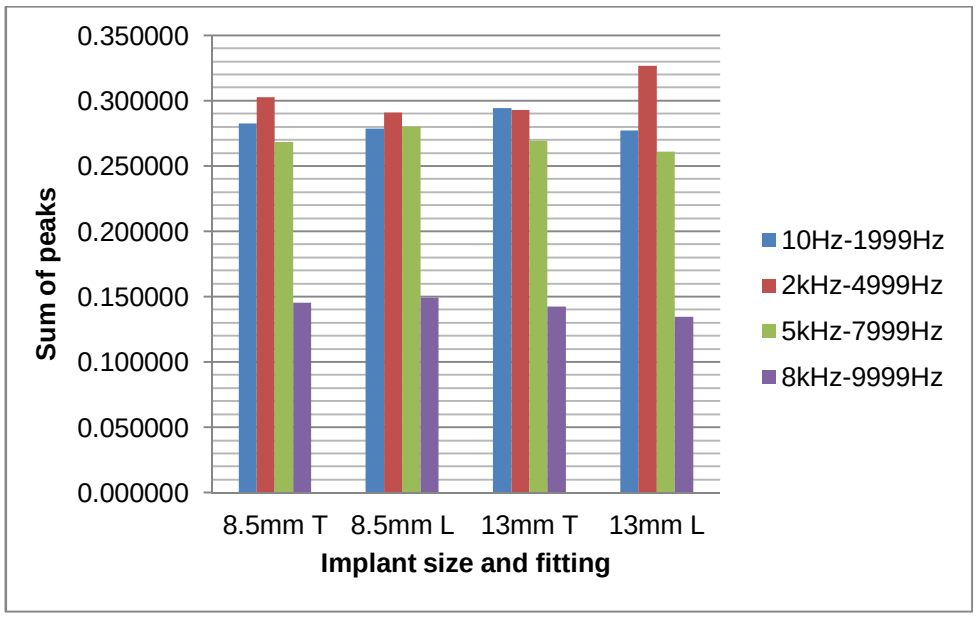

(b)

Figure 4.20: Demodulated analysis of transmitted air jet signals: (a) Mid-range frequency bands 0 – 49999Hz, (b) Low frequency bands 10 – 9999Hz. (Bar heights are cumulative over 10 – 20 records)

4.6 Deployability of the air jet source *in vivo*

Although the *in vivo* tests did not contain a controlled variable for interface quality, the same analytical tools were used to assess the characteristics of the AE signals as those for the air jet source in the previous section. This allowed an assessment of the effect of the various uncontrolled variables associated with working with living subjects in a chairside environment on the measures which have been used to distinguish the quality of the interface in the *in vitro* experiments.

Figure 4.21 shows the means and standard deviations of the 30 AE energy recordings for each of the two mountings per participant. Clearly the transmitted energy varied significantly between participants and this pattern was the same for each mounting of the sensor.

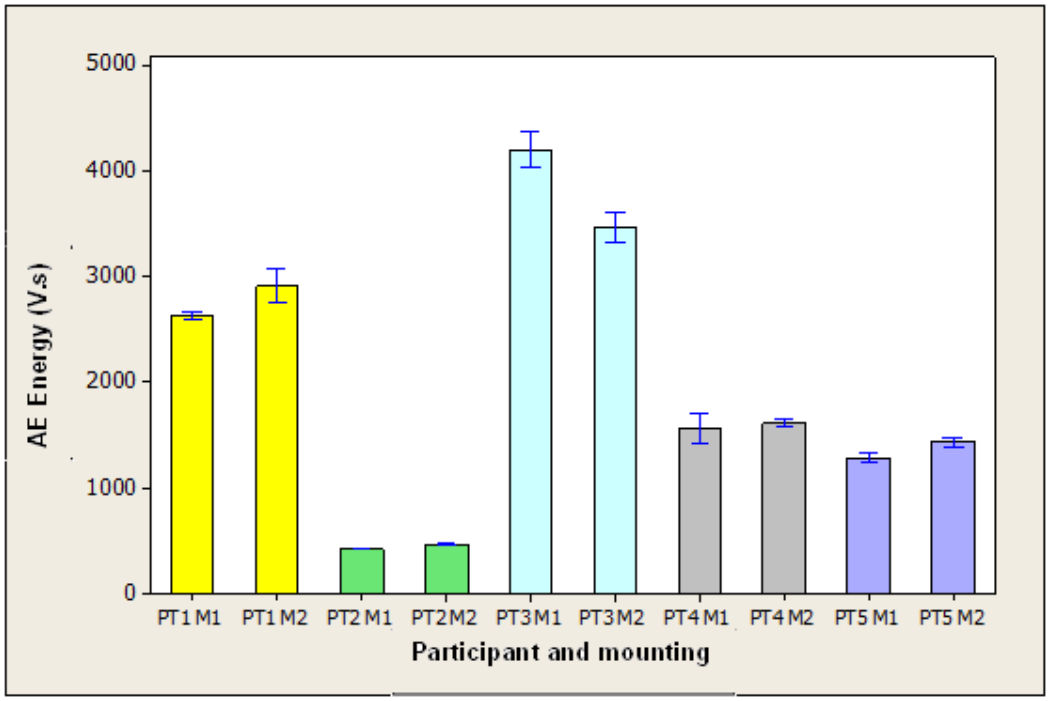

Figure 4.21: Transmitted AE energy for *in vivo* tests (PT = participant, M = mounting position)

ANOVA was carried out to examine the effect of the AE sensor mounting, by comparing all 30 records for M1 and M2 for each participant. The P-values are shown in Table 4.9, indicating a significant difference between M1 and M2 (except for Participant 4).

	PT1	**PT2**	**PT3**	**PT4**	**PT5**
P-Value	0.000823	1.32×10^{-10}	4.01×10^{-09}	0.55906	9.63×10^{-06}

Table 4.9: ANOVA for effect of mounting on transmitted AE energy *in vivo* (PT = participant)

Figure 4.22 shows the frequency ratios (high frequency range) for the in vivo tests. As with the energy, there are distinct differences between the participants, although these are less clearly indicated over the variation between mountings than was the case with energy.

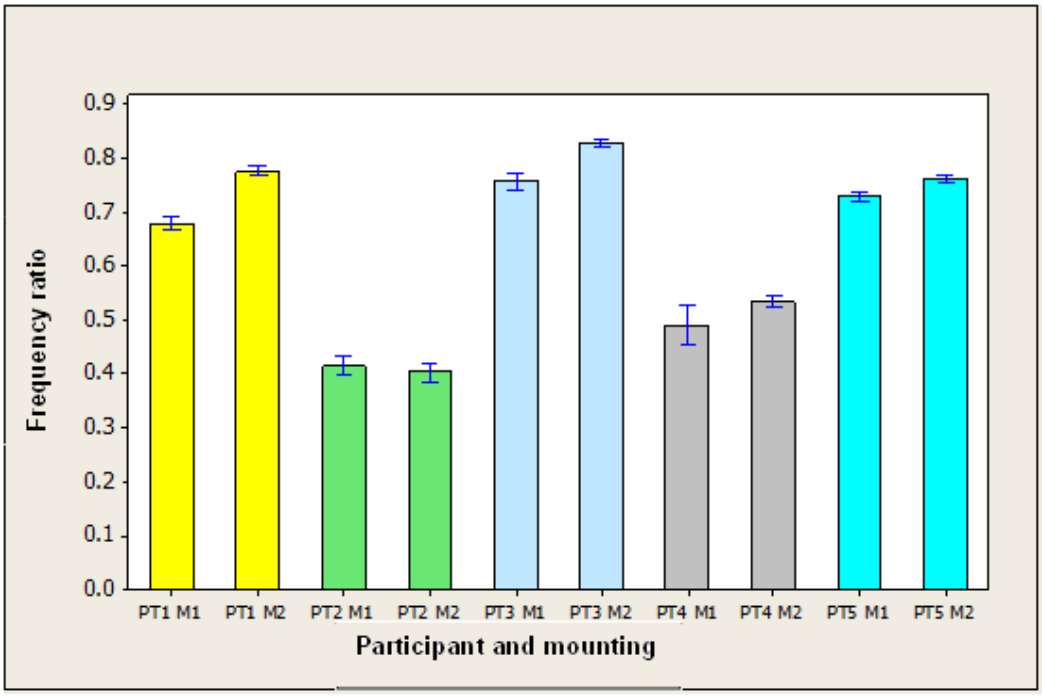

Figure 4.22: Transmitted frequency ratio (high frequency) for *in vivo* tests (PT = participant, M = mounting position)

ANOVA between M1 and M2 for each participant showed P-values as summarised in Table 4.10 which indicated a significant difference between mountings for all but Participant 2. Also, the data were re-grouped per participant (both mountings) and the participants tested against each other, yielding a P-value of 5.20×10^{-171}, which indicates significant differences between each participant.

	PT1	**PT2**	**PT3**	**PT4**	**PT5**
P-value	1.86×10^{-19}	0.340764	2.51×10^{-13}	0.022018	2.48×10^{-06}

Table 4.10: ANOVA for effect of mounting on transmitted AE frequency ratio *in vivo* (PT = participant)

As for the *in vitro* air jet tests, it was necessary to assess the consistency of the input, especially given that the time interval between each record was on average 7 to 10 seconds.

Figure 4.23 shows 30 AE energy recorded with time interval of 30 seconds for each of the mountings for each of the participants, and Table 4.11 summarises the linear

regression functions. As can be seen, most of the R^2 values are close to 1, indicating a clear trend, and 6 out of the 10 values of *a* are large positive figures, indicating that the energy increased with time. In one case (Participant 5, Mounting 2) there was a small decrease in energy with time.

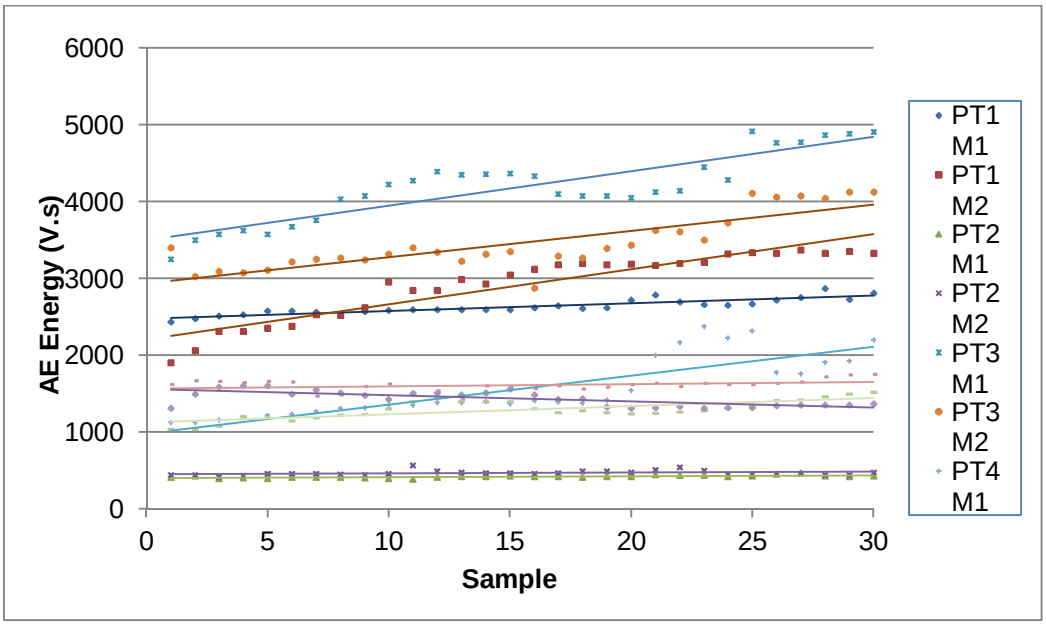

Figure 4.23: Change in transmitted AE energy with time for *in vivo* air jet tests (PT = participant, M = mounting position)

AE Energy Linear Regression		
	Function	**R^2**
PT1 M1	y = 10.135x + 2476.6	0.8125
PT1 M2	y = 45.701x + 2208.5	0.8830
PT2 M1	y = 1.275x + 404.81	0.4537
PT2 M2	y = 0.9253x + 460.67	0.0680
PT3 M1	y = 44.829x + 3505.2	0.7689
PT3 M2	y = 34.406x + 2935.9	0.6941
PT4 M1	y = 37.61x + 989.49	0.7208
PT4 M2	y = 2.9491x + 1569.3	0.1244
PT5 M1	y = 10.666x + 1130	0.5470
PT5 M2	y = -8.0717x + 1563.2	0.5121

Table 4.11: Trend in AE energy with time for *in vivo* air jet tests (PT = participant, M = mounting position)

Figure 4.24 shows the corresponding time evolution of frequency ratio for the in vivo air jet tests, and the functions are summarised in Table 4.12. This time the R^2 values were generally small, indicating that there was not a strong trend, although 7 out of the 10 values of *a* were again positive, indicating that the frequency ratio increases with time, albeit weakly.

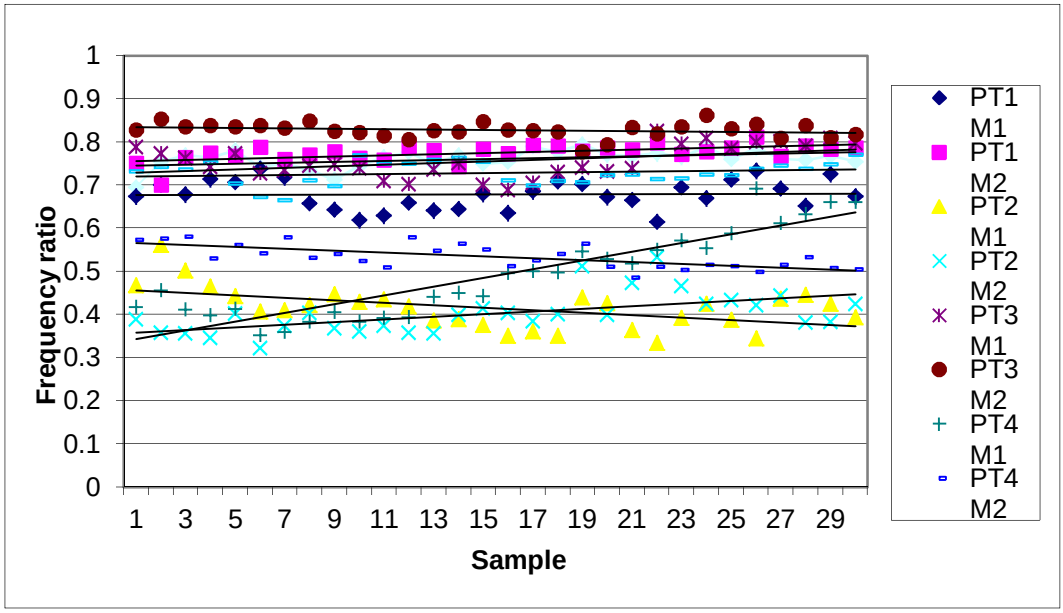

Figure 4.24: Change in transmitted AE frequency ratio with time for *in vivo* air jet tests (PT = participant, M = mounting position)

Frequency Ratio Linear Regression		
	Function	**R^2**
PT1 M1	y = 0.0001x + 0.6764	0.0009
PT1 M2	y = 0.0013x + 0.7551	0.3231
PT2 M1	y = -0.0029x + 0.4589	0.2683
PT2 M2	y = 0.0031x + 0.3549	0.3197
PT3 M1	y = 0.0018x + 0.7279	0.1856
PT3 M2	y = -0.0005x + 0.8353	0.0588
PT4 M1	y = 0.0102x + 0.3327	0.8221
PT4 M2	y = -0.0022x + 0.5682	0.4786
PT5 M1	y = 0.0006x + 0.7195	0.0366
PT5 M2	y = 0.0011x + 0.7446	0.1872

Table 4.12: Trend in AE frequency ratio with time for *in vivo* air jet tests(PT = participant, M = mounting position)

Finally, the *in vivo* test results were also subjected to demodulation using the same methods as for the *in vitro* air jet tests and the results are shown in Figure 4.25.

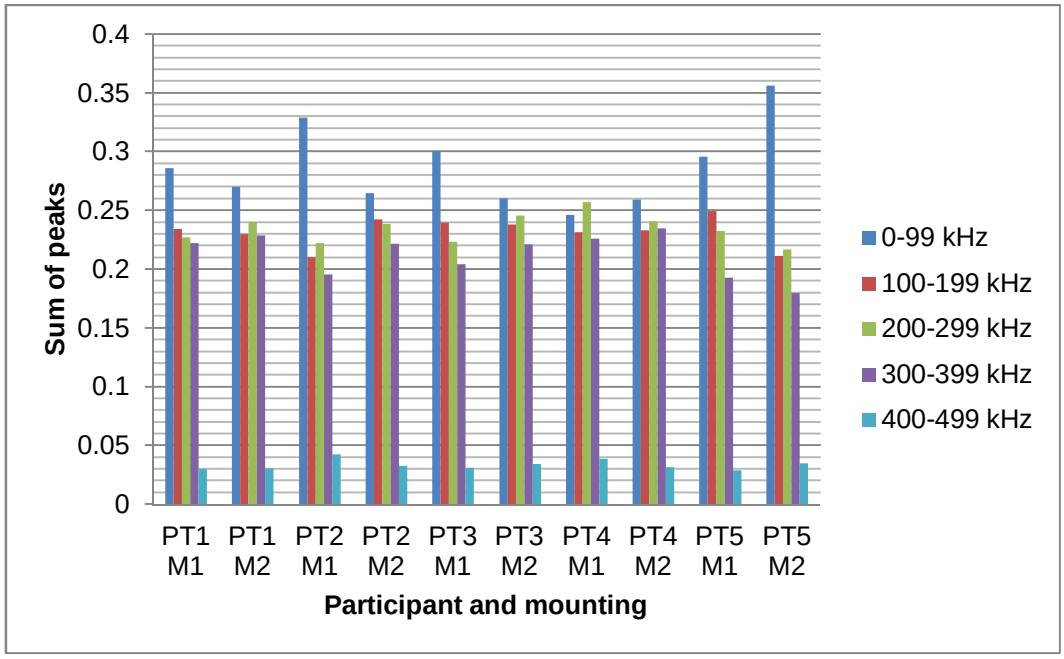

(a)

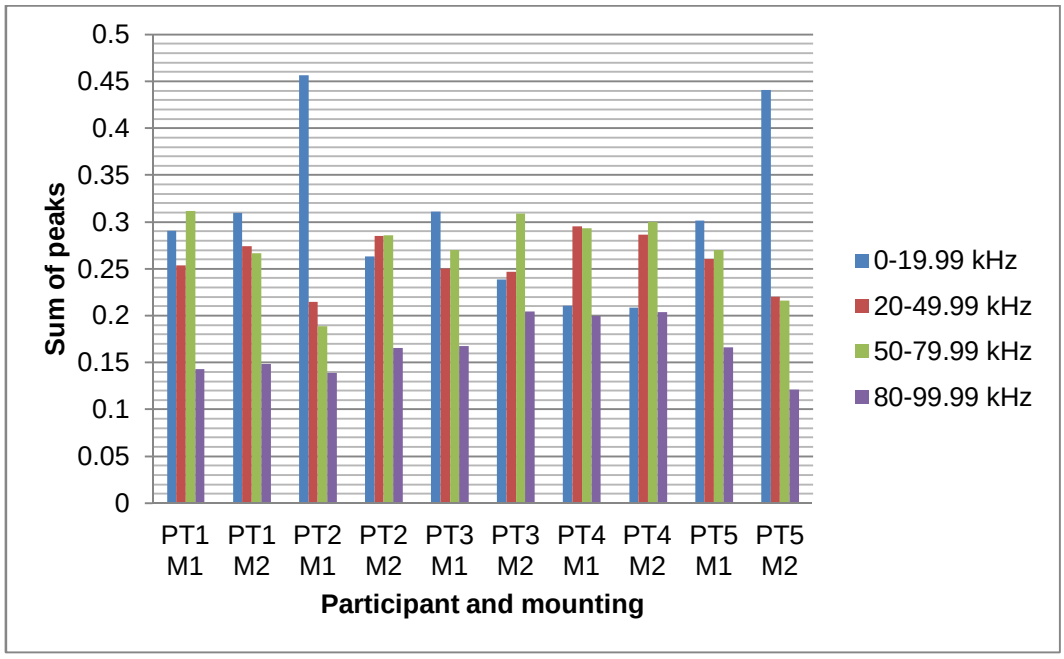

(b)

Figure 4.25: Demodulated analysis of air jet signals of the *in vivo* tests (a) Low frequency bands of 0-499 Hz; (b) Low frequency bands of 0-99.99 Hz (PT = participant, M = mounting position; bar heights are cumulative over 10 – 20 records)

The data is regrouped by frequency bands, ANOVA analysis was carried out to compare the signals between participants. The P-values are shown in Table 4.13 below, all are higher than 0.05 confidence level indicating no significant differences, except for frequency band 300 to 399 kHz.

Med-range frequency bands					
	0 - 99 kHz	100 – 199 kHz	200 – 299 kHz	300 – 399 kHz	400 – 499 kHz
P-values	0.332786	0.945742	0.434463	6.28×10^{-6}	0.551648
Low frequency bands					
	0 – 19.99 kHz	20 – 49.99 kHz	50 – 79.99 kHz	80 – 99.99 kHz	
P-values	0.357238	0.444003	0.477265	0.109671	

Table 4.13: Summary of ANOVA for sum of peaks *in vivo*

This part of the study was designed to assess the feasibility of transmission of AE signals generated by the air jet source applied on the implant *in vivo*, and to assess the variables that affect the transmission in each participant and the variability of transmission between individual participants and between individual integrated dental implants. It was not expected that any conclusions could be drawn about the stability or degree of integration of the implants on these participants; rather it was expected that any factors preventing application of the findings with the bovine bone models would be identified prior to a more extended study on participants with demonstrably different levels of integration.

The participant variables were scored from 0 to 5 (0 = minimum and 5 = maximum) as shown in Table 4.14, in order to give some figures to correlate with the energy and frequency ratio.

	PT 1	**PT 2**	**PT 3**	**PT 4**	**PT 5**
Difficulty of sensor placement	1	4	1	2	2
Thickness of soft tissue	2	4	2	2	3
Saliva level	1	3	1	2	2

General movement	2	4	1	3	1
Movement of tongue	2	4	1	2	3
Implant size	5	4	3	3	3
Total Score	**13**	**23**	**9**	**14**	**14**

Table 4.14: Participant variable scores

Figure 4.26 shows the relationship between the average transmitted AE energy and total participant score, which indicates that all of the patient variables influence the transmitted energy, assuming equal weighting between the variables. The strength of the effect is indicated by the slope, which is negative and the significance of the correlation by the R^2 value of almost 0.8. Figure 4.27 shows the individual effects of the scores, and it can be seen that the three strongest negative effects on transmitted energy are associated with the difficulty of placing the sensor and the participants' tongue and general movements. This gives a clear indication that some attention needs to be paid to making the application less intrusive for a patient. A high score on saliva level led to lower transmission of AE, which might be expected since an increase in the saliva level would lead to increase in participant's movement and hence impact on the transmission. This uncontrolled variable could be eliminated by the use of swabs of by irrigation during deployment of the test on a patient. The amount of patient soft tissue, as expected, reduced the amount of transmission, but this was a relatively weak effect in the face of the other participant-related variables. Finally, the larger implant sizes transmitted more energy (as was found in the *in vitro* tests). Again, this effect was quite weak, pointing to the need to reduce the uncontrolled participant-related variables in order to interrogate the interface using transmitted AE energy.

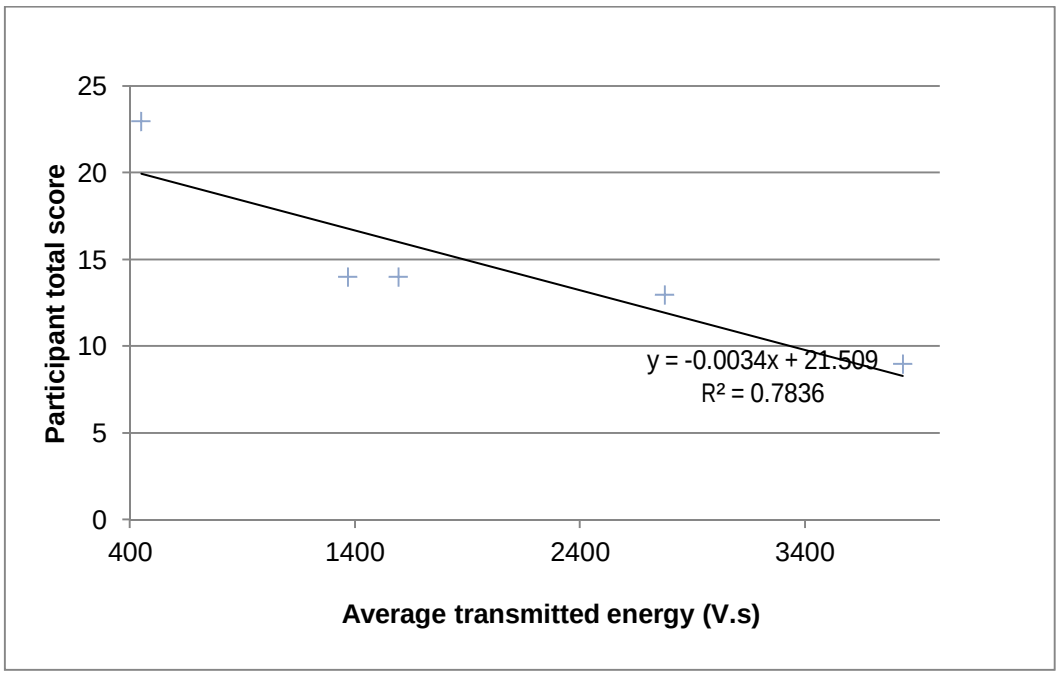

Figure 4.26: Effect of total participant score on transmitted AE energy

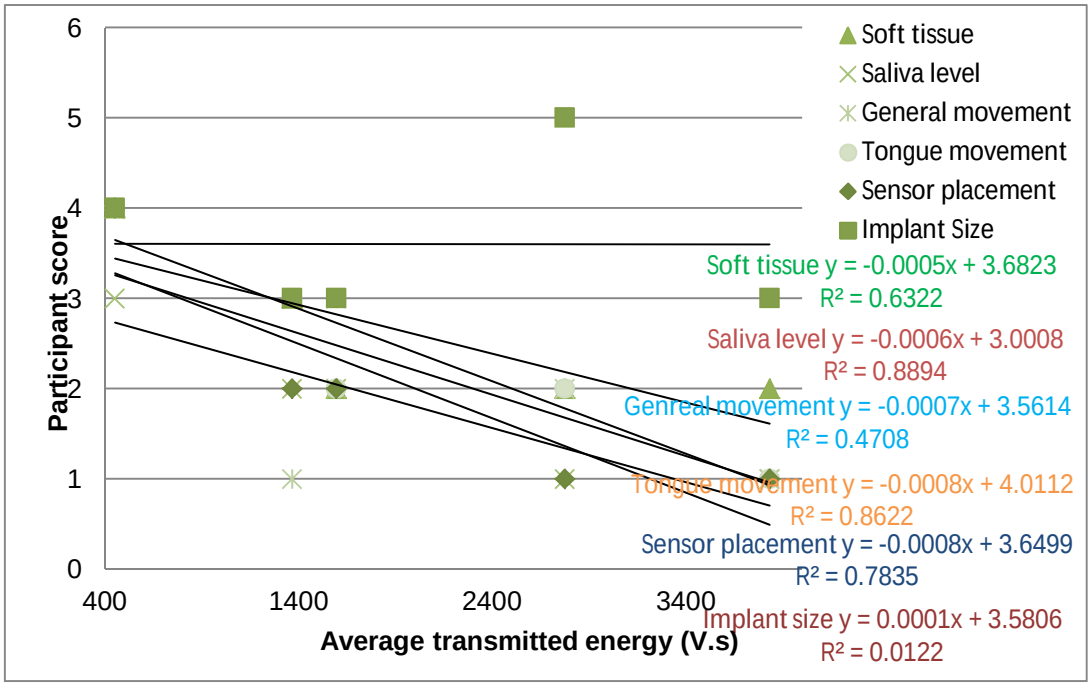

Figure 4.27: Effect of individual participant scores on transmitted AE energy

Figures 4.28 and 4.29 show the corresponding correlations between the patient variables and frequency ratio. As with energy, the frequency ratio reduces with total score and there is a similar ranking and sense of effect of the individual scores. This

is a useful general finding, since it indicates that frequency ratio might be a substitute for energy in an *in vivo* deployment, which would make some of the issues of calibration easier to surmount.

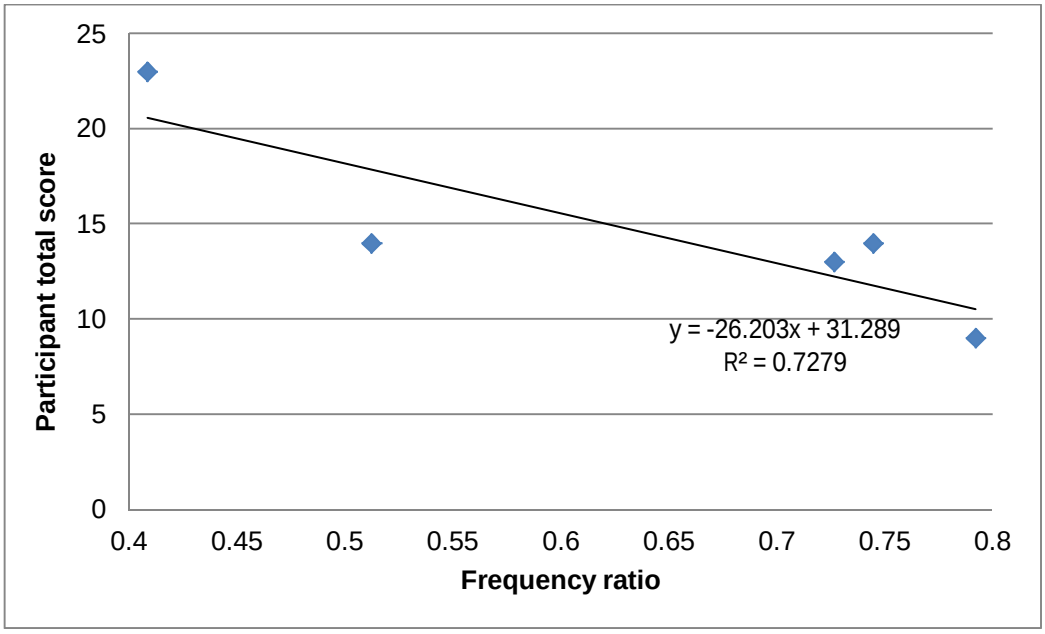

Figure 4.28: Effect of total participant score on transmitted AE frequency ratio

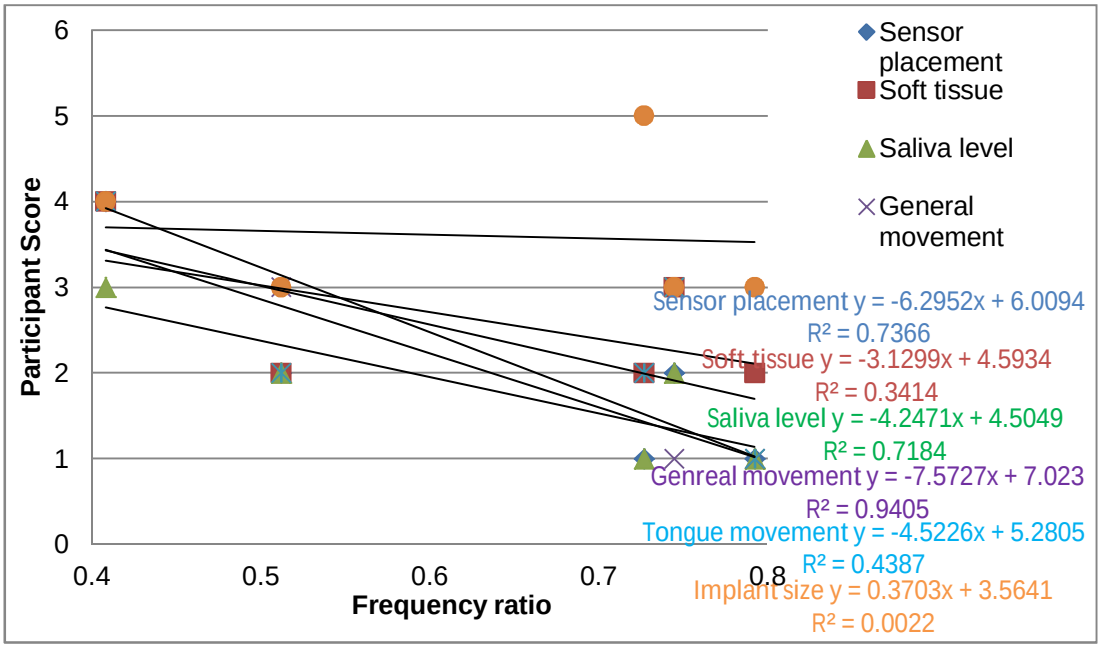

Figure 4.29: Effect of individual participant scores on transmitted AE frequency ratio

Finally on the matter of transmission, Figure 4.30 compares the transmission from the air jet source to the sensor in the systematic interface tests and the *in vivo* tests. The values shown are the average AE transmission per second of air jet flow and the averages for the bone tests are over all implant conditions for each of the samples of fresh bone. Equally, the averages for the *in vivo* tests are for both installations of the sensor over the full time range of the tests. Notwithstanding the fact that each of the bars in Figure 4.30 contains significant random and systematic variation (each of which is discussed in detail later), the data contain some useful findings about the transmission of AE in bone and flesh. First of all, the average transmission in the human subjects is about twice what it is in the bovine bones. There are a number of possible reasons for this, the two most likely being that the degree of hydration in the living subjects is likely to be, on average, better than it is for the fresh bones and that the interfaces in the human subjects is, as far as is known, in good condition. The comparison also indicates that the impediment to transmission offered by living flesh is not likely to be a limiting factor in the use of the technique, as is assumed, for example, by Stark *et al.* (2012). This is a significant advantage of AE over vibration for in vivo monitoring, as a number of authors (Qi *et al.* 2007) (Rowlands *et al.* 2008) have cited damping of vibrations as an impediment to the use of vibrometry for detecting implant loosening.

The other obvious finding form Figure 4.30 is that subject-to-subject variability is considerably greater for the living human subjects than for the bovine bones. This variability is studied in more detail in the following sections.

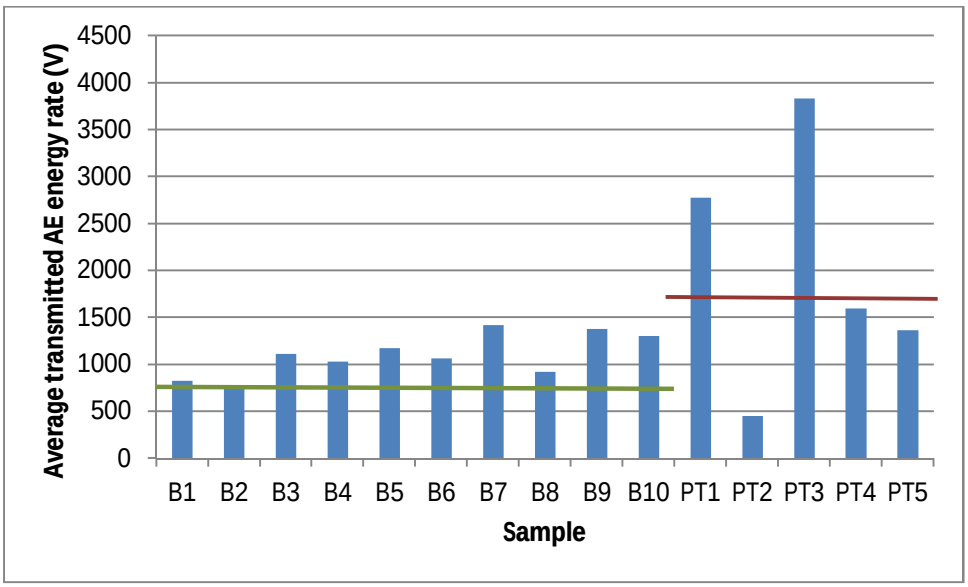

Figure 4.30: Average transmitted AE energy per second running of air jet source for *in vitro* bone implant tests and *in vivo* tests. Red line represents average for all human subjects, green line represents average for all bone samples.

4.7 Sources of AE

At the feasibility stage, several methods were assessed for their ability to generate AE signals in the oral cavity. Two instruments already in clinical use to measure tooth mobility were evaluated, the Hammer Impact Device (Elias *et al.* 1996), and the Periotest (Schulte *et al.* 1983), and, although the impact forces produced are harmless to the tooth structure, they did not produce sufficient AE because the rate of application of the load is not high enough. More success was found with fracture sources and biting on almonds, peanuts and carrots provided a range of sources, whose structure appeared to be dependent on the food type, harder more brittle foods producing much higher AE energy, concentrated into shorter bursts. Whereas each food type tested was reasonably reproducible, it is unlikely that this could constitute a reliable, reproducible standard source.

ASTM standards list a range of AE sources, some continuous and some discontinuous. Generally, discontinuous sources are preferred by researchers because the propagation of an impulse can be better tracked as it crosses a material (such as was done in the production of Figure 4.3). However, it was not considered desirable

to use fracture of a brittle material such as a glass capillary or pencil lead in the mouth and, as discussed above, biting on brittle foods is not sufficiently reproducible to use as a standard. Also, the available percussive devices did not produce a rapid enough rise time, which is perhaps the reason why these do not feature in standards for AE sources. This left a source based on the impingement of a high-speed gas stream as the most likely applicable approach for *in vivo* use.

The air jet source was based on the (standard) helium jet source, adapted to make use of the ubiquitous dental compressed air supply and to provide a reproducible means of delivery to an implant via a custom-built abutment. A potential advantage of continuous sources over discontinuous sources is that the input has a more complex structure which may be of use in probing the interface. The two measures used for pencil lead, AE energy and raw AE frequency ratio, could also be used for the air jet source, but successive demodulation also showed the air jet to contain a number of other characteristic frequencies obtained through demodulation. The spectrum was divided up into a number of bands and the total energy in each of these bands was characteristic of the source, but did not appear to vary in any systematic way with the condition of the implant in the *in vitro* or *in vivo* tests. On the positive side, however, the air jet source gave better discrimination of implant interface condition than did the pencil lead AE energy and raw AE frequency ratio.

The stability of the AE source for the *in vitro* tests was good, with no systematic change with time in either of the diagnostic indicators (AE energy and frequency ratio) over the time required to obtain 50 × 0.01s records (around 2½ minutes). For the *in vivo* tests, the stability was less good for the AE energy, increasing systematically with time by up to 50% over the time required to obtain 30 × 1s records (around 5 minutes), although the stability of the frequency ratio was much better. It is possible that the increase in energy was attributable to patient-related factors (e.g. salivation or sweating, which may have improved transmission) but changes in the notes of the source were also detected which point to the air supply not being sufficiently consistent.

Many of the applications of AE in implant monitoring are passive, in that the source is self-generated, for example by micro-fracture of cement particles or components (e.g. Roques *et al*., 2004 and Li *et al*., 2011). Such studies usually detect progressive damage by cumulative AE energy produced in an idealised geometry and rarely consider the propagation of the AE in a potential real situation. However, there is nothing to suggest that the sources are any weaker than a pencil lead fracture, so the findings of this work are of some relevance to the applicability of passive sensing. Recently, it has been suggested that the entire interface of a femoral implant could be monitored using embedded AE sensors, although the current work would tend to suggest that this might even be possible without embedding the sensors (Mavrogordato *et al.* 2011).

4.8 Using AE to interrogate the interface

The main series of experiments on the use of AE to distinguish between the two sizes of implant and between loose and tight fitting are summarised in Figures 4.13 and 4.14 for the pencil lead source and in Figures 4.16 and 4.18 for the air jet source.

As shown by the ANOVA, AE energy was found to discriminate adequately between the different implant conditions, as summarised in Table 4.15 for the pencil lead source and Table 4.16 for the air jet source. For a given bone, the transmitted energy was always reduced when the implant was loosely fitted for a given size and always reducing for a given tightness for the smaller fitting. The effect of tightness was typically to reduce the energy by about 50% when using the pencil lead source and by about 65% for the air jet source. The variation in the amount of change between bones was substantial for the pencil lead and rather less for the air jet. Also, the variation within a given category (e.g. 8.5mm tight) was also substantially less for the air jet source. Thus, it can be said that the air jet source was superior to the pencil lead source for interrogating the interface.

	Tight → Loose	**Within tight**
8.5 mm implants	-48% (-70% to -17%)	±46%
13 mm implants	-46% (-72% to -24%)	±32%

	13mm → 8.5mm	Within 13mm
Tight	-54% (-78% to -14%)	±32%
Loose	-51% (-76% to -18%)	±20%

Table 4.15: Change in AE energy transmitted from a pencil lead break when changing tightness or size of implant (ranges quoted in brackets)

	Tight → Loose	Within tight
8.5 mm implants	-65% (-76% to -55%)	±21%
13 mm implants	-65% (-77% to -50%)	±16%
	13mm → 8.5mm	**Within 13mm**
Tight	-38% (-66% to -15%)	±16%
Loose	-38% (-48% to -19%)	±16%

Table 4.16: Change in AE energy transmitted from air jet source when changing tightness or size of implant (ranges quoted in brackets)

By contrast, the ANOVA of the pencil lead tests suggested that frequency ratio would not be able to distinguish between the implant fitting conditions, although the air jet results did show statistically significant differences between the conditions. Tables 4.17 and 4.18 summarise the changes for the two tests in a format similar to that used for the AE energy discussion above. Clearly, frequency ratio can either increase or decrease with either tightness or implant size, based on the pencil lead tests and therefore such a measure could not be used to interrogate the interface. For the air jet source, it seems that frequency ratio may be able to distinguish between tight and loose fittings, but not between the two different sizes. In eight of the ten bones with 8.5 mm implants, the frequency ratio decreased going from tight to loose fitting and this increased to nine of the ten for the 13mm implants.

	Tight → Loose	Within tight
8.5 mm implants	-5% (-62% to +65%)	±17%
13 mm implants	9% (-18% to +62%)	±17%
	13mm → 8.5mm	**Within 13mm**
Tight	-9% (-48% to +36%)	±17%
Loose	-5% (-64% to +31%)	±12%

Table 4.17: Change in frequency ratio transmitted from a pencil lead break when changing tightness or size of implant (ranges quoted in brackets)

	Tight → Loose	Within tight
8.5 mm implants	-32% (-89% to +62%)	±25%
13 mm implants	-36% (-76% to +36%)	±20%
	13mm → 8.5mm	**Within 13mm**
Tight	-10% (-53% to +50%)	±20%
Loose	-8% (-71% to +128%)	±41%

Table 4.18: Change in frequency ratio transmitted from air jet source when changing tightness or size of implant (ranges quoted in brackets)

The clear difference in transmitted energy between the large and small implants and between the loose and tight indicated that the amount of material at the interface, i.e. the combined effects of the compression and the implant contact surface area, lead to improved transmission, which was in accord with the findings from orthopaedic implants (Qi 2000) . For the case of frequency ratio, a better (i.e. tighter) interface might be expected to transmit a higher proportion of high frequency AE as was found with the air jet source. Clearly, the causes of the random variation of frequency ratio need to be better understood, but the tests with the air jet at east suggest that this might be worthwhile.

One of the sources of random variation in the systematic tests was the quality of the bone itself. Whereas every effort was made to source bones from animals of similar size and age, Figure 4.31 shows the bedding of two 8.5mm implants inserted in the loose fitting conditions in two bovine ribs sourced from two different animals. The rib in Figure 4.31 (a) has a thicker layer of a compact bone on the surface, which produces better higher bone/implant contact, whilst (b) has a thinner compact layer and the cancellous bone has a more open structure, hence less solid contact with the dental implant.

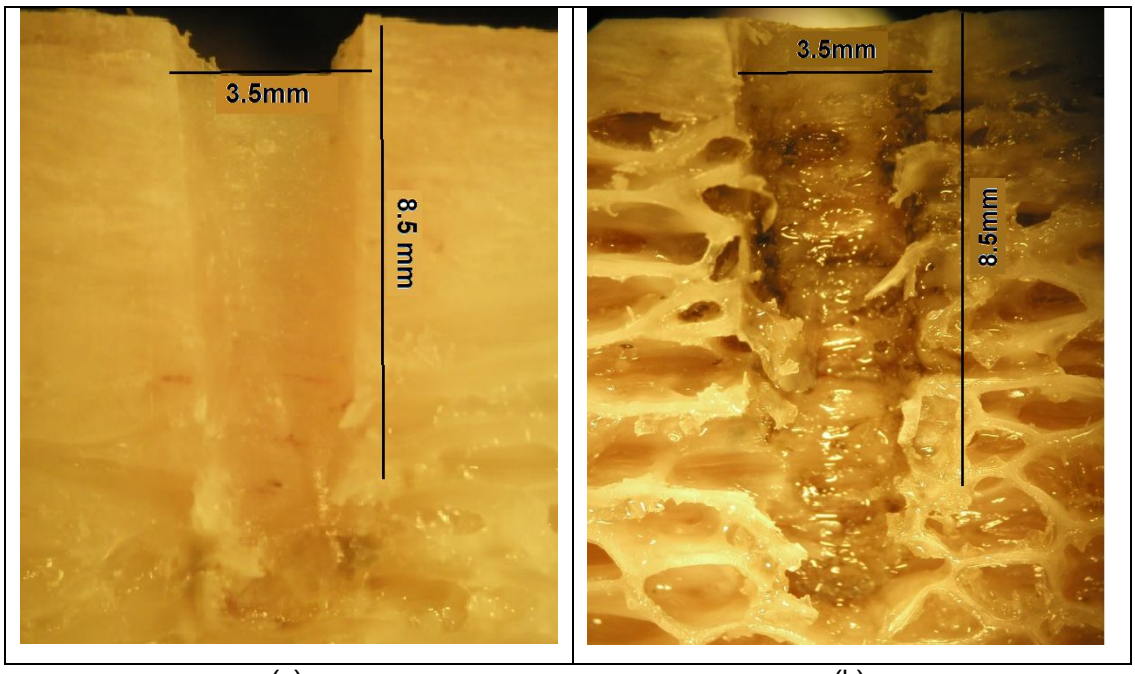

Figure 4.31: Comparisons between compact and cancellous bones: (a) Bovine rib with a compact structure, (b) Bovine rib with an open structure

4.9 AE applications in biomedical field

In the past 10 years, the Acoustic Emission has gained popularity as a monitoring method in the biomedical field, especially in Orthopedics. The AE technique offers the capability of monitoring the structural degradation passively and in real time, and can distinguish failure mechanisms and their location through the analysis of AE parameters.

Watanabe *et al* in 2001 used the acoustic emission method for monitoring the fracture healing of the rat femur. They found that some mechanical properties of the healing fractures can be estimated by monitoring the AE signals.

Davies *et al* 1996 used the AE to evaluate the cement-metal interface of the cemented femoral stems in autopsy-retrieved specimens. This study showed that acoustic emission signals arose from cracks that developed in the cement.

Hirasawa *et al* 2002 used acoustic emission to monitor the yield strength of healing fracture during external fixation in 35 patients with 39 long bones treated with external fixation. They found that the AE method had good potential as a reliable method for monitoring the mechanical status of healing bone.

Chapter 5

CONCLUSIONS

As presented at the outset, this work is the first to apply an AE method to monitor the stability of dental implants, offering several advantages over conventional and/or established techniques. Realising these advantages required a number of key questions to be answered, and these formed the basis of the research approach. First, it was necessary to determine if AE generated on the biting surface of a tooth could be detected by a sensor mounted on the face of a living subject. Second, it was necessary to assess to what extent the quality of the implant bone interface affected the transmission of AE generated by a standard source applied to a customised implant abutment. Third, a means of generating a reproducible source which could be deployed within the mouth needed to be developed and benchmarked against the standard source for the application. Finally, the overall feasibility of deploying the technique on a variety of subjects with implants needed to be assessed and the random and systematic sources of variation quantified. The detailed conclusions in each of these areas are given below.

5.1 Initial feasibility: *in vivo* transmission of AE

This study showed that an artificial AE source could be simulated intra-orally; the AE signals which were generated by biting on various types of hard or brittle food were successfully transmitted through human hard and soft tissues, and collected by an AE sensor mounted on the skin, thus demonstrating that a sufficiently strong AE source applied intra orally could be detected externally. There was a clear discrimination between different types of food and the location of the AE sensor on the face also had a significant effect on the strength of the recorded signal. Because the time structure of the source was not reproducible, even within a particular food type, this highlighted the need to develop a standard source, and because of the variable attenuation with sensor position, this highlighted the need for a study of this standard source applied to a range of different individuals with different sensor positions.

5.2 Preliminary transmission tests

Before carrying out the systematic interface transmission tests, a number of preliminary experiments were carried out to determine the best way to simulate a jaw with implant with various degrees of osseo-integration or stability, given that the model would be a bovine rib-bone. Also, the tests provided the opportunity to assess the variability in transmission between individuals, in this case the individual animals from which the bones came.

The surface transmission tests on showed the transmission through Glass Ionomer cement to be closest to the bone. This would suggest that complete osseo-integration could potentially be simulated using such cement.

The tests using a standard AE source on wet and dry bovine bones showed the transmission of AE energy through bone to be dependent upon its degree of hydration. It was also found that flooding the samples with water led to an increase in transmitted energy, but this appeared to affect transmission across the interface more than transmission though the bone. These findings have implication not only for this study, but also for passive AE monitoring.

5.3 Use of standard source to test interface

The main systematic tests using a standard AE source on fresh bovine bones were conducted to determine what, if any, features of the transmitted AE were attributable to the implant stability, simulated by changing the area (through implant size) and tightness of the contact. The transmitted AE energy and the ratio of high to low frequency in the raw spectrum were used as leading indicators. Frequency analysis is generally preferable to energy analysis as it avoids some of the difficulties associated with calibration.

A strong correlation was found between a simulation of primary stability of dental implants and the proportion of Acoustic Emission energy transmitted from the standard source to a sensor mounted on the surface of a bone *in vitro*. Tightly-fitting

implants transmitted more AE energy than those which were loosely–fitting. Implants with larger diameter and length (i.e. larger contact surface area) transmitted more AE energy than those with a smaller contact surface area.

The effect of the individual animal (i.e. the structure of the bone) was significant, although this did not obscure the effect of primary stability.

The patterns of the results from the high frequency analysis were not as distinct as the energy analysis but 70% of the data confirmed the results from the energy analysis.

Sectioning of a number of bones revealed a source of random variation in that, for a given nominal contact area and tightness, the conformity of the screw and bone varied because of the fairly open structure of the cancellous bone. Nevertheless, the findings were still clear despite this random variation.

These experiments showed that the Hsu-Nielson method was a reproducible source of AE signals for *in vitro* monitoring the stability of dental implants. However, the intra-oral application of this method to monitor osseo-integrated dental implants was impracticable due to concerns over the fractured portions of the pencil leads. Therefore, a new AE source was required for *in vivo* testing.

5.4 Development of air jet source

Consideration of the various options led to the selection of an air jet as an appropriate source for use in the mouth, and this required a number of practical and analytical developments, including the repetition of the tests with the standard source with varying degrees of integration. The two main conclusions from this work were as follows.

The air jet, as a continuous source, has a frequency structure which could be seen both in the impinging jet and in the transmitted signal. However, this structure was

not reproducible between examples and did not appear to be affected by the quality of the interface. It could thus be used as a "carrier wave".

The high frequency and energy features used for the pencil lead tests were stable over a period of several minutes, making the air jet a suitably reproducible source despite its continuous nature.

These features varied with simulated degree of integration in essentially the same way as with the pencil lead break tests, demonstrating that the air jet source was a reliable and reproducible substitute for a standard (pencil-lead) source.

Both the transmitted energy and the frequency ratio gave better discrimination between tightness of fit and implant size than did the air jet. Better understanding of the random sources of variation is desirable in the case of frequency ratio to make it more robust as a diagnostic indicator.

5.5 Deployability of the air jet source *in vivo*

The overall aim of this part of the study was to assess the transmission of AE signals generated by the air jet source from the oral cavity to an AE sensor positioned on the facial skin under practical clinical conditions. The energy and frequency analysis against a total patient "score" of systematic and random patient variables demonstrated the feasibility of the air jet method and the source.

The other aim was to examine the factors that might affect the AE transmission. The factors were divided into "engineering" variables (i.e. those associated with the reproducibility of the source, such as changes in air pressure over time), and patient variables, which were sub-divided into "random" (difficulty of sensor placement, saliva level, general movement and movement of the tongue) and "systematic" (thickness of the soft tissue and implant size).

The main engineering finding which needs to be addressed in a future implementation is that of "fade" of the source over time. This is relatively easily

managed by ensuring that the pressure source has sufficient top-up flow to ensure a constant pressure over several minutes of continuous use.

All of the random patient variables had the expected negative effect on AE energy transmission and the strength and degrees of the correlation were broadly similar even based on the subjective scale.

The systematic patient variables again showed the expected effects on AE energy transmission, with a negative correlation with amount of patient soft tissue and a positive correlation with size of implant. However, the systematic variables showed generally weaker correlations than the random ones, pointing to the need to control random variables by reducing the invasiveness of the technique.

The correlations of both random and systematic patent variables with frequency ratio, showed similar sensitivity to those with transmitted energy, except that the correlations were stronger in all cases. This is a useful finding as frequency ratio is a relative measure and avoids the problems of absolute calibration of sensors.

The study has only provided basic *in vivo* testing and the variables were quantified objectively. Furthermore there may be other, unsuspected variables. Most critically, the participants all had well-integrated implants, and so little variation was expected in transmission due to the quality of the interface.

Overall, this part of the study showed that the proposed system is deployable in practice and that the engineering issues can be overcome. Some developments are required in controlling the sources of random variation but, even so, it seems that systematic patient features can be measured.

5.6 Limitations of the study

There were various limitations in this study.

1. Although the AE method is sensitive and non-invasive, its nature is calibration-dependent when using energy features, although this can be overcome using frequency ratios.
2. Generally, continuous AE signals are more complex and difficult to analyse than burst signals. The air jet produced continuous signals, which required extensive analysis to extract the required information.
3. Limited methods of data analysis were used to examine the data.
4. Extra oral sensor placement proved to be difficult due to variations in facial anatomy and the participants' behaviour.
5. A number of patient-related variables affected the transmission of AE signals for the *in vivo* experiments.
6. A limited numbers of subjects with two mandibular implants were available to participate in the *in vivo* study. The five participants were elderly people with current medical conditions which made it difficult for them to cope with the tests.

5.7 Clinical relevance

Currently there is no one reliable and non-invasive method in monitoring the stability of dental implants. The AE method was investigated to address the above problems. It is non-invasive, and has been proven to be reliable *in vitro*. However the technique will require some refinement for clinical use.

5.8 Recommendations for further work

Future work should be aimed at refining the investigation carried out during this project. The following recommendations are suggested for further research:

1. *In vitro* studies using a standard source provided a baseline of AE transmission through implants placed in bovine bones with various sizes and fitting conditions. Further investigations could be carried out to understand the effect of geometry of the bone on AE transmission.
2. The air jet source proved to be reliable and safe; it could be used in other areas as an artificial AE source and calibration of AE systems.

3. Further work is recommended on refining the placement/stabilisation of AE sensors on a subject's face or the possibility of designing the sensor for intra oral placement.
4. Development of a standard comprehensive data analysis tool to examine the signals produced by the air jet.
5. Further animal/ human experiments could aid to understand the transmission of AE signals during the process of osseo-integration of dental implants

APPENDIX

APPENDIX A AE sensor calibration certificate

APPENDIX B Gas jet technique

The helium gas jet was first described by (McBride and Hutchison 1976), it has been used for the excitation and spectral calibration of an Acoustic Emission System (AES). The American Society for Testing and Materials (ASTM), (ASTM E976-99 1999), provided the following standards for the helium gas jet source to calibrate AE systems:

- Helium gas jet of 200 KPa (equivalent to approximately 29 PSI)
- Nozzle: 0.25mm diameter
- Diffused carbon steel block: 305mm x 75mm x 50mm

AE Instrumentation:

- Pre-Amplifier: +40dB Gain
- Filter: 100-400 kHz. Bandpass

Spectrum analysis:

- H.P. 8552B/8553B
- Centre Frequency: 250 kHz
- Bandwidth: 3kHz
- SCAN/DIV: 50 kHz
- SCAN TIME: 2S/DIV
- Input ATTEN: 0 dB
- LOG FEF: 0 dB, 10dB/DVISION
- VIDEO FILTER: 10 HZ

It was reported that this method allowed calibration of the entire AE system including the specimen, couplant, sensor and instrumentation without making mechanical contact between the exciting source and the specimen or structure of interest. The method appeared to have some possibility of being employed in the present investigation as it was based on non-mechanical contact with the specimen, which could provide an ideal intra-oral AE source without the risk to patients by fracturing objects in the Hsu Nielson method. On the other hand, the helium gas jet was originally designed to calibrate the AE system on metal blocks in the laboratory; it might not have been suitable for intra-oral use with patients. The health effects of

helium gas needed to be considered: inhalation of helium had possible effects of high voice, dizziness, dullness, headache and suffocation.

APPENDIX C Ethical approval

University Hospitals Division

Queen's Medical Research Institute
47 Little France Crescent, Edinburgh, EH16 4TJ

NHS Lothian

CPP/MJ/approval

07/10/2010

Research & Development
Room E1.12
Tel: 0131 242 3330
Fax: 0131 242 3343
Email:
R&DOffice@luht.scot.nhs.uk

Director:
Professor David E Newby

Dr Zannar Ossi
Edinburgh Postgraduate Dental Institute
4th Floor Lauriston Building
Lauriston Place
Edinburgh
EH3 9HA

Dear Dr Ossi,

Lothian R&D Project No: **2010/R/DEN/01**

Title of Research: Monitoring the stability of dental implants using acoustic emission

REC No: 10/S1103/04

CTA No: N/A **Eudract:** N/A

PIS: no version or date **Consent:** v1 12/01/2010

Protocol No: v1 12/01/2010

I am pleased to inform you that this study has been approved for NHS Lothian and you may proceed with your research, subject to the conditions below. This letter provides Site Specific approval for NHS Lothian.

Please note that the NHS Lothian R&D Office must be informed if there are any changes to the study such as amendments to the protocol, recruitment, funding, personnel or resource input required of NHS Lothian.

Substantial amendments to the protocol will require approval from the ethics committee which approved your study.

Please inform this office when recruitment has closed and when the study has been completed.

I wish you every success with your study.

Yours sincerely

Dr Christine P Phillips
Deputy R&D Director

enc Research Governance Certificate ☐ (to be signed and returned)

APPENDIX D AE Energy produced from different types of food

Almond				Peanut				Carrot		
MF	**Z**	**TMJ**		**MF**	**Z**	**TMJ**		**MF**	**Z**	**TMJ**
145.2339	102.5018	112.3439		17.4269	16.4948	13.2708		15.1632	29.1169	13.5572
140.781	99.8834	101.9551		17.3641	11.7752	13.6532		17.0316	20.5127	11.2426
144.407	101.7133	105.521		13.5537	13.9379	14.5181		18.6882	20.3874	12.5981
148.5589	101.9457	106.3428		22.1927	13.746	12.9847		19.9247	25.8641	12.5981
148.767	98.783	108.8235		15.7159	13.1611	14.0682		19.429	16.3928	0
144.8	113.7455	100.3886		18.3757	13.4194	0		16.6009	18.4488	11.6046
138.1016	102.3062	103.5053		22.9111	14.4228	13.5807		31.6019	19.3415	12.5868
149.1134	92.5982	101.0019		19.9718	12.98	15.2575		23.3165	17.015	14.2857
152.3638	108.6132	207.9697		18.857	13.4498	12.8354		19.251	22.037	14.0486
148.5969	106.799	209.3953		16.7076	12.3729	14.1743		32.2244	26.3721	14.1455
149.1178	113.8646	125.6449		17.4414	13.676	13.6035		19.7975	28.9466	13.6792
132.5035	101.5171	317.4007		15.4944	12.572	14.3827		43.1423	18.6422	12.0139
138.3813	99.5371	333.0161		15.7754	14.2301	12.6639		51.4325	27.7456	12.7227
138.9066	107.6428	106.6347		15.0019	14.2615	14.9175		15.7201	21.3822	12.3481
134.8746	114.0911	102.1259		13.2402	14.9283	14.178		45.0125	23.755	14.2077

MF-Mental Foramen, Z-Zygoma, TMJ-Temporomandibular joint

APPENDIX E Linear regression of AE energy (V) of air jet

	8.5mm T	**8.5mm L**	**13mm T**	**13mm L**
B1	y = -0.0245x + 8.8819 R^2 = 0.7242	y = -0.0022x + 3.4057 R^2 = 0.2336	y = 0.039x + 23.611 R^2 = 0.457	y = -8E-05x + 5.5689 R^2 = 0.0001
B2	y = 0.0157x + 7.0816 R^2 = 0.7579	y = 0.0026x + 3.2685 R^2 = 0.2451	y = 0.0498x + 15.978 R^2 = 0.6393	y = 0.0074x + 4.1959 R^2 = 0.5952
B3	y = 0.0699x + 8.4993 R^2 = 0.7168	y = 0.003x + 3.9094 R^2 = 0.1671	y = -0.0398x + 16.592 R^2 = 0.7411	y = -0.0199x + 8.3158 R^2 = 0.7411
B4	y = 0.0699x + 8.4993 R^2 = 0.7168	y = 0.0026x + 4.3394 R^2 = 0.0913	y = 0.0856x + 15.462 R^2 = 0.6198	y = 0.0068x + 5.2846 R^2 = 0.4752
B5	y = 0.0147x + 11.394 R^2 = 0.4003	y = 0.0038x + 3.6915 R^2 = 0.3232	y = 0.0186x + 19.889 R^2 = 0.1933	y = 0.0107x + 6.0008 R^2 = 0.5945
B6	y = 0.0699x + 8.4993 R^2 = 0.7168	y = -0.0048x + 4.2319 R^2 = 0.3199	y = 0.0127x + 17.459 R^2 = 0.1618	y = 0.0418x + 6.6233 R^2 = 0.7325
B7	y = 0.0054x + 14.084 R^2 = 0.0547	y = 0.0037x + 3.7357 R^2 = 0.4285	y = 0.0136x + 16.333 R^2 = 0.2599	y = -0.01x + 6.332 R^2 = 0.5757
B8	y = -0.0086x + 9.4046 R^2 = 0.1689	y = 0.0073x + 3.6255 R^2 = 0.4824	y = 0.0129x + 13.398 R^2 = 0.3628	y = 0.0013x + 5.8355 R^2 = 0.04
B9	y = 0.0084x + 13.571 R^2 = 0.264	y = 0.0063x + 3.3157 R^2 = 0.6768	y = 0.0106x + 17.779 R^2 = 0.1182	y = 0.001x + 6.2125 R^2 = 0.0107
B10	y = 0.0206x + 12.537 R^2 = 0.5507	y = 0.0038x + 3.0548 R^2 = 0.2461	y = 0.0078x + 18.75 R^2 = 0.069	y = -0.0071x + 6.2346 R^2 = 0.0696

APPENDIX F Linear regression of frequency ratio of air jet

	8.5mm T	**8.5mm L**	**13mm T**	**13mm L**
B1	y = -0.0007x + 0.4202 R^2 = 0.2818	y = -0.0003x + 0.3078 R^2 = 0.0957	y = -0.0001x + 0.8113 R^2 = 0.0161	y = 0.0002x + 0.3835 R^2 = 0.0172
B2	y = 0.001x + 0.5313 R^2 = 0.4034	y = -0.0002x + 0.2869 R^2 = 0.0426	y = 0.0004x + 0.3618 R^2 = 0.0719	y = 0.0003x + 0.4984 R^2 = 0.0304
B3	y = 0.0023x + 0.7564 R^2 = 0.437	y = 0.001x + 0.1573 R^2 = 0.3732	y = -0.0001x + 0.5965 R^2 = 0.0084	y = 0.0001x + 0.2367 R^2 = 0.0148
B4	y = -0.0013x + 0.6836 R^2 = 0.3967	y = 2E-05x + 0.0723 R^2 = 0.004	y = 0.0008x + 0.6074 R^2 = 0.1652	y = -7E-05x + 0.2389 R^2 = 0.0024
B5	y = 0.0003x + 0.5125 R^2 = 0.0088	y = 0.0004x + 0.4344 R^2 = 0.1129	y = 6E-05x + 0.7838 R^2 = 0.0023	y = 0.0005x + 0.3961 R^2 = 0.0886
B6	y = 0.0004x + 0.6855 R^2 = 0.1444	y = 0.0002x + 0.5382 R^2 = 0.0196	y = -0.0001x + 0.8113 R^2 = 0.0161	y = 0.0015x + 0.6748 R^2 = 0.5534
B7	y = -0.0001x + 0.7014 R^2 = 0.0078	y = 0.0012x + 0.3422 R^2 = 0.4108	y = 0.0007x + 0.67 R^2 = 0.3552	y = -0.0004x + 0.4695 R^2 = 0.1047
B8	y = 0.0005x + 0.3552 R^2 = 0.0658	y = 0.0007x + 0.4157 R^2 = 0.0851	y = -0.0001x + 0.7858 R^2 = 0.0213	y = 0.001x + 0.1638 R^2 = 0.5427
B9	y = 0.0003x + 0.4601 R^2 = 0.0403	y = 0.0004x + 0.7457 R^2 = 0.168	y = -2E-05x + 0.7891 R^2 = 0.0004	y = 0.0001x + 0.468 R^2 = 0.0034
B10	y = 0.0005x + 0.7192 R^2 = 0.1036	y = 0.0002x + 0.189 R^2 = 0.0428	y = -1E-04x + 0.765 R^2 = 0.0066	y = -0.0003x + 0.6665 R^2 = 0.0439

REFERENCE

ADA (1995-2000). The american dental association.

Adell, R. (1985). Tissue integrated prostheses in clinical dentistry. International Dental Journal 35(4): 259-265.

Adell, R., B. Eriksson, et al. (1990). Long-term follow-up study of osseointegrated implants in the treatment of totally edentulous jaws. Int J Oral Maxillofac Implants 5(4): 347-359.

Adell, R., U. Lekholm, et al. (1981). A 15-year study of osseointegrated implants in the treatment of the edentulous jaw. International Journal of Oral Surgery 10(6): 387-416.

Alander, P., L. V. J. Lassila, et al. (2004). Acoustic emission analysis of fiber-reinforced composite in flexural testing. Dental Materials 20(4): 305-312.

Albrektsson, T. (1993). On long-term maintenance of the osseointegrated response. Aust Prosthodont J 7 Suppl: 15-24.

Albrektsson, T., P. I. Branemark, et al. (1981). Osseointegrated titanium implants. Requirements for ensuring a long-lasting, direct bone-to-implant anchorage in man. Acta Orthop Scand 52(2): 155-170.

Albrektsson, T., E. Dahl, et al. (1988). Osseointegrated oral implants. A swedish multicenter study of 8139 consecutively inserted nobelpharma implants. J Periodontol 59(5): 287-296.

Albrektsson, T. and F. Isidor (1994). Consensus report of session iv. In: Lang np, karring t eds proceedings of the 1st european workshop on periodontology. London. Quintessence Pubishing Co Ltd 365–369.

Albrektsson, T. and L. Sennerby (1991). State-of-the-art in oral implants. Journal of Clinical Periodontology 18(6): 474-481.

Albrektsson, T., G. Zarb, et al. (1986). The long-term efficacy of currently used dental implants: A review and proposed criteria of success. Int J Oral Maxillofac Implants 1(1): 11-25.

Aparicio, C., B. Rangert, et al. (2003). Immediate/early loading of dental implants: A report from the sociedad espanola de implantes world congress consensus meeting in barcelona, spain, 2002. Clin Implant Dent Relat Res 5(1): 57-60.

Asaoka, K., K. Yoshida, et al. (1992). Effect of transient stress on acoustic emission behaviour during firing of dental porcelain. Journal of materials science 27(11): 3118-3122.

ASTM (1999). Astm e976-99: Standard guide for determining the reproducibility of acoustic emission sensor response. Annual Book of ASTM Standards. 3(03): 395-403.

ASTM E976-99 (1999). Standard guide for determining the reproducibility of acoustic emission sensor response, annual book of astm standards. (3.03): 395-403.

Atwood, D. A. (1971). Reduction of residual ridges: A major oral disease entity. J Prosthet Dent 26(3): 266-279.

Atwood, D. A. (1979). Bone loss of edentulous alveolar ridges. J Periodontol 50(4 Spec No): 11-21.

Barewal, R. M., T. W. Oates, et al. (2003). Resonance frequency measurement of implant stability in vivo on implants with a sandblasted and acid-etched surface. Int J Oral Maxillofac Implants 18(5): 641-651.

Becker, W. and B. E. Becker (1995). Replacement of maxillary and mandibular molars with single endosseous implant restorations - a retrospective study. Journal of Prosthetic Dentistry 74(1): 51-55.

Bergman, B. (1983). Evaluation of the results of treatment with osseointegrated implants by the swedish-national-board-of-health-and-welfare. Journal of Prosthetic Dentistry 50(1): 114-115.

Billi, F., C. Caneva, et al. (2000). Acoustic emission monitoring of fatigue strength of hydroxylapatite coatings on dental implants. 15th World Conference on Nondestructive Testing Roma (Italy) 15-21 October.

Block, M. S., A. Delgado, et al. (1990). The effect of diameter and length of hydroxylapatite-coated dental implants on ultimate pullout force in dog alveolar bone. J Oral Maxillofac Surg 48(2): 174-178.

Branemark, P. I. (1983). Osseointegration and its experimental background. Journal of Prosthetic Dentistry 50(3): 399-410.

Branemark, P. I. (1990). [osseointegration methods for rehabilitation in mouth, jaw and face regions]. Phillip J 7(6): 275-279.

Branemark, P. I., R. Adell, et al. (1969). Intra-osseous anchorage of dental prostheses. I. Experimental studies. Scand J Plast Reconstr Surg 3(2): 81-100.

Branemark, P. I., U. Breine, et al. (1969). Intra osseous anchorage of dental prostheses part 1 experimental studies. Scandinavian Journal of Plastic and Reconstructive Surgery 3(2): 81-100.

Buser, D., N. Broggini, et al. (2004). Enhanced bone apposition to a chemically modified sla titanium surface. Journal of Dental Research 83(7): 529-533.

Buser, D., R. K. Schenk, et al. (1991). Influence of surface characteristics on bone integration of titanium implants. A histomorphometric study in miniature pigs. J Biomed Mater Res 25(7): 889-902.

Carlsson, L., T. Rostlund, et al. (1986). Osseointegration of titanium implants. Acta Orthop Scand 57(4): 285-289.

Cawood, J. I. and R. A. Howell (1988). A classification of the edentulous jaws. Int J Oral Maxillofac Surg 17(4): 232-236.

Chaddad, K., A. F. H. Ferreira, et al. (2008). Influence of surface characteristics on survival rates of mini-implants. Angle Orthodontist 78(1): 107-113.

Chapman, R. J. (1989). Principles of occlusion for implant prostheses: Guidelines for position, timing, and force of occlusal contacts. Quintessence Int 20(7): 473-480.

Colombo, S., A. Giannopoulos, et al. (2005). Frequency response of different couplant materials for mounting transducers. NDT & E International 38(3): 187-193.

Cros, B., N. Brunet, et al. (2000). Increase in performances of focused microacoustic sensors by couplant adjustment. European Physical Journal-Applied Physics 9(1): 81-85.

Dao, T. T., J. D. Anderson, et al. (1993). Is osteoporosis a risk factor for osseointegration of dental implants? The International journal of oral & maxillofacial implants 8(2): 137-144.

das Neves, F. D., D. Fones, et al. (2006). Short implants--an analysis of longitudinal studies. Int J Oral Maxillofac Implants 21(1): 86-93.

Davies, J. E. (1998). Mechanisms of endosseous integration. Int J Prosthodont 11(5): 391-401.

Davies J.P, Tse M.K, Harris W.H (1996). Monitoring the integrity of the cement-metal interface of total joint components in vitro using acoustic emission and ultrasound. Journal of Arthroplasty 11 (5): 594-601.

Deporter, D., P. Watson, et al. (2002). Ten-year results of a prospective study using porous-surfaced dental implants and a mandibular overdenture. Clin Implant Dent Relat Res 4(4): 183-189.

Derhami, K., J. F. Wolfaardt, et al. (1995). Assessment of the periotest device in baseline mobility measurements of craniofacial implants. Int J Oral Maxillofac Implants 10(2): 221-229.

Douglass, J. B., L. Meader, et al. (1993). Cephalometric evaluation of the changes in patients wearing complete dentures: A 20-year study. J Prosthet Dent 69(3): 270-275.

Elias, J. J., J. B. Brunski, et al. (1996). A dynamic modal testing technique for noninvasive assessment of bone-dental implant interfaces. Int J Oral Maxillofac Implants 11(6): 728-734.

Ericsson, I., C. B. Johansson, et al. (1994). A histomorphometric evaluation of bone-to-implant contact on machine-prepared and roughened titanium dental implants. A pilot study in the dog. Clin Oral Implants Res 5(4): 202-206.

Eriksson, A. R. and T. Albrektsson (1983). Temperature threshold levels for heat-induced bone tissue injury: A vital-microscopic study in the rabbit. J Prosthet Dent 50(1): 101-107.

Esposito, M., J. M. Hirsch, et al. (1998). Biological factors contributing to failures of osseointegrated oral implants. (i). Success criteria and epidemiology. Eur J Oral Sci 106(1): 527-551.

Fennis, W. M., A. Tezvergil, et al. (2005). In vitro fracture resistance of fiber reinforced cusp-replacing composite restorations. Dent Mater 21(6): 565-572.

Fiorellini, J. P. and M. L. Nevins (2000). Dental implant considerations in the diabetic patient. Periodontology 2000 23: 73-77.

Franke Stenport, V. and C. B. Johansson (2003). Enamel matrix derivative and titanium implants. J Clin Periodontol 30(4): 359-363.

Friberg, B., T. Jemt, et al. (1991). Early failures in 4,641 consecutively placed branemark dental implants: A study from stage 1 surgery to the connection of completed prostheses. Int J Oral Maxillofac Implants 6(2): 142-146.

Geng, J. P., K. B. Tan, et al. (2001). Application of finite element analysis in implant dentistry: A review of the literature. J Prosthet Dent 85(6): 585-598.

Gibbs, C. H., P. E. Mahan, et al. (1981). Occlusal forces during chewing--influences of biting strength and food consistency. J Prosthet Dent 46(5): 561-567.

Hagi, D., D. A. Deporter, et al. (2004). A targeted review of study outcomes with short (< or = 7 mm) endosseous dental implants placed in partially edentulous patients. J Periodontol 75(6): 798-804.

Hamstad, M. (1985). Composite characterization techniques: Acoustic emissions. US Army Mantech Journal 10(3): 24-32.

Hamstad, M. and R. Moore (1986). Acoustic emission from single and multiple kevlar 49 filament breaks. Journal of Composites 20(1): 46-66.

Hermann, J. S., J. D. Schoolfield, et al. (2001). Crestal bone changes around titanium implants: A methodologic study comparing linear radiographic with histometric measurements. International Journal of Oral & Maxillofacial Implants 16(4): 475-485.

Hill, R. and S. M. A. El-Dardiry (1981). Variables in the use and design of acoustic emission transducers. Ultrasonics 19(1): 9-16.

Hirasawa Y, Takai S, Kim WC, Takenaka N, Yoshino N, Watanabe Y (2002). Biomechanical monitoring of healing bone based on acoustic emission technology. Clin Orthop Relat Res. (402):236-44.

HSU, N. N., J. A. SIMMONS, et al. (1977). An approach to acoustic emission signal analysis - theory and experiment Materials Evaluation 35(Oct): 100-106.

Huang, H. M., C. L. Chiu, et al. (2003). Early detection of implant healing process using resonance frequency analysis. Clin Oral Implants Res 14(4): 437-443.

Hutton, J. E., M. R. Heath, et al. (1995). Factors related to success and failure rates at 3-year follow-up in a multicenter study of overdentures supported by branemark implants. Int J Oral Maxillofac Implants 10(1): 33-42.

Isidor, F. (1997). Histological evaluation of peri-implant bone at implants subjected to occlusal overload or plaque accumulation. Clin Oral Implants Res 8(1): 1-9.

Ito, Y., D. Sato, et al. (2008). Relevance of resonance frequency analysis to evaluate dental implant stability: Simulation and histomorphometrical animal experiments. Clin Oral Implants Res 19(1): 9-14.

Ivanoff, C. J., K. Grondahl, et al. (1999). Influence of variations in implant diameters: A 3- to 5-year retrospective clinical report. International Journal of Oral & Maxillofacial Implants 14(2): 173-180.

Ivanoff, C. J., L. Sennerby, et al. (1997). Influence of implant diameters on the integration of screw implants. An experimental study in rabbits. Int J Oral Maxillofac Surg 26(2): 141-148.

Ivanoff, C. J., L. Sennerby, et al. (1996). Influence of mono- and bicortical anchorage on the integration of titanium implants. A study in the rabbit tibia. Int J Oral Maxillofac Surg 25(3): 229-235.

Iyer, S., C. Weiss, et al. (1997). Effects of drill speed on heat production and the rate and quality of bone formation in dental implant osteotomies .2. Relationship between drill speed and healing. International Journal of Prosthodontics 10(6): 536-540.

Jaffin, R. A. and C. L. Berman (1991). The excessive loss of branemark fixtures in type-iv bone - a 5-year analysis. Journal of Periodontology 62(1): 2-4.

Jaffin, R. A. and C. L. Berman (1991). The excessive loss of branemark fixtures in type iv bone: A 5-year analysis. J Periodontol 62(1): 2-4.

Jemt, T. (1991). Failures and complications in 391 consecutively inserted fixed prostheses supported by branemark implants in edentulous jaws: A study of treatment from the time of prosthesis placement to the first annual checkup. Int J Oral Maxillofac Implants 6(3): 270-276.

Jemt, T. and J. Johansson (2006). Implant treatment in the edentulous maxillae: A 15-year follow-up study on 76 consecutive patients provided with fixed prostheses. Clin Implant Dent Relat Res 8(2): 61-69.

Jemt, T. and U. Lekholm (1995). Implant treatment in edentulous maxillae: A 5-year follow-up report on patients with different degrees of jaw resorption. Int J Oral Maxillofac Implants 10(3): 303-311.

Jemt, T., B. Linden, et al. (1992). Failures and complications in 127 consecutively placed fixed partial prostheses supported by branemark implants from prosthetic treatment to first annual checkup. International Journal of Oral and Maxillofacial Implants 7(1): 40-44.

Johansson, C. and T. Albrektsson (1987). Integration of screw implants in the rabbit: A 1-year follow-up of removal torque of titanium implants. The International journal of oral & maxillofacial implants 2(2): 69-75.

Johansson, C. B. and T. Albrektsson (1991). A removal torque and histomorphometric study of commercially pure niobium and titanium implants in rabbit bone. Clinical Oral Implants Research 2(1): 24-29.

Johns, R. B., T. Jemt, et al. (1992). A multicenter study of overdentures supported by branemark implants. Int J Oral Maxillofac Implants 7(4): 513-522.

Kaiser, J. (1950). A study of acoustic phenomenon in tensile test. Dissertiation, University of bristol, UK.

Kaneko, T. (1991). Pulsed oscillation technique for assessing the mechanical state of the dental implant-bone interface. Biomaterials 12(6): 555-560.

Kaneko, T., Y. Nagai, et al. (1986). Acoustoelectric technique for assessing the mechanical state of the dental implant bone interface. Journal of Biomedical Materials Research 20(2): 169-176.

Klein, M. O., K. A. Grotz, et al. (2008). Ultrasound transmission velocity for noninvasive evaluation of jaw bone quality in vivo before dental implantation. Ultrasound in Medicine and Biology 34(12): 1966-1971.

Lang, N. P., A. C. Wetzel, et al. (1994). Histologic probe penetration in healthy and inflamed peri-implant tissues. Clin Oral Implants Res 5(4): 191-201.

Langer, B., L. Langer, et al. (1993). The wide fixture: A solution for special bone situations and a rescue for the compromised implant. Part 1. Int J Oral Maxillofac Implants 8(4): 400-408.

Lazzara, R. J., S. S. Porter, et al. (1998). A prospective multicenter study evaluating loading of osseotite implants two months after placement: One-year results. J Esthet Dent 10(6): 280-289.

Lazzara, R. J., T. Testori, et al. (1999). A human histologic analysis of osseotite and machined surfaces using implants with 2 opposing surfaces. Int J Periodontics Restorative Dent 19(2): 117-129.

Lekholm, U., K. Grondahl, et al. (2006). Outcome of oral implant treatment in partially edentulous jaws followed 20 years in clinical function. Clin Implant Dent Relat Res 8(4): 178-186.

Lekholm, U. and G. Zarb (1985). Patient selection and preparation. In: Branemark pi, zarb ga, albrektssoon t, editors. Tissue-integrated prostheses. osseointegration in clinical dentistry. Chicago: Quintessence: 199-209.

Li, C. and E. Nordlund (1993). Effects of couplants on acoustic transmission. (1): 63-69.

Lim, S.-A., J.-Y. Cha, et al. (2008). Insertion torque of orthodontic miniscrews according to changes in shape, diameter and length. Angle Orthodontist 78(2): 234-240.

Lin, C. T., S. Y. Lee, et al. (2000). Degradation of repaired denture base materials in simulated oral fluid. J Oral Rehabil 27(3): 190-198.

Linder, L., T. Albrektsson, et al. (1983). Electron-microscopic analysis of the bone titanium interface. Acta Orthopaedica Scandinavica 54(1): 45-52.

Long, M. and H. J. Rack (1998). Titanium alloys in total joint replacement - a materials science perspective. Biomaterials 19(18): 1621-1639.

Lundskog, J. (1972). Heat and bone tissue. An experimental investigation of the thermal properties of bone and threshold levels for thermal injury. Scand J Plast Reconstr Surg 9: 1-80.

Manz, M. C., H. F. Morris, et al. (1992). An evaluation of the periotest system. Part ii: Reliability and repeatability of instruments. Dental implant clinical research group (planning committee). Implant Dent 1(3): 221-226.

Mavrogordato, M., M. Taylor, et al. (2011). Real time monitoring of progressive damage during loading of a simplified total hip stem construct using embedded acoustic emission sensors. Medical Engineering & Physics 33(4): 395-406.

McBride, S. L. and T. S. Hutchison (1976). Helium gas-jet spectral calibration of acoustic-emission transducers and systems. Canadian Journal of Physics 54(17): 1824-1830.

Meredith, N. (1998). Assessment of implant stability as a prognostic determinant. Int J Prosthodont 11(5): 491-501.

Meredith, N., D. Alleyne, et al. (1996). Quantitative determination of the stability of the implant-tissue interface using resonance frequency analysis. Clin Oral Implants Res 7(3): 261-267.

Meyer, U., U. Joos, et al. (2004). Ultrastructural characterization of the implant/bone interface of immediately loaded dental implants. Biomaterials 25(10): 1959-1967.
Misch, C. E. (1993). Progressive loading of bone with implant prostheses. J Dent Symp 1: 50-53.

Misch, C. E., M. W. Bidez, et al. (2001). A bioengineered implant for a predetermined bone cellular response to loading forces. A literature review and case report. J Periodontol 72(9): 1276-1286.

Miyamoto, I., Y. Tsuboi, et al. (2005). Influence of cortical bone thickness and implant length on implant stability at the time of surgery--clinical, prospective, biomechanical, and imaging study. Bone 37(6): 776-780.

Mostardi, R. A., S. O. Meerbaum, et al. (1999). In vitro response of human fibroblasts to commercially pure titanium. J Biomed Mater Res 47(1): 60-64.

Naert, I., M. Quirynen, et al. (1992). A study of 589 consecutive implants supporting complete fixed prostheses. Part ii: Prosthetic aspects. J Prosthet Dent 68(6): 949-956.

Niinomi, M. (1998). Mechanical properties of biomedical titanium alloys. Materials Science and Engineering A 243(1-2): 231-236.

Nishimura, I., R. Hosokawa, et al. (1992). The knife-edge tendency in mandibular residual ridges in women. J Prosthet Dent 67(6): 820-826.

Nivesrangsan, P. (2004). Multi source, multi sensor approaches to monitor diesel engine using acoustic emission. Heriot-Watt University, Mechanical Engineering, Thesis.

Nkenke, E., M. Hahn, et al. (2003). Implant stability and histomorphometry: A correlation study in human cadavers using stepped cylinder implants. Clin Oral Implants Res 14(5): 601-609.

Olson, J. W., A. F. Shernoff, et al. (2000). Dental endosseous implant assessments in a type 2 diabetic population: A prospective study. International Journal of Oral & Maxillofacial Implants 15(6): 811-818.

Ostman, P. O., M. Hellman, et al. (2005). Direct implant loading in the edentulous maxilla using a bone density-adapted surgical protocol and primary implant stability criteria for inclusion. Clin Implant Dent Relat Res 7 Suppl 1(1): S60-69.

Ostman, P. O., M. Hellman, et al. (2008). Immediate occlusal loading of implants in the partially edentate mandible: A prospective 1-year radiographic and 4-year clinical study. Int J Oral Maxillofac Implants 23(2): 315-322.

Ottoni, J. M. P., F. L. Oliveira, et al. (2005). Correlation between placement torque and survival of single-tooth implants. International Journal of Oral & Maxillofacial Implants 20(5): 769-776.

Qi, G. (2000). Attenuation of acoustic emission body waves in acrylic bone cement and synthetic bone using wavelet time-scale analysis. Journal of Biomedical Materials Research 52(1): 148-156.

Qi, G., B. Zhang, et al. (2007). Microdamages: An insight to mechanical performance of stem-cement.

Quirynen, M., I. Naert, et al. (1992). Fixture design and overload influence marginal bone loss and fixture success in the branemark system. Clin Oral Implants Res 3(3): 104-111.

Rigo, E. C. S., A. O. Boschi, et al. (2004). Evaluation in vitro and in vivo of biomimetic hydroxyapatite coated on titanium dental implants. Materials Science & Engineering C-Biomimetic and Supramolecular Systems 24(5): 647-651.

Roberts, W. E., K. E. Simmons, et al. (1992). Bone physiology and metabolism in dental implantology: Risk factors for osteoporosis and other metabolic bone diseases. Implant dentistry 1(1): 11-21.

Roberts, W. E., R. K. Smith, et al. (1984). Osseous adaptation to continuous loading of rigid endosseous implants. American Journal of Orthodontics and Dentofacial Orthopedics 86(2): 95-111.

Roques, A., M. Brown, et al. (2004). Investigation of fatigue crack growth in acrylic bone cement using the acoustic emission technique. Biomaterials 25(5): 769-778.

Rowlands, A., F. A. Duck, et al. (2008). Bone vibration measurement using ultrasound: Application to detection of hip prosthesis loosening. Medical Engineering & Physics 30(3): 278-284.

Saadoun, A. P. and M. L. LeGall (1992). Clinical results and guidelines on steri-oss endosseous implants. Int J Periodontics Restorative Dent 12(6): 486-495.

Schatzker, J., J. G. Horne, et al. (1975). Effect of movement on holding power of screws in bone. Clinical Orthopaedics and Related Research(111): 257-262.

Schliephake, H., A. Sewing, et al. (2006). Resonance frequency measurements of implant stability in the dog mandible: Experimental comparison with histomorphometric data. Int J Oral Maxillofac Surg 35(10): 941-946.

Schnitman, P. A. and L. B. Shulman (1979). Recommendations of the consensus development conference on dental implants. J Am Dent Assoc 98(3): 373-377.

Schou, S., P. Holmstrup, et al. (2002). Probing around implants and teeth with healthy or inflamed peri-implant mucosa/gingiva. A histologic comparison in cynomolgus monkeys (macaca fascicularis). Clin Oral Implants Res 13(2): 113-126.

Schrooten, J., H. Van Oosterwyck, et al. (1999). Adhesion of new bioactive glass coating. J Biomed Mater Res 44(3): 243-252.

Schulte, W., B. d'Hoedt, et al. (1983). [periotest--a new measurement process for periodontal function]. Zahnarztl Mitt 73(11): 1229-1230, 1233-1226, 1239-1240.

Sennerby, L., L. G. Persson, et al. (2005). Implant stability during initiation and resolution of experimental periimplantitis: An experimental study in the dog. Clinical Implant Dentistry and Related Research 7(3): 136-140.

Skalak, R. (1983). Biomechanical considerations in osseointegrated prostheses. J Prosthet Dent 49(6): 843-848.

Smith, D. E. and G. A. Zarb (1989). Criteria for success of osseointegrated endosseous implants. J Prosthet Dent 62(5): 567-572.

Sones, A. D. (1989). Complications with osseointegrated implants. J Prosthet Dent 62(5): 581-585.

Song, Y.-Y., J.-Y. Cha, et al. (2007). Mechanical characteristics of various orthodontic mini-screws in relation to artificial cortical bone thickness. Angle Orthodontist 77(6): 979-985.

Spray, J. R., C. G. Black, et al. (2000). The influence of bone thickness on facial marginal bone response: Stage 1 placement through stage 2 uncovering. Ann Periodontol 5(1): 119-128.

Spray, J. R., J. J. Garnick, et al. (1978). Microscopic demonstration of the position of periodontal probes. J Periodontol 49(3): 148-152.

Sullivan, D. Y., R. L. Sherwood, et al. (1996). The reverse-torque test: A clinical report. Int J Oral Maxillofac Implants 11(2): 179-185.

Sullivan, D. Y., R. L. Sherwood, et al. (1997). Preliminary results of a multicenter study evaluating a chemically enhanced surface for machined commercially pure titanium implants. J Prosthet Dent 78(4): 379-386.

Tallgren, A. (1972). The continuing reduction of the residual alveolar ridges in complete denture wearers: A mixed-longitudinal study covering 25 years. J Prosthet Dent 27(2): 120-132.

Taylor, T. D. (1998). Prosthodontic problems and limitations associated with osseointegration. The Journal of Prosthetic Dentistry 79(1): 74-78.

Tolman, D. E. and W. R. Laney (1992). Tissue-integrated prosthesis complications. Int J Oral Maxillofac Implants 7(4): 477-484.

Tortora, G. and S. Grabowski (2000). Principles of anatomy and physiology, 9th ed. Biological Sciences Textbooks Inc 6: 160-182.

Tricio, J., D. Vansteenberghe, et al. (1995). Implant stability related to insertion torque force and bone-density - an in-vitro study. Journal of Prosthetic Dentistry 74(6): 608-612.

Truhlar, R. S., F. Lauciello, et al. (1997). The influence of bone quality on periotest values of endosseous dental implants at stage ii surgery. J Oral Maxillofac Surg 55(12 Suppl 5): 55-61.

Turkyilmaz, I., C. Tumer, et al. (2007). Relations between the bone density values from computerized tomography, and implant stability parameters: A clinical study of 230 regular platform implants. Journal of Clinical Periodontology 34(8): 716-722.

Uribe, R., M. Penarrocha, et al. (2005). Immediate loading in oral implants. Present situation. Med Oral Patol Oral Cir Bucal 10 Suppl 2: E143-153.

Wang, Y. and B. W. Darvell (2008). Failure behavior of glass ionomer cement under hertzian indentation. Dent Mater 24(9): 1223-1229.

Watanabe Y, Takai S, Arai Y, Yoshino N, Hiranawa Y. Prediction of mechanical properties of healing fracture using acoustic emission. J Orthop Res. 2001; 19:548-553.

Weinberg, L. A. and B. Kruger (1995). A comparison of implant/prosthesis loading with four clinical variables. Int J Prosthodont 8(5): 421-433.

Wennström, J. and R. Palmer (1999). Consensus report of session 3: Clinical trials. In: Lang, n., karring, t. & lindhe, j., eds. Proceedings of the 3rd european workshop on periodontology. Implant Dentistry. Berlin, PA: Quintessence: 255-259.

Weyant, R. J. (1994). Characteristics associated with the loss and peri-implant tissue health of endosseous dental implants. Int J Oral Maxillofac Implants 9(1): 95-102.

Williams, R. (1980). Acoustic emission. Adam Hilger Ltd, Bristol.

Zarb, G. A. and A. Schmitt (1990). The longitudinal clinical effectiveness of osseointegrated dental implants: The toronto study. Part iii: Problems and complications encountered. J Prosthet Dent 64(2): 185-194.